ADSORPTION OF CHLORINATED HYDROCARBONS

ON SILICA GEL

By

SHING-LIN KUO

Bachelor of Engineering
Tamkang University
Taipei, Taiwan, R.O.C.
1977

Master of Science
University of Wyoming
Laramie, Wyoming
1983

Submitted to the Faculty of the Graduate College
of the Oklahoma State University
in partial fullfillment of the requirements
for the Degree of
DOCTOR OF PHILOSOPHY
December, 1987

ADSORPTION OF CHLORINATED HYDROCARBONS

ON SILICA GEL

Thesis Approved:

Anthony L. Hines
Thesis Adviser

Mayis Seapan

William F. McGuinan

Jan A. Wagner

Norman N. Durham
Dean of the Graduate College

PREFACE

A survey of indoor air pollutants is conducted in this work. A gravimetrical adsorption apparatus was designed and used to remove six chlorinated hydrocarbon pollutants using silica gel as the adsorbent. The results showed that silica gel can be effectively used to remove pollutants.

A new analytic isotherm model was developed. This model assumes that the adsorbent consists of a distribution of energetically different sites which can be represented by a Morse-type energy distribution function with the local isotherm on a site can be described by the Jovanovic equation. The new model provides an excellent correlation of the experimental data for various gas-solid systems and also gives a more accurate and yet simpler description of adsorption behaviors on heterogeneous adsorbents than other heterogeneous isotherm equations.

Langmuir and BET models were also used to correlate the adsorption data for six chlorinated hydrocarbons on silica gels. It was found that the Langmuir model provided better correlations for the isotherm data for the heavier adsorbates than for the light ones, while the BET model provided good correlations for the isotherm data only up to 35 percent saturation pressure for each adsorbate.

Diffusion coefficients of chlorinated hydrocarbon pollutants were also investigated using spherical silica gel bead as the adsorbent. Pressure effect on the diffusion coefficients was studied. It is found that the spherical silica gel bead exhibited a homogeneous-like behavior and the Fickian diffusion model can be used to correlate the adsorption data and subsequently, calculated the diffusion coefficients of the chlorinated hydrocarbon pollutants.

I wish to express my sincere appreciation to all the people who assisted me during the course of this study. I am especially grateful to my major adviser, Dr. Anthony L. Hines, for his guidance, encouragement, and interest. Appreciation is also extended to the other committee members, Dr. Mayis Seapan, Dr. Jan Wagner, and Dr. William F. McTernan for their assistance and advisement in the course of this work.

Special thanks is due to the School of Chemical Engineering, Oklahoma State University for the financial support I received during the course of this work.

I want to express my deepest appreciation to my parents, Shooa-Ren Kuo and Won-Chi Jen, and other family members for their constant support, encouragement, and understanding.

Finally, I wish to thank Shirley Hagar for the excellent typing of this work.

TABLE OF CONTENTS

LIST OF TABLES

CHAPTER II

CHAPTER III

CHAPTER IV

CHAPTER V

CHAPTER VI

LIST OF FIGURES

CHAPTER II

CHAPTER III

CHAPTER IV

CHAPTER V

CHAPTER VI

NOMENCLATURE

CHAPTER II

E	=	Constant characteristic energy
E_o	=	Constant characteristic energy of a standard adsorbate
m	=	Constant in the generalized isotherm equation
P	=	Pressure
P^s		Saturation pressure
R	=	Gas constant
T	=	Temperature
$\bar{V}$	=	Molar volume of adsorbed phase
W	=	Volume of adsorbed phase
W_o	=	Volume adsorbed at saturation

Greek Letters

β	=	Affinity coefficient, E/E_o
ϵ	=	Adsorption potential

CHAPTER III

A	=	Saturation adsorption capacity
b	=	Jovanovic parameter defined by Eq. [4]
b_o	=	Limiting value of b at infinite temperature
e	=	Adsorption energy parameter
E	=	Energy distribution function
g	=	Energy parameter defined by Eq. [6]
K	=	$K_1^2 K_2$
K_o	=	Parameter in Morse-type energy distribution function
K_1	=	Parameter in Morse-type energy distribution function
K_2	=	Parameter in Morse-type energy distribution function
K_ℓ	=	Local Henry's law constant
P	=	System pressure
Q	=	Overall adsorption isotherm

Q_ℓ = Local adsorption isotherm

q = Isosteric heat of adsorption

R = Universal gas constant

T = System temperature

CHAPTER IV

A = Surface area of a molecule

a = Langmuir parameter defined in Eq. [2]

b = Jovanovic parameter defined in Eq. [5]

b_o = Limiting value of b at infinite temperature

C = BET constant defined in Eq. [3]

E = Energy distribution function

g = Adsorption energy parameter

ΔH_c = Heat of condensation

ΔH_s = Isosteric heat of adsorption

K_1 = Parameter in Morse-type energy distribution function

K_2 = Parameter in Morse-type energy distribution function

K_ℓ = Henry's law constant

m = Saturation adsorption capacity

N = Overall adsorption isotherm

N_ℓ = Local adsorption isotherm

N_m = Monolayer adsorption capacity

P = System pressure

R = Universal gas constant

T = System temperature

CHAPTER V

A = Surface area of a molecule

a = Langmuir parameter defined in Eq. [2]

b = Jovanovic parameter defined by Eq. [5]

b_o = Limiting value of b at infinite temperature

C = BET constant defined in Eq. [3]

E	=	Energy distribution function
g	=	Adsorption energy parameter
K_1	=	Parameter in Morse-type energy distribution function
K_2	=	Parameter in Morse-type energy distribution function
K_ℓ	=	Henry's law constant
m	=	Saturation adsorption capacity
N	=	Overall adsorption isotherm
N_ℓ	=	Local adsorption isotherm
P	=	System pressure
P_s	=	Saturation pressure
q	=	Isosteric heat of adsorption
q_c	=	Heat of condensation
R	=	Universal gas constant
T	=	System temperature

CHAPTER VI

C	=	Concentration profile of adsorbate inside a spherical adsorbent
C_o	=	Initial adsorbent concentration
C_1	=	Surface concentration of adsorbent
D	=	Effective diffusion coefficient
D_g	=	Gas diffusivity
D_k	=	Knudsen diffusion coefficient
D_ℓ	=	Liquid diffusivity
D_o	=	Preexponential or frequency factor
D_s	=	Surface diffusion coefficient
E_a	=	Activation energy of surface diffusion
ΔH_s	=	Isosteric energy of adsorption
M_t	=	Amount of adsorbate adsorbed
M_∞	=	Amount of adsorbate adsorbed at $T \rightarrow \infty$
R	=	Radius of a spherical adsorbent bead, gas constant
T	=	Temperature

CHAPTER I

INTRODUCTION

INTRODUCTION

Gas adsorption is a very broad subject and is usually divided into two broad classes, namely, physical adsorption and chemisorption. Physical adsorption is usually very rapid and is reversible, the adsorbate being removable without change by lowering the pressure. It is supposed that this type of adsorption occurs as a result of the same type of relatively nonspecific intermolecular forces that are responsible for the condensation of a vapor to a liquid and are usually described as Van der Waal's forces. Thus, in physical adsorption the heat of adsorption should be in the range of heats of condensation. Physical adsorption is usually important only for gases below their critical temperature, i.e., for vapors.

Physical adsorption is dependent on the nature of the adsorbate and adsorbent to a small extent only. In contrast to chemisorption, in principle all sites can be covered by physical adsorption below the critical temperature, as far as the geometric structure of the adsorbent permits. There exists, however, sites where physical adsorption preferentially takes place. They are, for example, OH groups in the case of physical adsorption of oxygen-containing substances and of some sulphur compounds, and oxygen ions of oxides in the case of adsorption of similar compounds.

Davidson silica gels are microporous, granular, amorphous form of silica, prepared by the hydrolysis of soluble sodium silicate with sulfuric acid to produce sodium sulfate and silicic acid. It is commonly accepted that the surface of a hydrated silica is covered with hydroxyl groups which are attached to silicon atoms. The adsorption and

other surface properties of silica gels are known to depend on the presence of these silanol hydroxyl groups on the surface. When the silica gel is heated during reactivation, it undergoes dehydration because some of the hydroxyl groups leave the surface as water vapor. The degree of dehydroxylation of the surface is a function of the regeneration temperature and may alter the adsorptive strength of the surface.

An adsorbent surface is considered as homogeneous when the adsorption sites have identical properties; whereas, it is considered as heterogeneous when the sites have varying properties. The heterogeneity of the adsorbent surface usually results in different adsorptive strength of the adsorption sites. The degree of heterogeneity of the adsorbent surface plays an important role in the determination of the adsorption isotherm shapes and can be evaluated by comparing the variations of isosteric heats of adsorption at different loadings. When sites with equivalent properties are distributed over the surface at random, adsorption is always localized. Therefore, the equilibrium of adsorption on sites with identical properties will obviously be described by one of the localized adsorption models. When the energy of adsorption sites can be described by means of a continuous distribution function, the adsorption isotherm for the entire heterogeneous surface can be obtained by integrating the product of the localized isotherm and the energy distribution function.

A complete description of adsorption kinetics includes not only the adsorption isotherm models, but also the relationship between the rate of adsorption and pressure, temperature and the extent of adsorption. The rate of uptake (Reference 2, Chapter VI) may be limited by: (1) the

rate of mass transfer of the gas to the adsorbent surface; (2) the rate of mass transfer within pores in the adsorbent; (3) the rate of transfer of heat liberated by the adsorption process from the adsorbed molecule to the adsorbent; (4) the rate of activated migration of the adsorbed particles along the surface of the adsorbent to the site which is most favorable for adsorption; and (5) the rate of surface process, requiring, for example, that an activation energy by supplied.

In this work, the adsorption isotherm data for six chlorinated hydrocarbons, including chloromethane, dichloromethane, trichloromethane, tetrachloromethane, 1,1,1-trichloroethane and tetrachloroethylene on Davidson silica gels were measured gravimetrically at 288, 293, and 298K. A constant reactivation temperature and vacuum were used to regenerate the adsorbent prior to each isotherm measurement. A new theoretical isotherm model for adsorption on a heterogeneous surface was developed and tested. The new isotherm model as well as several localized isotherm models, including the Langmuir model and the BET equation, were used to correlate the adsorption data obtained in this study. Diffusion of the above mentioned chlorinated hydrocarbons through spherical silica gel beads were also studied at three temperatures and the diffusion rate controlling step was determined by evaluating the contribution of each diffusion mechanism to the diffusion process.

CHAPTER II

ADSORPTION OF CHLORINATED HYDROCARBON POLLUTANTS ON SILICA GEL

ADSORPTION OF CHLORINATED HYDROCARBON POLLUTANTS ON SILICA GEL

Shing-Lin Kuo and Anthony L. Hines*

School of Chemical Engineering
Oklahoma State University
Stillwater, Oklahoma 74078

*To whom correspondence should be directed.

ABSTRACT

A survey of indoor air pollutants was conducted. The removal of six chlorinated hydrocarbons, including chloromethane, dichloromethane, trichloromethane, tetrachloromethane, 1,1,1-trichloroethane, and tetrachloroethylene was performed using adsorption methods. The equilibrium uptakes of the six indoor pollutants on silica gel were determined gravimetrically at 25°C and at pressures up to saturation. The modified potential theory proposed by Dubinin and his co-workers was used to correlate the adsorption data.

ADSORPTION OF CHLORINATED HYDROCARBON POLLUTANTS ON SILICA GEL

INTRODUCTION

Air pollution has traditionally meant pollution of the outdoor air-exhaust spewing from motor vehicles or smoke billowing from factories and refineries. Recently, however, studies have shown that indoor air is often dirtier than outdoor air. The Environmental Protection Agency (EPA) reported that toxic chemicals found in every home--from paint to cleaning solvents--are three times more likely to cause cancer than outdoor airborne pollutants, even in areas next to chemical plants (1). Since most people spend more than 60 percent of their time inside their homes and 20 percent of America's single-family homes could contain more cancer-causing gases than some people think is healthy, scientists are concerned that high indoor pollutant levels might have adverse health effects.

Two factors that have aggravated the indoor-air problem are new chemical products and houses that are better insulated. Concern has also increased as researchers have learned more about the hazards of many of the chemicals that have long been in people's homes (2). A typical house harbors dozens of products that release organic chemicals. Many household-chemical products, such as spray paints, insecticides, and furniture polish, come in aerosol form. This causes tiny droplets of the product to be dispersed in the air and subsequently adds an additional chemical (the propellant) to those that are already present in the basic product. On the other hand, the nationwide drive to save energy by weatherproofing has made the air inside many homes and offices more polluted than the outside air.

CLASSIFICATIONS OF INDOOR AIR POLLUTANTS

The pollutants that pose the greatest threats inside homes and offices are not necessarily the same ones that pose the greatest problems outdoors. A summary of the sources with possible concentrations and threats of some indoor air pollutants is given in Table 1. As can be seen, there are a large variety of indoor air pollutants that pose a myriad of health threats to humans. Of all the indoor air pollutants, the chlorinated hydrocarbons, radon, formaldehyde, cigarette smoke, and unvented combustion products have drawn the most attention. The reason for concern about the chlorinated hydrocarbons, particularly dichloromethane, is that it is present in large amounts in several widely used consumer products. Each year approximately 135 million cans of paint stripper are used which contain from 50 to 80 percent dichloromethane. It has been estimated that three of every thousand who use a dichloromethane-based paint stripper no more than once per year between age 25 and 70 could develop cancer. Thus, dichloromethane is considered to pose the highest cancer risk of any household chemical.

REMOVAL OF INDOOR AIR POLLUTANTS

Indoor air pollution problems have just recently been brought to the attention of researchers, but most of the studies so far have focused only on determining the types and levels of the indoor air pollutants. Studies on the removal of indoor air pollutants are very limited and the results have not always been satisfactory. Complete removal of indoor air pollutants is a difficult task because of the

diversity of the pollutants, many of which exhibit different properties and pose different health threats. The techniques developed so far for the removal of air pollutants have targeted a particular type of pollutant. For example, radon gas, toxic household chemicals, paint strippers, and combustion products can be directed away from the house by venting and then introducing fresh air into the home. Another method is to place filters in the forced-air heating or central air-conditioning systems to help in removing particulates and some organic pollutants. The techniques described above may be used to solve specific indoor air pollution problems, but only when the outdoor air is much cleaner than that which exists indoors. In view of the interest in using solar energy to heat and cool homes and offices, it may be feasible to use the same adsorbent found in solar cooling systems to also remove many indoor air pollutants. In this work a silica gel that has found use in dehumidification applications is evaluated as a possible candidate for adsorbing several chlorinated hydrocarbons from indoor air.

EXPERIMENTAL SECTION

The adsorbent used in this study was type PA40, 80-100 mesh silica gel supplied by Davison Chemical Co. All but one of the indoor chlorinated air pollutants given in Table 1 were investigated. These are: chloromethane, dichloromethane, trichloromethane, and tetrachloromethane, which are a homologous series, and two other indoor air pollutants: 1,1,1-trichloroethane and tetrachloroethylene. All of the above chemicals were obtained from Fisher Scientific Co. and had purities greater than 99.5%.

The experimental adsorption studies were carried out gravimetrically using a Cahn R-2000 electrobalance housed in a vacuum bottle. The adsorption apparatus was designed such that either gases or vapors could be studied. The sample weight was monitored with a strip chart recorder connected to the electrobalance control unit. A refrigerated-heater bath with a copper circulation coil wrapped around the sample hangdown tube was used to control the adsorption temperature. A special vapor supply flask was used as the pollutant container. A vacuum system which consisted of two vacuum pumps, a sorption trap, and a diffusion pump were used to obtain a vacuum of 1×10^{-4} mm Hg for the system. The leak rate of the complete system was approximately 0.005 mm Hg/h. Two thermistor gauges were used to monitor the pressure when the system was evacuated and during adsorption runs. In addition, pressures up to 1 atm were measured with a Wallace and Tiernan absolute pressure gauge. A schematic diagram of the apparatus is shown in Figure 1.

The electrobalance was calibrated to agree with the output signal of the recorder. The weight changes of the silica gel sample due to the adsorption of indoor air pollutants were detected by the electrobalance. The silica gel sample was regenerated by evacuating the system and applying heat at 423K to the sample hangdown tube. Heating was continued until a constant sample weight was obtained. This typically required from 4 to 10 h. Following regeneration, the adsorbent was cooled to the adsorption temperature and the adsorbate was introduced into the system. After equilibrium was reached, as indicated by a constant sample weight, the pressure and weight were recorded. Equilibrium isotherm data were taken from very low pressure

up to saturation. Desorption measurements were made by reducing the system pressure.

ANALYSIS OF DATA

Adsorption isotherms were obtained for chloromethane, dichloromethane, trichloromethane, tetrachloromethane, 1,1,1-trichloroethane, and tetrachloroethylene on silica gel at 298k after overnight regeneration of the adsorbent at 423K in vacuo. The experimental equilibrium values are presented in Figures 2 and 3. The maximum error introduced by the buoyancy effect on the adsorption measurements was evaluated and found to be less than 0.5%. Since this error was small, the buoyancy effect on the adsorption measurement was neglected. The weight of the sample was measured to within 10 μg with an error in the weight measurement of 0.0005%. Pressure was measured with an accuracy of ± 0.15 mm Hg. Except for the lowest pressures, the maximum error in pressure measurements was less than 0.3%. The average error over the entire adsorption range was estimated to be less than 1%. Several of the data points were reproduced with an error no greater than 1%.

The adsorption isotherms of all six indoor air pollutants on silica gel were Type I, according to the BDDT classification (4,5), and showed no apparent hysteresis when desorbing. The absence of capillary condensation, as noted from the equilibrium data, indicates that the silica gel contains mostly micropores. For a homologous series of chemicals, the amount of adsorbate removed by the silica gel increased as the molecular weight of the adsorbate increased as can be seen from Figures 2 and 3. The fact that the maximum uptake of each adsorbate by the silica gel was in the range of 0.395 - 0.445g adsorbate/g silica gel

suggests that silica gel is an effective adsorbent for removing indoor air pollutants.

The potential theory proposed by Polanyi (6,7) has been applied successfully for both monolayer and multilayer adsorption of gases and vapors on porous as well as nonporous adsorbents. The Polanyi theory in its original form assumes that the adsorbent exerts long-range attractive forces on the gas or vapor surrounding it. These forces give rise to a potential field with the potential decreasing as the distance from the adsorbent increases. The adsorption potential is described by

$$\varepsilon = RT \ln\left(\frac{P^s}{P}\right) \qquad (1)$$

where P^s is the saturation pressure of the vapor at system temperature, P is pressure of the adsorption system and R is gas constant. Thus, a plot of the volume adsorbed versus the adsorption potential should yield a characteristic curve that is independent of temperature.

Dubinin (8) correlated equilibrium adsorption data for different gases and vapors on the same adsorbent by using a single characteristic curve. He suggested that for vapors of similar compounds, the adsorption potentials at equal adsorption volumes should have a constant ratio which is given by the ratio of the molar volumes of the adsorbed phases. Thus, a plot of the volume adsorbed versus the adsorption potential divided by the molar volume should yield a single characteristic curve for the adsorption of similar materials on the same adsorbent at different temperatures. The theory of pore filling proposed by Dubinin and co-workers (9,10,11) is particularly suited for describing the adsorption on microporous solids. As shown by Bering et

al. (10), the volume adsorbed in the pores can be described by the expression

$$W = W_o \exp\left[-\left(\frac{\varepsilon}{\beta E_o}\right)^m\right] \qquad (2)$$

where E_o is a constant characteristic energy of a standard adsorbate, β is the affinity coefficient, W_o is the volume of adsorption space at saturation and m is a constant. According to Eq. (2), a plot of $\ell n\ W$ vs. $(\varepsilon)^m$ should yield a straight line with a slope of $-(1/\beta E_o)^m$ and an intercept of W_o. If the adsorption of several compounds on one adsorbent can be described by Eq. (2) using only one value for the exponent m, then one of these isotherms may be used to predict the isotherms of the other compounds. By setting the affinity coefficient of the standard material equal to 1, which is dichloromethane in this study, the constants W_o and E_o can be determined from the standard isotherm. The affinity coefficient for other isotherms can be approximated by the ratio of the parachors as shown by Bering et al. (9).

The generalized correlation is presented in Figure 4 according to the modified Polanyi theory. As noted, the experimental data can be approximated by a single characteristic curve. Because the generalized isotherm equation given by Eq. (2) contains three parameters, W_o, E_o, and m, the correlation of the data is possible if the parameter m is the same for all adsorbates on a single adsorbent. A value of 1.42 was found to produce the best least-squares fit to the data. The generalized equation obtained is

$$W = 0.301 \exp[-(\varepsilon/1.374\beta)^{1.42}] \quad (3)$$

The above equation was used to predict the adsorption equilibrium data for chloromethane, dichloromethane, trichloromethane and tetrachloromethane using affinity coefficients of 0.95, 1.0, 1.15, and 1.30, respectively. The absolute percent deviation between the predicted and the experimental values is less than 10% except at pressure below 20 mmHg. It is interesting to note that values of m range from 1.2 to 1.8 for highly activated carbon and from 3.0 to 6.0 for zeolites. Dubinin (8) reported an m equal to 1.0 for one type of silica gel.

CONCLUSION

A survey of indoor air pollutants was conducted. The removal of six pollutants, including chloromethane, dichloromethane, trichloromethane, tetrachloromethane, 1,1,1-trichloroethane, and tetrachloroethylene was investigated using adsorption methods. The adsorption isotherms of the six chlorinated hydrocarbons on silica gel were determined gravimetrically at 25°C and at pressures up to saturation. The generalized adsorption isotherm equation proposed by Dubinin and his co-workers was used to correlate the adsorption data. On the basis of this study, it was concluded that silica gel can be effectively used to both dehumidify as well as remove pollutants from indoor air.

Nomenclature

E	=	Constant characteristic energy
E_o	=	Constant characteristic energy of a standard adsorbate
m	=	Constant in the generalized isotherm equation
P	=	Pressure
P^s		Saturation pressure
R	=	Gas constant
T	=	Temperature
$\bar{V}$	=	Molar volume of adsorbed phase
W	=	Volume of adsorbed phase
W_o	=	Volume adsorbed at saturation

Greek Letters

β	=	Affinity coefficient, E/E_o
ε	=	Adsorption potential

LITERATURE CITED

1. U. S. News and World Report, Sept. 23, 71 (1985).
2. Consumer Reports, October, 600 (1985).
3. E. Meyer, Chemistry of Hazardous Materials; Prentice-Hall, Englewood Cliffs, New Jersey, 1977.
4. S. Brunauer, P. H. Emmett, and E. J. Teller, Am. Chem. Soc., 60, 309 (1938).
5. S. Brunauer, L. S. Deming, W. E. Deming, and E. J. Teller, Am. Chem. Soc., 62, 1723 (1940).
6. M. Polanyi, Z. Physik, 2, 111 (1920).
7. M. Polanyi, Verh. Deut. Physik, Ges., 18, 55 (1916).
8. M. M. Dubinin, Chem. Rev., 60, 235 (1960).
9. B. P. Bering, M. M. Dubinin, and V. V. Superinsky, J. Colloid Interface Sci., 21, 378 (1966).
10. B. P. Bering, M. M. Dubinin, and V. V. Superinsky, J. Colloid Interface Sci., 38, 186 (1972).
11. M. M. Dubinin, J. Colloid Interface Sci., 23, 487 (1967).

LIST OF TABLES

TABLE I

Sources, Possible Concentrations, Indoor-to-Outdoor Concentration Ratios, and Threats of Some Indoor Air Pollutants

Pollutant	Sources of Indoor Pollution	Possible[a] Concentration	I/O Ratio	Threats[3]
Dichloro-methane	Paint strippers and thinners	NA	>1	Nerve disorders, diabetes
Trichloro-methane	Chlorine-treated water in hot showers	NA	>1	Anesthetic, eye irritation, cancer
Tetrachloro-ethylene	Dry-cleaning-fluid fumes on clothes	NA	>1	Nerve disorders, damage to liver and kidneys, possible cancer
1,1,1-Trichloro-ethane	Aerosol sprays	NA	>1	Dizziness, irregular breathing
Chloromethane	Solvents, aerosol sprays	NA	>1	Nerve disorders, possible cancer
Tetrachloro-methane	Solvents, combustion	NA	>1	Headache, dizziness, cancer
Radon and Progeny	Radioactive soil, groundwater, building materials	0.1-30 nCi/m^3	>>1	Lung cancer
Formaldehyde	Insulation, particle board, furniture stuffing	0.05-1.0 ppm	>1	Irritation of eyes and throat
Carbon Monoxide	Combustion equipment, engines, faulty furnaces, unvented gas stoves	100 ppm	>>1	Headaches, irregular breathing
Nitrogen Dioxide	Combustion, gas stoves, water heaters, dryers, cigarettes, engines	200-1000 $\mu g/m^3$	>>1	Irritated lungs, children's colds
Benzo-a-pyrene	Wood stoves, tobacco smoke	NA	>>1	Lung cancer

TABLE I (Continued)

Pollutant	Sources of Indoor Pollution	Possible[a] Concentration	I/O Ratio	Threats[3]
para-Dichloro-benzene	Air fresheners, mothball crystals	NA	>1	Cancer
Sulfur Dioxide	Heating system	20 $\mu g/m^3$	<1	Choking, coughing, irritation of eyes and throat
Sulfate	Matches, gas stoves	5 $\mu g/m^3$	<1	Choking, chest pain, colds
Carbon Dioxide	Combustion, humans, pets	3000 ppm	>>1	Irregular breathing
Ozone	Electric arcing, UV light sources	20 ppb 200 ppb	<1 >1	Headache, coughing, chest pain, build-up of fluid in lungs
Asbestos	Fireproofing	<1 fiber/CC	1	Lung cancer
Mineral and Synthetic Fibers	Products, clothes, rugs, wallboard	NA	-	Lung damage, cancer
Viable Organisms	Humans, pets, rodents, insects, plants, fungi, humidifiers, air conditioners	NA	>1	Coughing, any kind of disease is possible
Respirable Particles	Stoves, fireplaces, cigarettes, condensation of volatiles, resuspension, cooking, aerosol sprays	100-500 $\mu g/m^3$	>>1	Irritation of eyes, skin, and respiratory membranes, anesthetic, arrest respiration

[a] Concentrations listed are only illustrative of those reported indoors. NA (Not Appropriate to list a concentration).

LIST OF FIGURES

SYMBOLS INDEX FOR FIGURE 1

A	Adjustable relief valve - 1/4"
B	Needle valve - 1/4"
C	Bellows vacuum valve - 1/4"
D	Bellows vacuum valve - 1/2"
E	Bellows vacuum valve - 1/2"
F	Bellows vacuum valve - 1/2"
G	Needle valve - 1/4"
H	Needle valve - 1/4"
BF	Constant temperature bath or furnace
CU	Balance control unit
DIT	Dry ice trap
DP	Difussion pump
FB	Feed bottle
HT	Hangdown tube
MP	Mechanical vacuum pump, holding pump
RC	Recorder
RP	Mechanical vacuum pump, roughing pump
TVG	Thermistor vacuum gauage
WTG	Wallace and Tiernan gauge

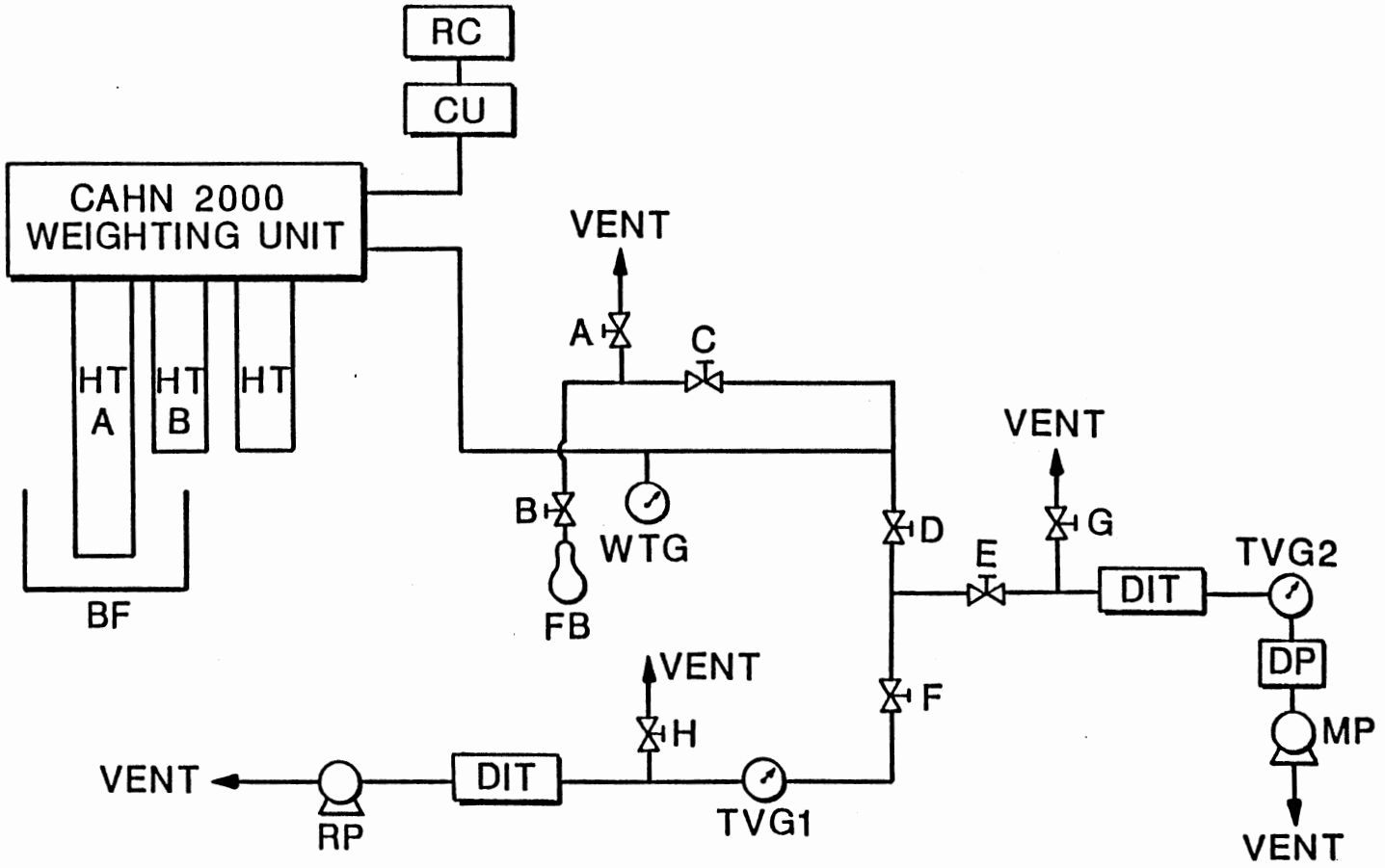

Figure 1. Schematic Diagram of Adsorption Apparatus.

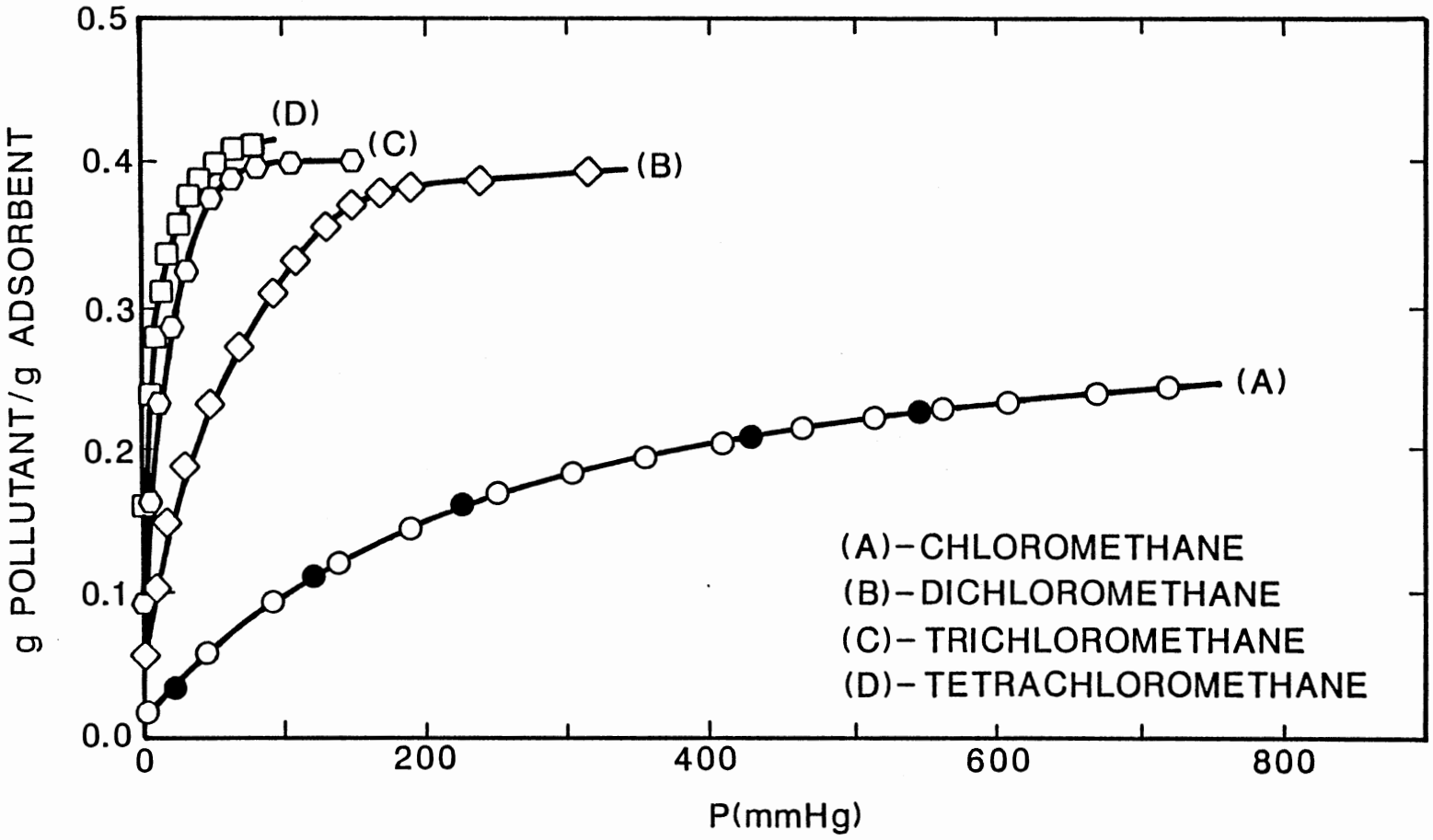

Figure 2. Adsorption Isotherms of Chloromethane, Dichloromethane, Trichloromethane and Tetrachloromethane on Silica Gel at 25°C (Solid Symbols Represent Desorption Data).

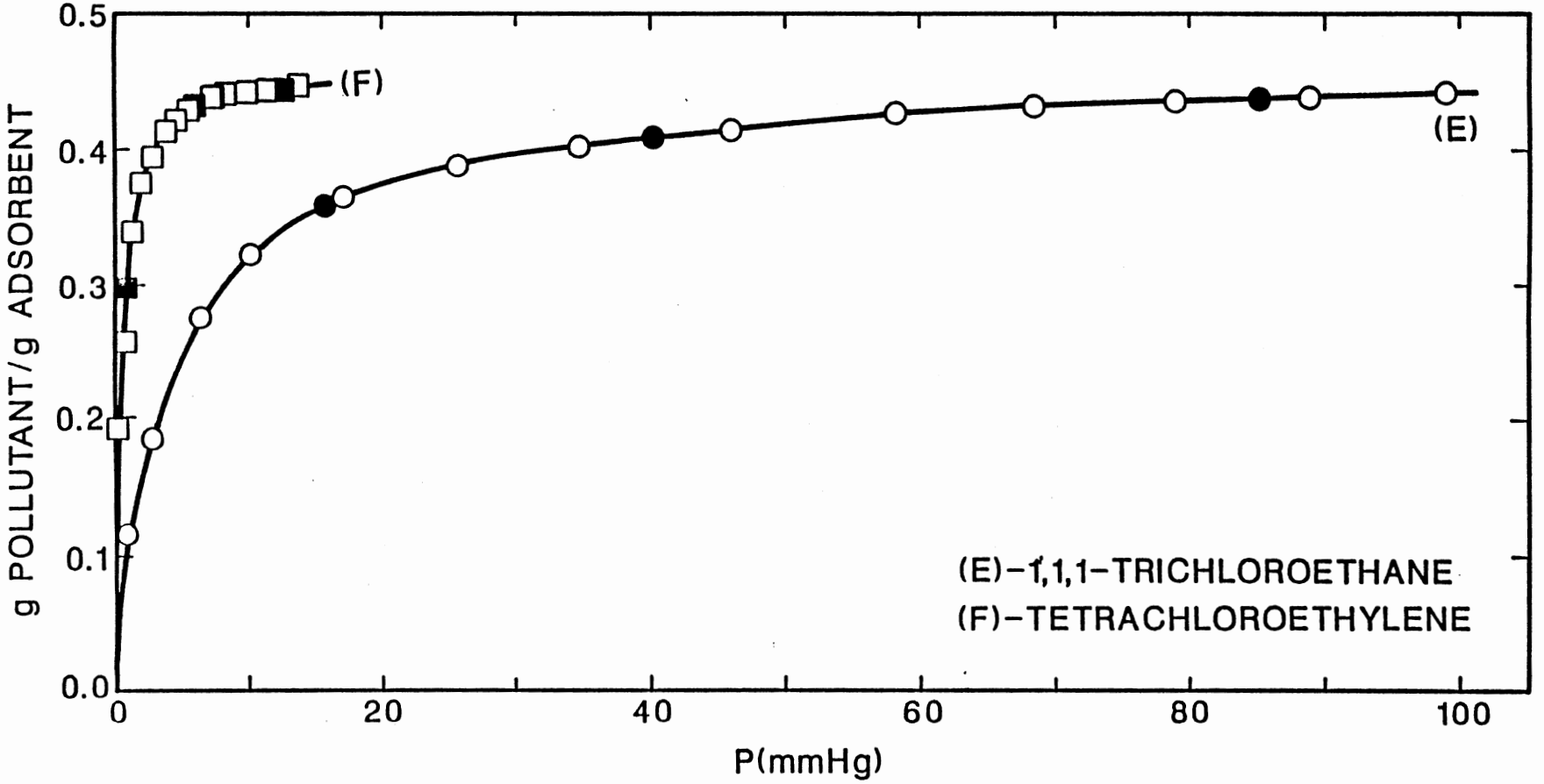

Figure 3. Adsorption Isotherms of 1,1,1-Trichloroethane and Tetrachloroethylene on Silica Gel at 25 ^{o}C (Solid Symbols Represent Desorption Data).

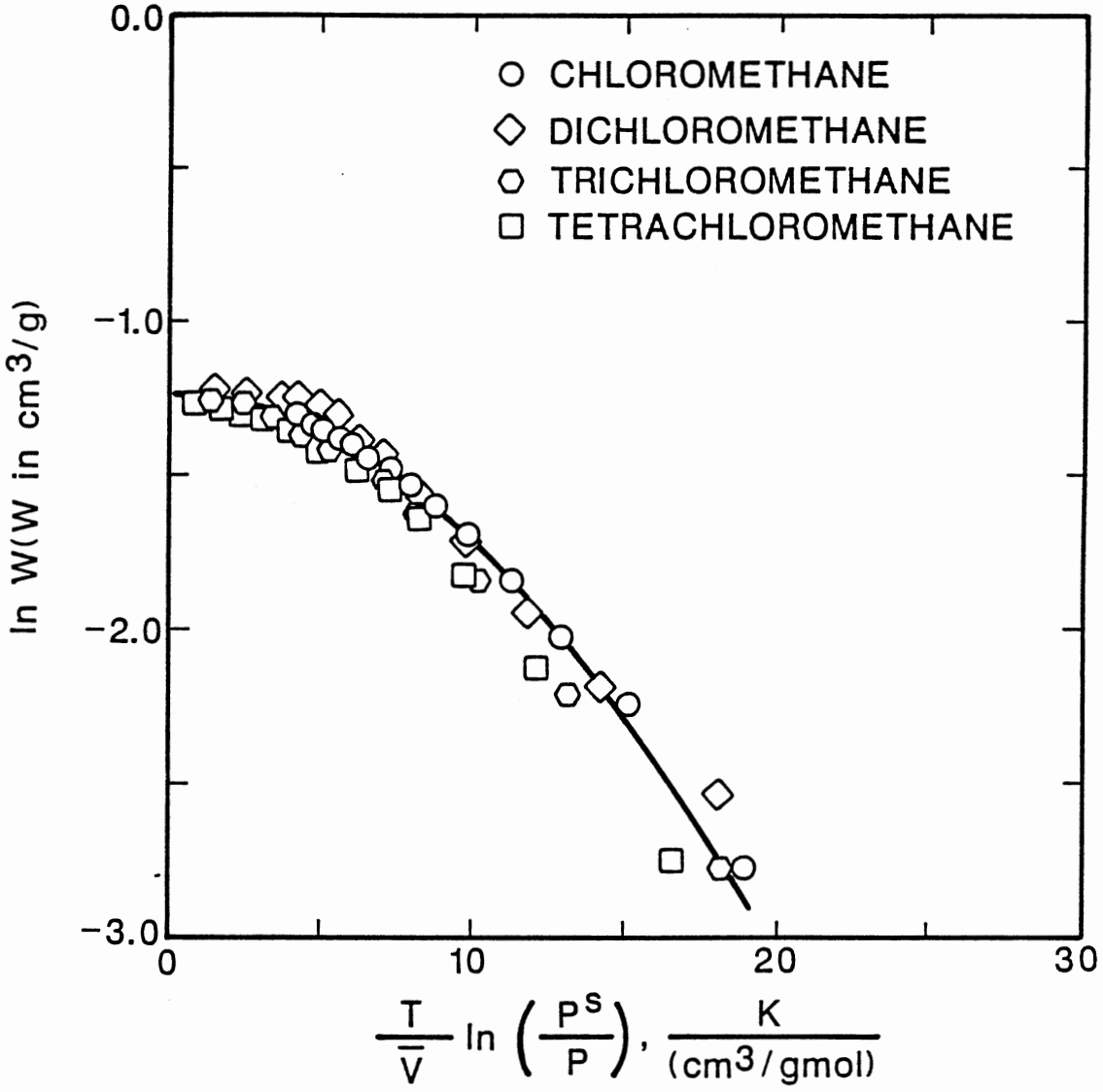

Figure 4. Generalized Adsorption Correlation on Silica Gel.

CHAPTER III

NEW THEORETICAL ISOTHERM FOR ADSORPTION ON HETEROGENEOUS ADSORBENTS

NEW THEORETICAL ISOTHERM FOR ADSORPTION ON HETEROGENEOUS ADSORBENTS

Shing-Lin Kuo and Anthony L. Hines*

School of Chemical Engineering
Oklahoma State University
Stillwater, Oklahoma 74078

*To whom correspondence should be directed.
Keywords: Theoretical Adsorption Isotherm

ABSTRACT

A new analytic isotherm equation is derived for adsorption of gases on microporous heterogeneous adsorbents. The model assumes that the adsorbent consists of a distribution of energetically different sites which can be represented by a Morse-type energy distribution function with the local isotherm on a site can be described by the Jovanovic equation. The model has three parameters, the saturation adsorption capacity and two energy distribution parameters. All of these parameters are related to the Henry's law constants.

The new model was tested using experimental data that included the adsorption of CH_4, C_2H_4 and CO_2 on various activated carbons at different temperatures and pressures. The new model provides an excellent correlation of the experimental adsorption data for the above gases. A comparison of the new model with other isotherm equations showed that the new model gives a more accurate and yet simpler description of adsorption behaviors on heterogeneous adsorbents.

NEW THEORETICAL ISOTHERM FOR ADSORPTION ON HETEROGENEOUS ADSORBENTS

INTRODUCTION

Numerous theories and semitheories describing pure gas adsorption isotherms have been reported by Ponec et al. (1974) and by Sing (1973). However, most of these were often restricted to particular types of systems and to limited ranges of conditions. Some models do not even conform with the basic constraints that are imposed by physics. The primary reason of failure is the inabilty of the simplified models to simulate the very complex gas-solid and lateral molecular interactions which occur during adsorption. The other reason for failure is that most models use only a single constant to describe the complicated adsorption space. This severely distorts the actual situation. In the excellent review of common adsorption equations and their limitations given by Sircar and Gupta (1981), it is indicated that most adsorption equations violate the basic requirements of thermodynamics.

It is well known that for a large class of solid-vapor systems, the heterogeous structure of the adsorbing surface plays an important role in the process of physical adsorption. A detailed review of the subject is given by Jaroniec et al. (1981). The popular approach is to assume that the heterogeneous adsorbent consists of a distribution of energetically homogeneous sites and the overall heterogeneous adsorption isotherm can be obtained by the integration of the contributions of each site as shown by Ross and Oliver (1964):

$$Q(P,T) = \int_0^\infty Q_\ell(P,T,e)\ E(e)de \qquad [1]$$

where Q(P,T) represents the overall adsorption isotherm on the heterogeneous adsorbent. The term, $Q_\ell(P,T,e)$, describes a specific adsorption isotherm for homotattic sites of adsorptive energy e. Both Q and Q_ℓ are amounts adsorbed per unit mass of the adsorbent. The energy term, E(e), is the site energy distribution function for e and E(e)de is the fraction of total sites having energy between e and e + de. The choice of the integration limits is rather arbitrary and their justification depends upon the characteristics of the energy distribution function. If the energy distribution function is represented by a continuous probability density function of e, the normalization requires that

$$\int_0^\infty E(e)de = 1 \qquad [2]$$

The limits of integration in Eqs. [1] and [2] are zero and infinity, representing, respectively, a very weakly adsorptive site and a site with irreversible adsorption. Equation [1] has three unknown functions, viz. Q(P,T), $Q_\ell(P,T,e)$ and E(e). Only Q(P,T) can be measured experimentally. The energy term, E(e), can then be calculated from the experimental adsorption data, using Eq. [1] and assuming an analytic expression for Q_ℓ or vice versa. As shown by Ross and Morrison (1973) and by House and Jaycock (1978), most of the published studies have focused on numerically estimating E(e) from experimental Q(P,T) data by assuming a well known expression for Q_ℓ, such as the Langmuir model, step isotherm, Fowler-Guggenheim, Hill-Deboer, or Viral equations of state. Other efforts to obtain analytic expressions for E(e) correspond to well known adsorption equations for Q(P,T), such as the generalized

Freundlich, Dubinin-Radushkevich, and Toth isotherms, by assuming that $Q_{\ell}(P,T,e)$ can be described by the Langmuir or the step isotherm (Sips, 1950; Jaroniec, 1975; Misra, 1969).

Few studies have been done to derive analytic expressions for Q(P,T) which are very useful to design engineers for extrapolating data, calculating multicomponent equilibria and modeling of adsorptive separation processes. Misra (1970, 1973) used an exponential form of the probability density function as well as the constant probability function in conjunction with the Langmuir and the Jovanovich local isotherm equations to obtain analytic functions for Q(P,T). The resulting isotherms, however, did not have a defined Henry's law region as required by the physics of adsorption (Hill, 1960). The isotherms were also not tested using real data. Cerofolini et al. (1978) used the Langmuir local isotherm in conjunction with a condensation approximation for the adsorption-energy distribution to obtain an expression for an overall isotherm equation. The resulting isotherm does reduce to the Henry isotherm in the very low pressure limit. However, it was not tested using real data. Recently, Sircar (1984) developed an expression for Q(P,T) by assuming that the Langmuir model represented the local isotherm and the energy distribution had a gamma probability density form. Sircar's model does successfully describe the adsorption of various gases on activated carbons and zeolites over large ranges of pressure and temperature. However, the resulting equation is very cumbersome to use. Sircar (1984) later developed a much simpler model with the same degree of versatility by using the Jovanovic local isotherm model in conjunction with the gamma energy distribution function.

In this study a new heterogeneous adsorption equation is developed using the Jovanovic model as the local isotherm in conjunction with a Morse-type potential as the energy distribution function. The new model is tested using experimental data. The effect of the choice of energy distribution function on the adsorbent heterogeneity is analyzed.

THEORY

It is assumed that the local isotherm for a homogeneous surface is given by the equation of Jovanovic (1969):

$$Q_\ell(P,T,e) = A[1 - \exp(-bP)] \qquad [3]$$

where A is the saturation adsorption capacity and b is the Jovanovic parameter given by

$$b = b_o \exp(q/RT) \qquad [4]$$

In the above expression, b_o is a constant that represents the limiting value of b as T becomes infinitely large, q is the isosteric heat of adsorption for the site and R is the gas constant. The Jovanovic equation reduces to the linear isotherm in the Henry's law region as the pressure becomes very small. The local Henry's law constant is given by

$$\left[\frac{\partial Q_\ell}{\partial P}\right]_T = K_\ell(T) = Ab \qquad [5]$$

or

$$K_\ell(T) = Ab_o \quad \text{as } T \to \infty$$

For a heterogeneous adsorbent q can vary theoretically between zero and infinity, corresponding respectively to a value for E of zero and infinity. Thus b can vary between b_o and infinity. In this study we define a new energy parameter, g, as

$$g = b_o[\exp (q/RT) - 1] \qquad [6]$$

Equation [6] shows that the energy function, g, also varies between zero and infinity, corresponding respectively to q approaching zero and infinity. Each site is characterized by a specific value of g. We assume that the energy distribution on the adsorbent can be described by a modified Morse-type probability density function of g.

The original form of Morse potential energy function (Morse, 1929) that describes molecular potential is

$$E(r) = A + De^{-2a(r-r_o)} - 2De^{-a(r-r_o)}. \qquad [7]$$

where r represents the distance that separates molecules, r_o represents the equilibrium internuclear separation about which the molecule vibrates, a represents the vibration frequency of the molecule, D represents the dissociation energy that is required to increase r until the atoms separate to infinity, and A represents the energy separation and is given so that the potential curve of neutral molecule are reckoned from the lowest vibration level of the lowest electronic state of the neutral molecule.

When the Morse potential was used to describe the energy probability density function of the heterogeneous adsorbents, we assumed

that the energy distribution along the adsorbent surface can be represented by the following expression

$$E(g) = K_o[e^{-K_1 g} - K_2 e^{-g}] \qquad 0 \leq g \leq \infty \qquad [8]$$

$$\int_o^\infty E(g)\, dg = 1 \qquad [9]$$

where g is the energy parameter that accounts for the distance between gas molecule and adsorptive site, K_o is the parameter that represents the energy which is required to increase the distance between the bulk phase and adsorptive site to infinity, K_1 is the parameter that accounts for the vibration frequency of the bulk phase, and K_2 is the parameter that represents the minimum energy corresponding to the equilibrium separation between the bulk phase and adsorptive site.

The constants K_o, K_1, and K_2 are a function of temperature. The normalization requirements given by Eq. [9] yield the following value for K_o:

$$K_o = \frac{K_1}{1 - K_1 K_2} \qquad [10]$$

Equations [6], [8], [9], and [10] can be combined to obtain

$$\int_o^\infty K_o[e^{-K_1 g} - K_2 e^{-g}]\, [g + b_o]\, d(\frac{q}{RT}) = 1.0 \qquad [11]$$

Equation [11] shows that the probability function for the heterogeneous adsorbent is given in terms of q/RT as

$$E(\frac{q}{RT}) = \frac{K_1}{1 - K_1 K_2} [e^{-K_1 g} - K_2 e^{-g}) [g + b_o] \qquad [12]$$

It can be seen from Eq. [12] that E(q/RT) has a skewed Gaussian-like shape when K_1 is greater than 0. Even for K_1 approaching 0, E(q/RT) goes to zero as q approaches 0, since b_o is usually a very small quantity, i.e. ($b_o < 10^{-4}$) for most practical systems. Thus E(q/RT) has a skewed Gaussian-like shape for all values of K_1. The term E(q/RT) also approaches the Dirac-delta function in the limit as K_1 approaches infinity, representing an energetically homogeneous adsorbent. As an example, Figure 1 shows the shapes of E(g) according to Eq. [8] for $b_o = 10^{-4}$, $K_2 = -0.01$, and $K_1 = 10, 50, 100$. Figure 2 shows the corresponding E(q/RT) functions according to Eq. [12].

The overall isotherm can be obtained by using Eq. [1] as

$$Q = \int_o^\infty Q_\ell E(g)\, dg \qquad [13]$$

Equations [3], [4], [6], [8], and [10] may be substituted into Eq. [13] and then integrated to obtain the following analytic expression for the overall adsorption isotherm for a heterogeneous adsorbent:

$$Q(P,T) = A[1 - e^{-b_o P} (\frac{1}{1 - K_1 K_2}) (\frac{K_1}{P + K_1} - \frac{K_1 K_2}{P + 1})] \qquad [14]$$

It follows from Eq. [14] that

$$Q(P,T) = 0 \text{ when } P \to 0 \qquad [15]$$

and

$$Q(P,T) = A \text{ when } P \to \infty \qquad [16]$$

Also

$$\left[\frac{\partial Q}{\partial P}\right]_T = A\left[b_o + \frac{1 - K}{K_1 - K}\right] = K_\ell(T) \text{ when } P \to 0 \qquad [17]$$

where $K = K_1^2 K_2$. Equations [15] and [16] give the correct limits of an isotherm equation for a microporous adsorbent. Equation [17] shows that Eq. [14] reduces to the linear isotherm in the limit as P approaches zero, as required by the physics of adsorption thermodynamics. Equation [17] also shows that the model parameters are related to the Henry's law constant, K_ℓ.

Equation [14] gives the overall isotherm for a heterogeneous adsorbent for the case in which the local isotherm is described by the Jovanovic model and the surface energy distribution is given by Eq. [8]. Other energy distribution functions have been previously used but with the same local isotherm model used in this study (Misra, 1973; Sircar, 1984; Rudzinski and Jaroniec, 1974).

The local Jovanovic isotherm reduces to the following form as T approaches infinity:

$$Q_\ell = A[1 - \exp(-b_o P)] \qquad [18]$$

By substituting Eqs. [8], [10], and [18] into Eq. [13], it can be shown that the overall isotherm Q also has the same form as Eq. [18] in the limit when T becomes infinitely large. Ross and Oliver (1964) pointed out the existence of such homogeneous-like behavior of a heterogeneous adsorbent at high temperatures.

Since physical adsorption is an exothermic process, the Henry's law constant expressed here as Ab_o, becomes very small when T approaches infinity. Hence, b_o is usually very small ($b_o << 1$) as shown in Table 1. Consequently, $b_oP << 1$ in moderate pressure ranges, and Eqs. [14] and [17] can for all practical purposes be approximated as

$$Q(P,T) = A[1 - (\frac{1}{1 - K_1K_2}) (\frac{K_1}{P + K_1} - \frac{K_1K_2}{P + 1})] \qquad [19]$$

and

$$A[\frac{1 - K}{K_1 - K}] = K_\ell(T) \text{ when } P \to 0 \qquad [20]$$

where $K = K_1^2K_2$. The new adsorption isotherm given by Eq. [19] can be used to describe equilibrium adsorption data on heterogeneous adsorbents. The equation has three parameters viz. A, the saturation capacity and the two energy distribution parameters, K_1 and K_2. Furthermore, A, K_1, and K_2 are related to the Henry's law constant by Eq. [20]. Thus, there are actually only two adjustable parameters in the new adsorption isotherm if good low pressure isotherm data are available to define K_ℓ.

ISOSTERIC HEAT OF ADSORPTION

The isosteric heat of adsorption, q, for the heterogeneous adsorbent at an adsorbate loading Q can be obtained by using the thermodynamic relationship

$$\frac{q}{RT^2} = \left[\frac{\partial(\ell nP)}{\partial T}\right]_Q \qquad [21]$$

Thus, differentiating Eqs. [18] and [19] with respect to T at constant loading Q gives

$$\frac{q}{RT^2} = \frac{\frac{d}{dT}\{[1 - \frac{Q}{A}][1 - K_1K_2]\} + \frac{1}{P+1}\frac{d(K_1K_2)}{dT} - \frac{1}{P+K_1}\frac{dK_1}{dT}}{\frac{PK_1K_2}{(P+1)^2} - \frac{PK_1}{(P+K_1)^2}} \qquad [22]$$

TEST OF NEW ADSORPTION ISOTHERM

The applicability of the adsorption Eqs. [19] and [20] was evaluated using published experimental adsorption data for several systems. The data used for testing the model included adsorption data of methane and ethylene on BPL activated carbon obtained by Reich (1974) and carbon dioxide on BPL carbon and MSC V carbon obtained by Sircar (1981) over large ranges of pressure and temperature. These systems were chosen because the adsorbents were truly microporous and showed significantly varying degrees of affinity of adsorption on the carbons as indicated by the difference in the K_ℓ and b_o values given in Table I. The adsorption data also exhibited significant departure from the homogeneous Jovanovic behavior. According to the Jovanovic model shown

by Eq. [3], a plot of $\ell n(1 - \frac{Q}{A})$ versus pressure should yield a straight line with a slope equal to -b. A few examples of such plots using the isotherm data at 260.2K are shown in Figure 3. The A values used in the plots correspond to the apparent saturation levels of the isotherms at 260.2K. The nonlinearity of the plots demonstrate that the activated carbon is heterogeneous for these adsorbates. Therefore, more sophisticated isotherm models should be used to correlate the heterogeneous adsorption systems.

Equations [19] and [20] were then used to describe the isotherm data. A trial and error procedure was used to obtain the best fit parameters. The Henry's law constants were estimated from the initial slopes of the isotherms. A value of A was chosen and K_2 was calculated using Eq. [20] for different values of K_1. The entire isotherm was then generated using Eq. [19]. If the calculated isotherm was not within ±2% of the experimental data in the entire pressure range, a new value of A was chosen and the procedure repeated. The best fit model parameters are given in Table II.

Figures 4 - 7 show the experimental data (circles) and the best fit curves (dashed lines) by the proposed new heterogeneous isotherm model for various adsorption systems. The second model proposed by Sircar (1984) was also used to correlate the experimental data for comparison purposes, and these were denoted by the solid lines. It may be seen from the figures that the new heterogeneous model describes the isotherm data extremely well over large ranges of pressure and temperature for both carbons. The new heterogeneous model also provides better correlations of the experimental data than does Sircar's model as can be seen from the figures. The BPL activated carbon was a relatively large

pore carbon with approximately 60% of its pore volume consisting of pores below 30 Å in diameter, with the remaining pores being larger than 100 Å in diameter. The MSC V activation carbon had relatively smaller pores with most of the pore diameters falling in the 5 Å range. The system temperatures for CH_4 on BPL carbon and CO_2 on MSC V carbon are above their respective critical temperature ranges while isotherm data for C_2H_4 and CO_2 on BPL carbons were obtained at temperatures that were below their respective critical temperatures. Table II shows that A varied slightly over the large range of temperatures. The parameter K_1 was found to be a strong function of temperatures for all systems, and K_1 increased with increasing temperatures. The parameter K_2 also proved to be strongly temperature dependent and it also increased with increasing temperatures.

It may be noted from the above that the heterogeneous adsorption model derived by the assumption of a local Jovanovic isotherm and a Morse-type energy distribution function is capable of describing the adsorption characteristics of various gases and vapors on microporous adsorbents which exhibit significantly different affinities of adsorption. Previous studies by Sircar (1984) have shown that these isotherms could also be described by various combinations of Q(P,T,e) and E(e) functions. However, there are two limitations: (1) The local and overall isotherms must satisfy the key limiting properties imposed by the physics of adsorption thermodynamics and (2) only a few combinations will allow analytic integration of Eq. [1].

CONCLUSIONS

This study indicates that adsorbent heterogeneity plays an important role in determining the shape of any isotherm. Different adsorption systems will exhibit substantially different heterogeneity of adsorption which can not be predicted a priori. Experimental data is needed for each gas-solid system for estimation of adsorbent heterogeneity.

The new heterogeneous adsorption model developed in this work successfully describes experimental isotherms of various gases and vapors on different microporous adsorbents over a large range of temperatures and pressures. The practical usefulness of any overall isotherm model will obviously depend on its mathematical simplicity. The heterogeneous isotherm model developed in this work provides a useful tool for the correlation of isotherm data on heterogeneous surfaces because it is easy to use and it provides a more accurate description of experimental data than does other existing models of this type.

NOTATION

A	=	Saturation adsorption capacity
b	=	Jovanovic parameter defined by Eq. [4]
b_o	=	Limiting value of b at infinite temperature
e	=	Adsorption energy parameter
E	=	Energy distribution function
g	=	Energy parameter defined by Eq. [6]
K	=	$K_1^2 K_2$
K_o	=	Parameter in Morse type energy distribution function
K_1	=	Parameter in Morse type energy distribution function
K_2	=	Parameter in Morse type energy distribution function
K_ℓ	=	Local Henry's law constant
P	=	System pressure
Q	=	Overall adsorption isotherm
Q_ℓ	=	Local adsorption isotherm
q	=	Isosteric heat of adsorption
R	=	Universal gas constant
T	=	System temperature

LITERATURE CITED

Cerofolini, G. F., M. Jaroniec, and S. Sokolowski, "A Theoretical Isotherm for Adsorption on Heterogeneous Surface," J. Colloid and Polymer Sci., 256, 471 (1978).

Hill, T. L., An Introduction to Statistical Thermodynamics, Addison-Wesley, Reading, Mass. (1955).

House, W. A., and M. J. Jaycock, "A Numerical Algorithm for the Determination of the Adsorptive Energy Distribution Function from Isotherm Data," J. Colloid and Polymer Sci., 256, 52 (1978).

Jaroniec, M., "Adsorption on Heterogeneous Surfaces: The Exponential Equation for the Overall Adsorption Isotherm," Surface Sci., 50, 553 (1975).

Jaroniec, M., A. Patrykiejew, and M. Borowko, Progress in Surface and Membrane Science, Vol. 14, Academic Press, New York (1981).

Jovanovic, D. S., "Physical Adsorption of Gases I: Isotherms for Monolayer and Multilayer Adsorption," Kolloid-Z. Z. Polym., 235, 1203 (1969).

Misra, D. N., "Jovanovich Adsorption Isotherm for Heterogeneous Surfaces," J. Colloid Interface Sci., 43, 85 (1973).

Misra, D. N., "New Adsorption Isotherm for Heterogeneous Surfaces," J. Chem. Phys., 52, 5499 (1970).

Misra, D. N., "Adsorption on Heterogeneous Surfaces: A Dubinin-Radushkevich Equation," Surface Sci., 18, 367 (1969).

Morse, P. M., "Diatomic Molecules According to the Wave Mechanics II. Vibrational Levels," Phys. Rev., 34, 57 (1929).

Ponec, V., Z. Knor, and S. Cerry, Adsorption on Solids, CRC Press, Ohio (1974).

Reich, R., Ph.D. Dissertation, Georgia Institute of Technology, Georgia (1974).

Ross, S., and I. D. Morrison, "Computed Adsorptive-Energy Distribution in the Monolayer (Cademon)," Surface Sci., 52, 103 (1975).

Ross, S., and J. P. Oliver, On Physical Adsorption, Wiley, New York (1964).

Rudzinski, W., and M. Jaroniec, "Adsorption on Heterogeneous Surfaces: A New Method for Evaluating the Energy Distribution Function," Surface Science, 42, 552 (1974).

Sing, K. S. W., Adsorption at the Gas/Solid Surface: Colloid Science I, Bertholomew Press, Dorking (1973).

Sips, R., "On the Structure of a Catalyst Surface, II," J. Chem. Phys., 18, 1024 (1950).

Sircar, S., "Effect of Local Isotherm on Adsorbent Heterogeneity," J. Colloid and Interface Sci., 101, 452 (1984).

Sircar, S., "New Adsorption Isotherm for Energetically Heterogeneous Adsorbents," J. Colloid and Interface Sci., 98, 306 (1984).

Sircar, S., "Sorption of Carbon Dioxide on Activated Carbons: Effect of the Heat of Sorption During Kinetic Measurements," Carbon, 19, 153 (1981).

Sircar, S., and Gupta R., "A Semi-Empirical Adsorption Equation for Single Component Gas-Solid Equilibria," AIChE J., 27, 806 (1981).

LIST OF TABLES

TABLE I

Henry's Law Constants for the Systems Investigated

Adsorption System	T(^{o}K)	K_{ℓ} (mmol/g psia)	b_o(psia^{-1})
CH_4 on BPL carbon	212.7	0.60969	
	260.2	0.12861	9.25×10^{-6}
	301.4	0.04219	
C_2H_4 on BPL carbon	212.7	1.8240	
	260.2	1.6501	-
	301.4	0.4069	
CO_2 on BPL carbon	212.7	4.0870	2.26×10^{-6}
	260.2	0.40215	
	301.4	0.11023	
CO_2 on MSC V carbon	303.1	0.41032	4.56×10^{-8}
	339.8	0.08914	

TABLE II

Best Fit Model Parameters

System	T(^{o}K)	A (mmol/g)	K_1 (psia)	$-K_2$ (psia^{-1})
CH_4 ON BPL carbon	301.4	6.00	200.0	0.00001
	260.2	6.70	85.0	0.00009
	212.7	7.70	32.0	0.00163
C_2H_4 on BPL carbon	301.4	5.90	30.0	0.00128
	260.2	6.80	17.0	0.00428
	212.7	8.20	6.0	0.01195
CO_2 on BPL carbon	301.4	8.80	107.0	0.00003
	260.2	10.40	42.0	0.00037
	212.7	10.80	40.0	0.01418
CO_2 on MSC V carbon	339.8	3.30	63.8	0.00424
	303.1	3.75	0.145	1156.09

LIST OF FIGURES

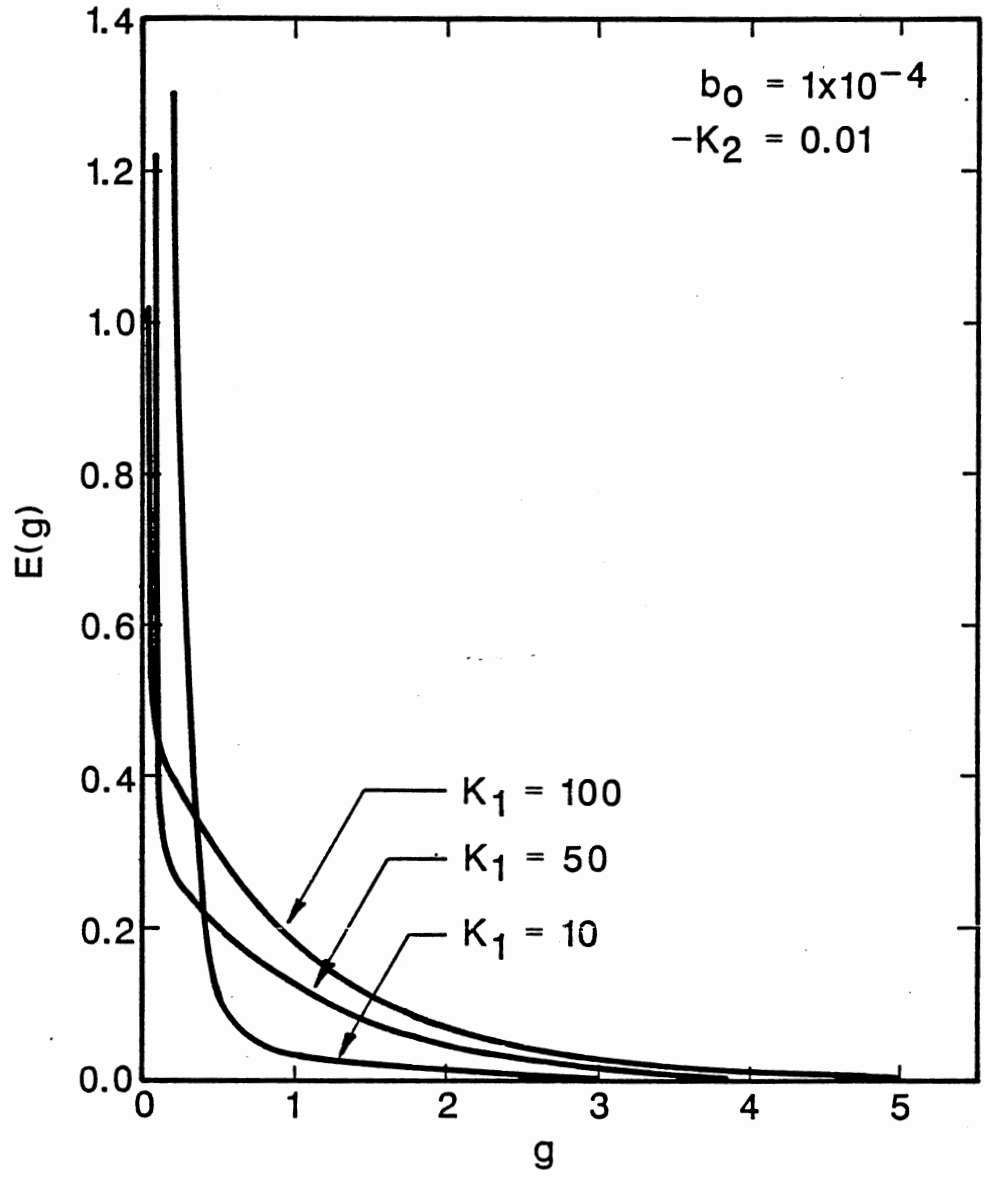

Figure 1. Plots of Energy Distribution Function for Different K_1 in g Domain.

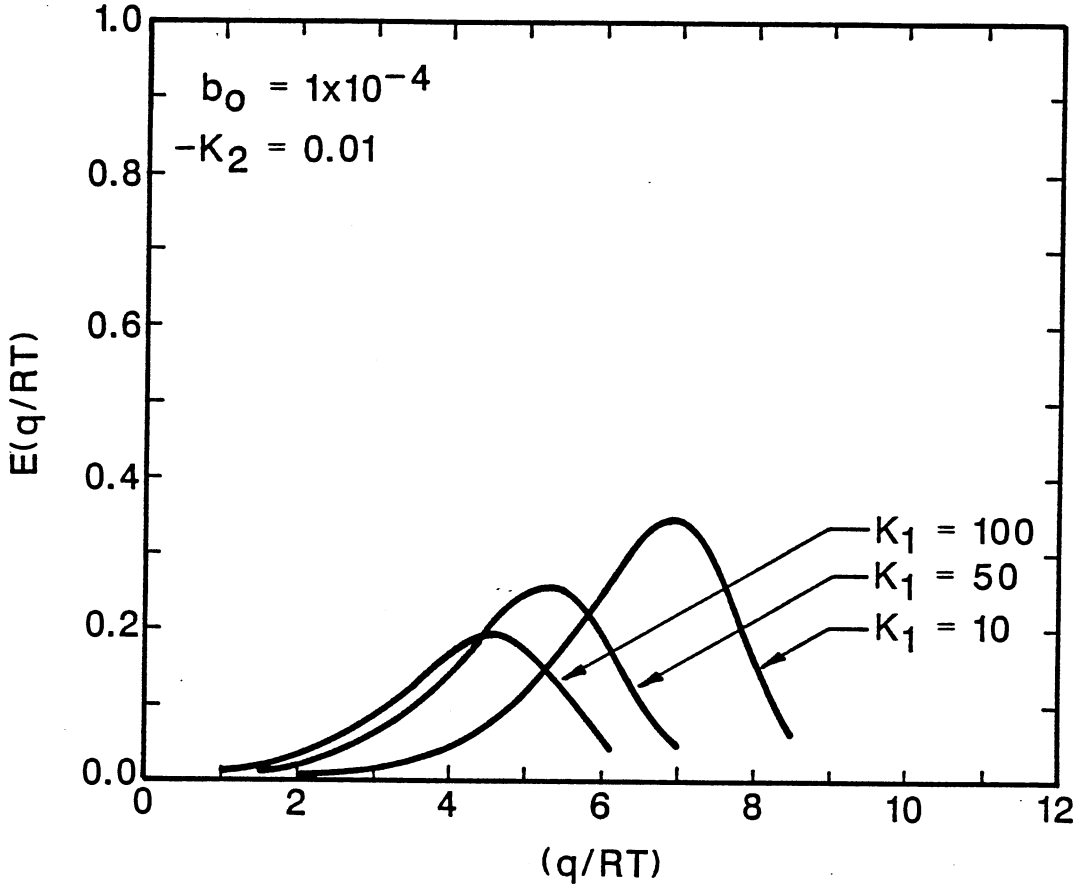

Figure 2. Plots of Probability Functions for Different K_1 in q/RT Domain.

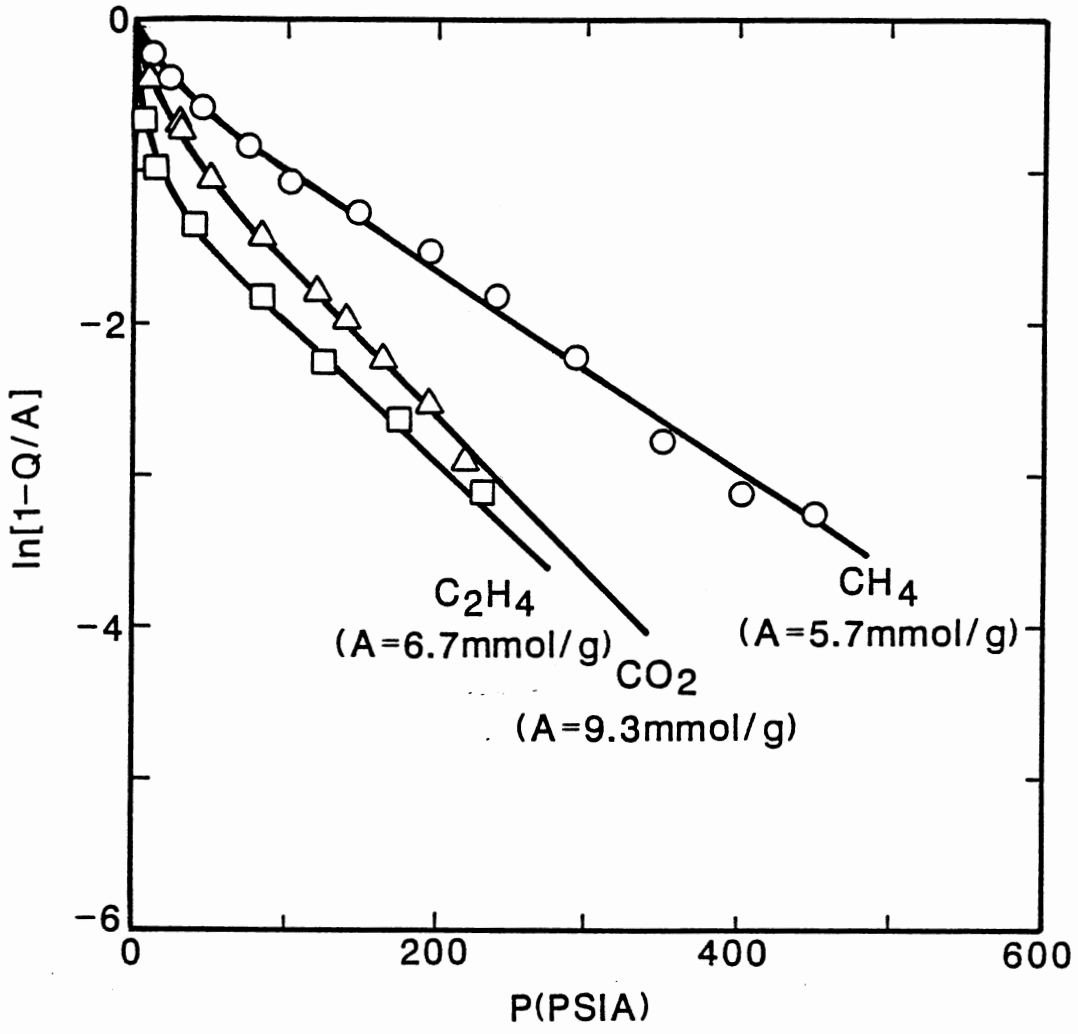

Figure 3. Linearized Jovanovic Plots for Various Gases Adsorbed on BPL Carbon at 260.2 K.

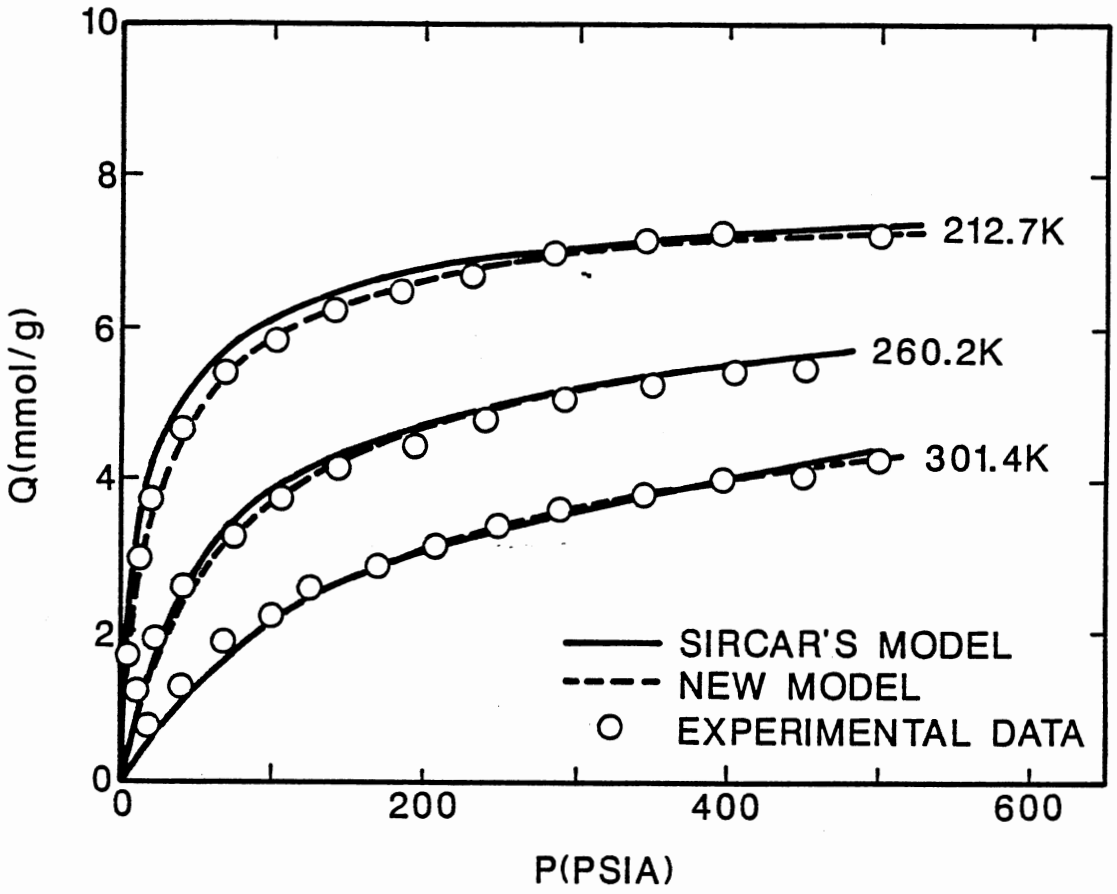

Figure 4. Adsorption of Methane on BPL Carbon.

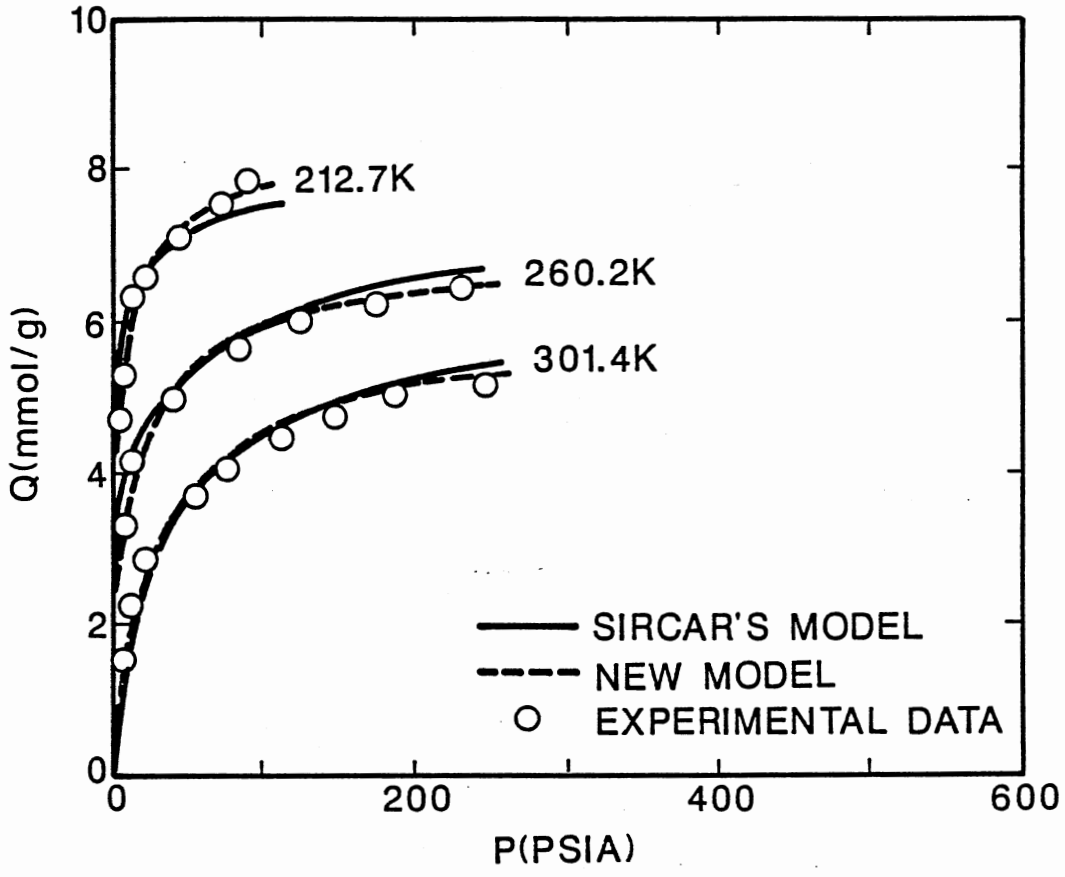

Figure 5. Adsorption of Ethylene on BPL Carbon.

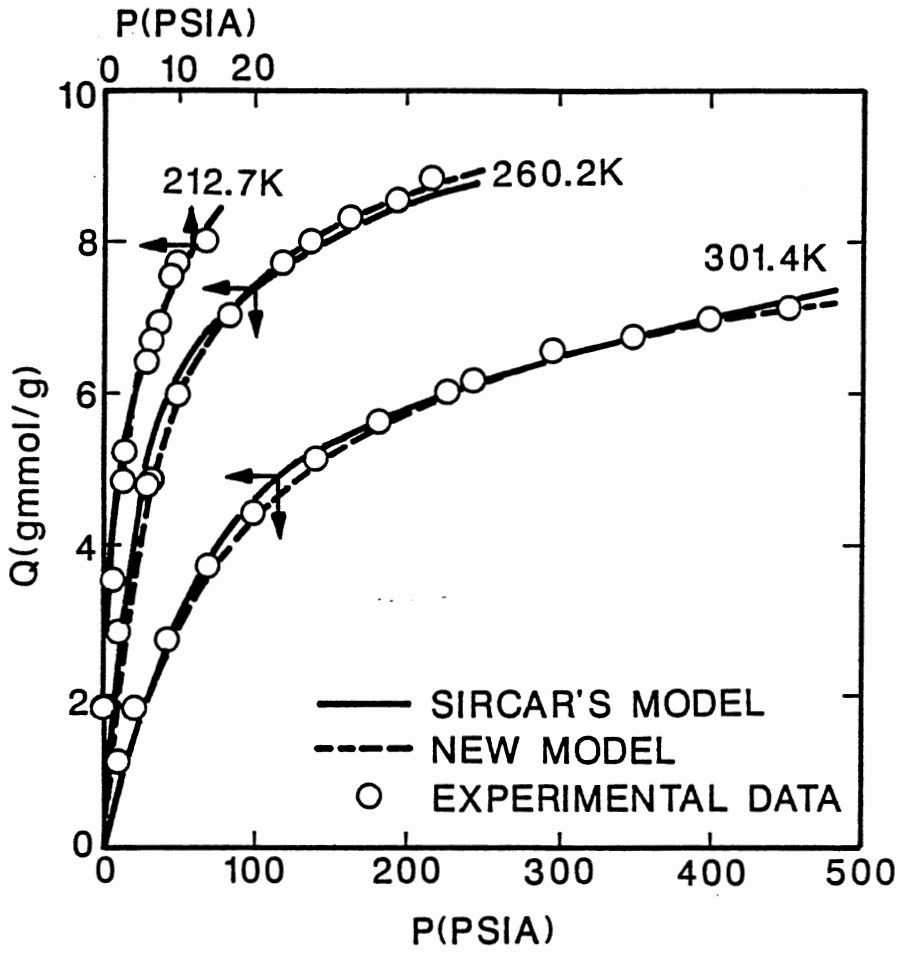

Figure 6. Adsorption of Carbon Dioxide on BPL Carbon.

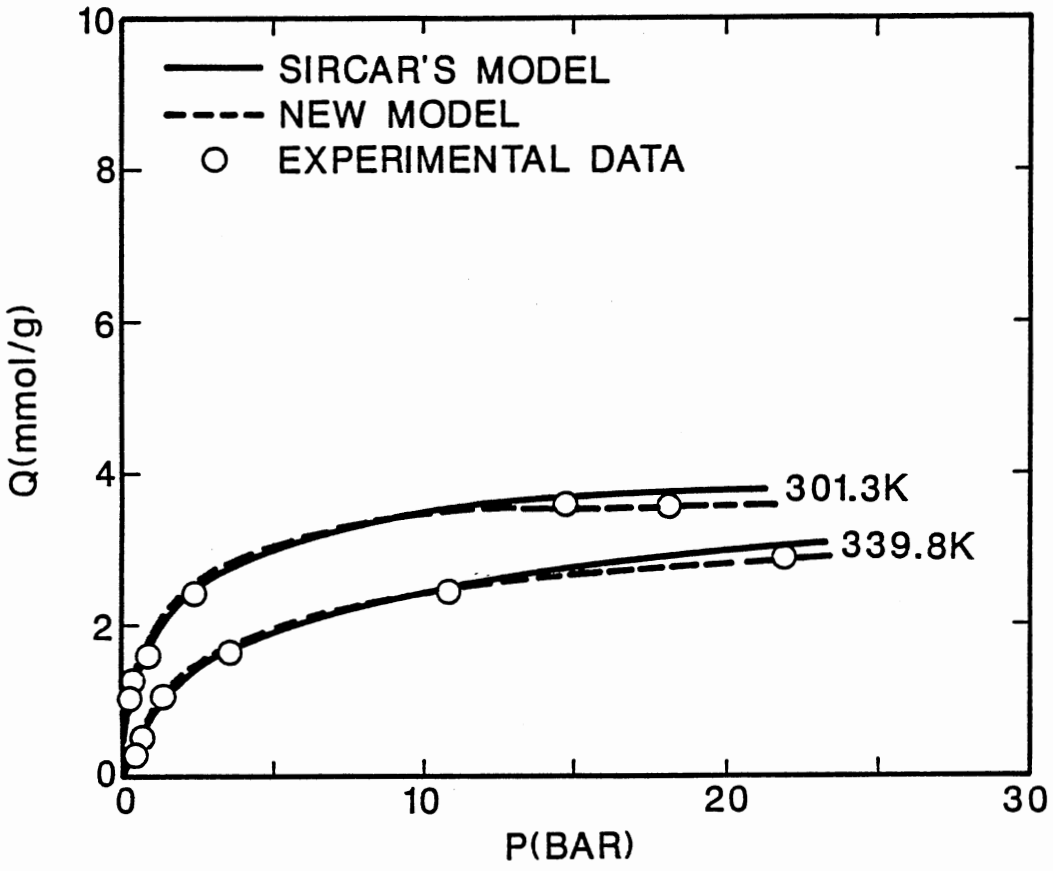

Figure 7. Adsorption of Carbon Dioxide on MSCV Carbon.

CHAPTER IV

APPLICATION OF A NEW HETEROGENEOUS ISOTHERM MODEL TO PREDICT THE ADSORPTION OF CHLORINATED HYDROCARBONS ON SILICA GEL

APPLICATION OF A NEW HETEROGENEOUS ISOTHERM MODEL TO PREDICT THE ADSORPTION OF CHLORINATED HYDROCARBONS ON SILICA GEL

Shing-Lin Kuo and Anthony L. Hines*

School of Chemical Engineering
Oklahoma State University
Stillwater, Oklahoma 74078

*To whom correspondence should be directed.

ABSTRACT

Adsorption studies of the homologous series chloromethane, dichloromethane, trichloromethane, and tetrachloromethane on silica gel were carried out at 288, 293, and 298K.

Experimental data were compared with the calculated equilibrium uptake as predicted by the Langmuir and the BET models as well as the Kuo and Hines isotherm model for heterogeneous systems. It was found that Kuo and Hines isotherm model provided the best correlation of the experimental data. The Langmuir model provided better correlations for the isotherm data for the heavier adsorbates than for lighter ones, while the BET model provided good correlations to the isotherm data only up to 35 percent saturation pressure for each adsorbate.

APPLICATION OF A NEW HETEROGENEOUS ISOTHERM MODEL TO PREDICT THE ADSORPTION OF CHLORINATED HYDROCARBONS ON SILICA GEL

INTRODUCTION

Indoor air pollution has drawn considerable attention from researchers in recent years (1,2,3). The high indoor/outdoor pollutant concentration ratio has made scientists believe that indoor air is often dirtier than that found outdoors, and the indoor air pollutants are the primary sources of many family diseases. Of all the indoor air pollutants, dichloromethane and trichloromethane are considered to be two of the most dangerous. Dichloromethane often comes into the home in the form of paint strippers and is considered to pose the highest cancer risk of any household chemical (1). Trichloromethane is introduced into the home with chlorine-treated water in hot showers and is also considered to be one of the leading causes of cancer. Chloromethane and tetrachloromethane are also thought to be responsible for many respiratory symptoms, although they are not present in large amounts as compared to the other household chemicals. Although the effects of indoor air pollutants on human health have been studied extensively, relatively few studies have been made in which the pollutants were removed from the air.

In this study, the adsorption of chloromethane, dichloromethane, trichloromethane, and tetrachloromethane on silica gel were measured gravimetrically at three different temperatures. The adsorption isotherm data were correlated using the Langmuir and the BET models as well as the new heterogeneous adsorption model developed in a previous study by Kuo and Hines (4).

EXPERIMENTAL SECTION

Materials and Apparatus. The silica gel used in this study was type PA 40, 80 - 100 mesh supplied by Davison Chemical Co. The chlorinated hydrocarbons consisted of the homologous series chloromethane, dichloromethane, trichloromethane, and tetrachloromethane. The chloromethane was obtained from Union Carbide and had a minimum purity of 99.5%. The dichloromethane, trichloromethane, and tetrachloromethane were obtained from Fisher Scientific Co. with purities of 99.9%, 99.9% and 99.5%, respectively.

The experimental adsorption studies were carried out gravimetrically using a Cahn R-2000 electrobalance which has a sensitivity of 0.1 micrograms. The adsorption apparatus was housed in a vacuum bottle assembly and was designed such that either gases or vapors could be studied. The assembly was equipped with two sample hangdown tubes surrounded by a cylindrical shell through which water could flow to keep the balance temperature relatively constant during sample regeneration and during the adsorption study. The system was designed such that a sample weight of 3.5 grams could be tested. The sample weight was monitored with a strip chart recorder connected to the electrobalance control unit. A refrigerated-heated bath and circulator with a temperature control of ± 0.1K was used to control the adsorption temperature. A special vapor supply flask was used to introduce the liquid adsorbates into the system. A vacuum system which consisted of two vacuum pumps, a sorption trap, and a diffusion pump were used to obtain a vacuum of 1×10^{-4} mmHg for the adsorption system during regeneration. The leak rate of the complete system was approximately 0.05 mmHg/h. Two thermistor gauges were used to monitor the pressure

when the system was being evacuated and during the adsorption runs. Pressures up to 760 mmHg were measured with a Wallace and Tiernan absolute pressure gauge with an accuracy of ± 0.02 mmHg. The error of the weight measurement was estimated to be ± 10 μg.

Procedure. The electrobalance was calibrated to agree with the output signal of the strip chart recorder. The weight changes of the silica gel due to adsorption were detected by the electrobalance. The adsorbent was regenerated by evacuating the system and applying heat at 423K to the sample hangdown tube. Heating was continued until a constant sample weight was obtained. This typically required from 4 to 10h. After regeneration, the adsorbent was cooled to the adsorption temperature and the adsorbate was introduced into the system. After equilibrium was reached, as indicated by a constant sample weight, the pressure and weight were recorded. Equilibrium adsorption data were collected from very low pressures up to saturation. Following adsorption, desorption measurements were made by reducing the system pressure.

Bouyancy tests were conducted to determine the effects of the gas on the weight readings other than from the effect of actual gas adsorption. This procedure was exactly like the one used in collecting data, except that glass beads were placed in the sample pan rather than the adsorbent. The maximum error introduced by the buoyancy effect upon the measured adsorbed weight was estimated to be less than 0.5% for each adsorbate.

RESULTS AND DISCUSSION

Equilibrium Data. Adsorption isotherms were obtained for chloromethane, dichloromethane, trichloromethane, and tetrachloromethane on silica gel at 288, 293, and 298K after overnight regeneration of the adsorbent at 423K in vacuo. The experimental equilibrium data are presented in Table I. The weight of the sample was measured to within 10 μg. Since the regenerated sample weight was 0.2137g, the error in weight measurement was 0.005%. Pressure was measured with an accuracy of ± 0.15 mmHg. Except for the lowest pressures, the maximum error in pressure measurements was less than 0.3%. The average error over the entire adsorption range was estimated to be less than 1%. Several of the data points were reproduced with an error no greater than 1%.

The adsorption data for all four chemicals on silica gel were Type I according to the Brunauer classification (5) and showed no apparent hysteresis when desorbing. The absence of capillary condensation, as shown by the equilibrium data, indicates that the silica gel contains mostly micropores. For the homologous series, the amount of adsorbate removed by the silica gel increased as the molecular weight of the adsorbate increased as shown in Table I. The fact that the maximum uptake of each adsorbate by the silica gel was in the range of 0.395-0.435g adsorbate/g silica gel suggests that silica gel is an effective adsorbent for removing any of the chlorinated hydrocarbons found in this homologous series. The maximum uptake of each adsorbate was also plotted with respect to the molar volume of each adsorbate as shown in Figure 1. It can be seen from the figure that the maximum adsorption capacities for the homologous series fall on a single curve for each temperature. This suggests that the maximum capacity curve may

be used to predict the maximum uptake of other compounds in the homologous series.

The isosteric heats of adsorption were calculated at constant adsorbent loading from the relationship

$$\Delta H_s = R\left[\frac{\partial(\ell nP)}{\partial(1/T)}\right]_N \qquad [1]$$

The heterogeneity of the adsorbent surface is usually caused by the differences among the adsorptive strength of the sites. The heterogeneity of the adsorption system can be detected from the shape of the adsorption isotherms and is usually evaluated by comparing the isosteric heats of adsorption at different loadings. As can be seen from Table II, the isosteric heats of adsorption in the beginning of the adsorption process exhibit the commonly observed trend of a decreasing amount of heat being given off as the loading on the surface is increased. This is due to pore filling in that the more active sites will adsorb gas molecule first. As the adsorption proceeds, most of the more active sites will be filled with the adsorbed molecules and the remaining less active sites will give off less amount of heat due to less amount of adsorption. However, the heats of adsorption remains practically constant after certain surface loading, which is considered to be near monolayer coverage, is reached. The fact that the heats of adsorption remains constant at different loadings indicates that the surface of the adsorbent is homogeneous. Since the heats of adsorption shown in Table II are of the same order of magnitude as the heats of condensation, it may be concluded that the adsorption of the chlorinated hydrocarbons is primarily the result of physical forces.

The heats of adsorption data for chlorinated hydrocarbons on PA 40 silica gels were also compared to that for the adsorption of water on the same material. The heats of adsorption for water adsorbed on PA 40 silica gels at 8 different loadings ranging from 0.11 to 0.25 gH_2O/g solid were investigated by Rojas (6) and were found to be in the range of 11.14 to 11.42 kcal/gmol. The study of this work confirms the work of Rojas in that PA 40 silica gels consists of homogeneous surface.

Data Correlation. The Langmuir model (7-9) was used to correlate the equilibrium data. The Langmuir equation, which can be derived by using statistical thermodynamics or kinetic considerations, has the form

$$N_{\ell} = \frac{maP}{1 + aP} \qquad [2]$$

where N_{ℓ} is the equilibrium uptake, P is the pressure, m is a characteristic constant defined as the amount of adsorption which would saturate the unit surface with a monolayer, and the term a is a characteristic constant often defined as the "capillarity" of the substances. When Eq. [2] was used to correlate the adsorption data by applying a regressional analysis technique, it was found that the Langmuir model did not successfully correlate the adsorption data for the lighter chlorinated hydrocarbons. However, the Langmuir model provided better correlations for the equilibrium isotherm data for the higher molecular weight chlorinated hydrocarbons.

The BET isotherm (10) was also used to correlate the adsorption isotherm data. The BET model, which was obtained by extending the Langmuir isotherm to apply to multilayer adsorption, has the form

$$\frac{P}{N_{\ell}(P_s-P)} = \frac{1}{CN_m} + \frac{(C-1)}{CN_m}\frac{P}{P_s} \qquad [3]$$

where P_s is the saturation or vapor pressure, C is a constant for the particular adsorption system, N_{ℓ} is the uptake, and N_m is the monolayer adsorption capacity. If $P/[(P_s - P)N_{\ell}]$ is plotted versus P/P_s, a straight line should be obtained over the region in which the BET equation holds. This line will have a slope of $(C-1)/(CN_m)$ and an intercept of $1/(CN_m)$. When such plots were made, it was found that the BET model correlated the experiment data successfully only for the region $P/P_s \leq 0.35$ for each of the chlorinated hydrocarbons. This is not surprising considering that the BET model satisfies the Henry's law requirement in the low pressure region and it holds primarily for Types II and III isotherms. Since the BET model holds for the low pressure region, it was used to obtain the monolayer coverage and the surface area occupied by the molecules. The results are shown in Table III. As can be seen from the table and the equilibrium data, multilayer coverage occured for all of the chlorinated hydrocarbons on silica gels. The calculated surface area occupied by one molecule of the chlorinated hydrocarbons was found to be in the range of $2.55 - 7.96 \times 10^{-19}$ m^2/molecule.

For a large class of solid-vapor systems the heterogeneous structure of the adsorbent phase plays an important role in the process of physical adsorption. The traditional one-parameter models frequently fail in describing the adsorption behavior on microporous adsorbents. Most of the traditional isotherm models do not even conform to the basic constraints imposed by the physics of adsorption thermodynamics (11). The popular approach for the adsorption on a heterogeneous surface is to

assume that the heterogeneous adsorbent consists of a distribution of energetically distinct sites and the overall adsorption isotherm can be obtained by the integration of the contributions of each site (12). This can be expressed as

$$N(P,T) = \int_0^\infty N_\ell(P,T,g) \quad E(g)dg \qquad [4]$$

where $N(P,T)$ is the overall adsorption isotherm on the heterogeneous adsorbent, $N_\ell(P,T,g)$ describes a specific adsorption isotherm for homogeneous sites of adsorptive energy g, and $E(g)$ is the site energy distribution for g.

Several combinations of local isotherm equations for $N_\ell(P,T,g)$ and energy distribution functions for $E(g)$ have been used to derive analytical expressions for $N(P,T)$ (4,13,14). The most versatile isotherm that can be used to describe the adsorption behaviors on heterogeneous surfaces is probably the one derived by Kuo and Hines (4) in a previous study (4). In that work, it was assumed that the local isotherm for homogeneous sites can be described by Jovanovic model (15) as

$$N_\ell(P,T,g) = m[1 - e^{-bP}] \qquad [5]$$

with the energy distribution function being represented by a Morse-type probability density function (16) given by

$$E(g) = \frac{K_1}{1 - K_1K_2} [e^{-K_1g} - K_2e^{-g}] \qquad [6]$$

In Eqs. [5] and [6], m is the saturation adsorption capacity, K_1 and K_2 are parameters in the energy distribution function, and b is the Jovanovic parameter which can be related to the heat of adsorption by

$$b = b_o \exp(-\Delta H_s/RT) \qquad [7]$$

The resulting overall adsorption isotherm for adsorption on a heterogeneous adsorbent is

$$N(P,T) = m[1 - (\frac{1}{1 - K_1K_2})(\frac{K_1}{P + K_1} - \frac{K_1K_2}{P + 1})] \qquad [8]$$

where m, K_1 and K_2 are related to the Henry's law constant, K_ℓ, by

$$m[\frac{1 - K_1^2K_2}{K_1 - K_1^2K_2}] = K_\ell \quad \text{as} \quad P \to 0 \qquad [9]$$

In deriving Eqs. [8] and [9] Kuo and Hines (4) neglected the b_o contribution to the overall isotherm equation, since b_o is usually very small ($b_o << 1$) for most systems.

Equations [8] and [9] were used to correlate the adsorption data for chloromethane, dichloromethane, trichloromethane and tetrachloromethane on silica gel. The adsorbates showed varying degrees of affinity of adsorption on the silica gel as indicated by the differences in the Henry's law constants and b_o values given in Table IV. According to the Jovanovic model, a plot of $\ell n(1 - \frac{N}{m})$ versus pressure should

yield a straight line with a slope equal to -b. A few examples of such plots for the systems studied using the isotherm data at 288K are shown in Figure 2. The nonlinearity of the plots indicated that a more sophisticated isotherm model would be necessary to correlate the adsorption isotherm data. Equations [8] and [9] were then used by employing a trial and error procedure to obtain the best fit parameters. The Henry's law constants were estimated from the initial slopes of the isotherms. A value of m was chosen and K_2 was calculated using Eq. [9] for different value of K_1. The entire isotherm was then generated using Eq. [8]. If the calculated isotherm was not within ± 2% of the experimental data over the entire pressure range, a new value of m was chosen and the procedure repeated. The best fit model parameters are given in Table V.

Figures 3 - 6 show the experimental data and the best fit curves obtained from Eqs. [8] and [9] for chloromethane, dichloromethane, trichloromethane, and tetrachloromethane on silica gel. As shown in the figures, the heterogeneous isotherms obtained by using the Kuo and Hines model describes the isotherm data extremely well over the entire range of pressure and temperature.

The energy probability density function $E(\Delta H_s/RT)$ may be obtained by defining the energy parameter $g = b_o[\exp(\Delta H_s/RT) - 1]$ and combining it with Eqs. [6] and [7] to give

$$E(\Delta H_s/RT) = \frac{K_1}{1 - K_1K_2} [e^{-K_1 g} - K_2 e^{-g}] [g + b_o] \qquad [10]$$

Figure 7 shows graphs of $E(\Delta H_s/RT)$ versus $\Delta H_s/RT$ for all of the systems at 288K. As noted in the figure, Eq. [10] gives skewed Gaussian-like energy distribution functions, which are characteristic of the Morse-type probability density function. Since the distributed E functions for all the systems are very similar as shown in Figure 7, it may be concluded that silica gel exhibits the same degree of heterogeneity for all of the chlorinated hydrocarbons in the homologeous series.

Comparisons of the experimental equilibrium data correlations using different isotherm models can be made by calculating the average absolute percent deviation over the entire pressure range for each adsorption system. the adsorption isotherm data for the chlorinated hydrocarbons on silica gel at three temperatures were correlated by using the Langmuir, BET, and Kuo and Hines models, and the results of the average absolute percent deviation predicted by each model are shown in Table VI. As can be seen from the table, the Kuo and Hines model provided the best correlation for the experimental isotherm data. The Langmuir model provided better correlations for the isotherm data for the heavier adsorbates than for the lighter ones, while the BET model gave the worst correlations for all of the chlorinated hydrocarbons. This is not surprising when considering that the BET model only holds for pressure up to 35% saturation of the chlorinated hydrocarbons.

CONCLUSIONS

The adsorption of the homologous series chloromethane, dichloromethane, trichloromethane, and tetrachloromethane was investigated using silica gel as the adsorbent. The adsorption isotherms of the four chlorinated hydrocarbons on silica gel were

determined gravimetrically at 288, 293, and 298K and pressures up to saturation. The maximum adsorption capacities for the homologous series fell on a single curve for each temperature, which suggests that the maximum capacity curve may be used to predict the maximum uptake of other compounds in the homologous series. On the basis of this study, it was concluded that silica gel can be effectively used to adsorb many chlorinated hydrocarbons.

The isotherm data for the adsorption of the four chlorinated hydrocarbons on silica gel were correlated by using the Kuo and Hines adsorption isotherm model as well as the Langmuir and the BET models. It was found that the Kuo and Hines model provided the best correlation for the experimental isotherm data. The Langmuir model provided better correlations for the isotherm data for the heavier adsorbates than for lighter ones, while the BET model provides good correlations for the isotherm data only up to 35% saturation pressure for each of the chlorinated hydrocarbons.

NOTATION

A	=	Surface area of a molecule
a	=	Langmuir parameter defined in Eq. [2]
b	=	Jovanovic parameter defined in Eq. [5]
b_o	=	Limiting value of b at infinite temperature
C	=	BET constant defined in Eq. [3]
E	=	Energy distribution function
g	=	Adsorption energy parameter
ΔH_c	=	Heat of condensation
ΔH_s	=	Isosteric heat of adsorption
K_1	=	Parameter in Morse-type energy distribution function
K_2	=	Parameter in Morse-type energy distribution function
K_ℓ	=	Henry's law constant
m	=	Saturation adsorption capacity
N	=	Overall adsorption isotherm
N_ℓ	=	Local adsorption isotherm
N_m	=	Monolayer adsorption capacity
P	=	System pressure
P_s	=	Saturation pressure
R	=	Universal gas constant
T	=	System temperature

LITERATURE CITED

1. Consumer Reports, October, 60 (1985).

2. U. S. News and World Report, September, 71 (1985).

3. S. L. Kuo and A. L. Hines, "Adsorption of Chlorinated Hydrocarbon Pollutants on Silica Gel," submitted for review, 1987.

4. S. L. Kuo and A. L. Hines, "New Theoretical Isotherm for Adsorption on Heterogeneous Adsorbents," submitted for review, 1987.

5. S. Brunauer, The Adsorption of Gases and Vapors, Vol. 1, Princeton University Press, Princeton, New Jersey (1945).

6. F. J. Rojas V. , M.S. Thesis, Colorado School of Mines, Colorado (1981).

7. I. Langmuir, J. Am. Chem. Soc., 38, 2221 (1916).

8. I. Langmuir, J. Am. Chem. Soc., 39, 1848 (1917).

9. I. Langmuir, J. Am. Chem. Soc., 40, 1361 (1918).

10. S. Brunauer, P. H. Emmett, and E. Teller, J. Am. Chem. Soc., 60, 309 (1938).

11. S. Sircar and R. Gupta, AIChE J., 27, 806 (1981).

12. S. Ross and J. P. Oliver, On Physical Adsorption, Wiley, New York, 1964.

13. S. Sircar, J. Colloid and Interface Sci., 98, 306 (1984).

14. S. Sircar, J. Colloid and Interface Sci., 101, 452 (1984).

15. D. S. Jovanovic, Kolloid-Z. Z., Polym. 235, 1203 (1968).

16. P. M. Morse, Phys. Rev., 34, 57 (1929).

LIST OF TABLES

TABLE I

Adsorption Isotherm Data for Chlorinated Hydrocarbons on Silica Gel

Adsorbate	288°K		293°K		298°K	
	P,mmHg	N,mmol/g	P,mmHg	N,mmol/g	P,mmHg	N,mmol/g
Chloromethane	31.1	1.155	4.1	0.407	3.2	0.356
	105.8	2.504	40.0	1.142	45.8	1.109
	189.4	3.433	96.3	2.083	93.8	1.826
	259.2	3.954	161.1	2.886	139.6	2.366
	350.0	4.406	234.5	3.480	190.7	2.865
	445.1	4.755	310.0	3.941	249.6	2.332
	531.8	5.004	375.8	4.255	304.1	3.601
	615.2	5.174	457.9	4.526	354.5	3.839
	700.0	5.329	512.7	4.725	409.6	4.056
	559.4	5.066	603.0	4.906	464.4	4.253
	382.5	4.535	674.0	5.049	516.0	4.401
	220.0	3.676	572.7	4.836	562.0	4.526
	62.4	1.803	401.6	4.333	609.8	4.632
	6.4	0.534	285.7	3.811	670.0	4.736
			130.8	2.549	720.0	4.826
			12.2	1.023	547.8	4.483
					428.0	4.126
					227.5	3.151
					122.2	2.182
					22.4	0.656
Dichloromethane	3.0	0.961	2.8	0.785	2.5	0.671
	6.4	1.374	8.9	1.384	8.4	1.219
	14.9	2.045	17.7	1.890	19.3	1.746
	23.7	2.489	29.2	2.438	32.0	2.210
	36.8	3.057	42.2	2.892	50.3	2.727
	49.8	3.491	55.0	3.274	70.5	3.202
	63.9	3.873	68.9	3.594	94.2	3.666
	78.2	4.143	83.7	3.904	110.2	3.914
	95.4	4.400	98.7	4.173	128.0	4.183
	108.8	4.513	114.0	4.389	148.4	4.359
	122.3	4.606	128.8	4.482	169.0	4.462
	140.4	4.709	146.7	4.565	189.7	4.513
	158.6	4.751	163.2	4.617	240.2	4.565
	208.7	4.854	193.3	4.668	315.6	4.637
			233.3	4.709		

TABLE I (Continued)

Adsorbate	288°K		293°K		298°K	
	P,mmHg	N,mmol/g	P,mmHg	N,mmol/g	P,mmHg	N,mmol/g
Trichloromethane	1.4	0.976	1.6	0.899	1.5	0.779
	6.3	1.764	3.1	1.205	6.1	1.367
	12.2	2.271	8.7	1.793	13.7	1.955
	19.8	2.704	16.7	2.373	23.0	2.410
	29.1	2.998	25.6	2.734	32.2	2.719
	39.3	3.248	37.8	3.101	51.4	3.138
	50.0	3.380	49.9	3.270	64.4	3.255
	60.2	3.439	63.8	3.365	82.1	3.329
	71.4	3.468	74.2	3.395	107.2	3.351
	87.3	3.498	89.7	3.410	150.3	3.373
	105.9	3.519	114.1	3.432		
Tetrachloromethane	0.8	0.656	0.5	0.399	0.6	0.405
	2.0	0.947	1.1	0.604	1.2	0.559
	4.7	1.483	3.2	0.987	4.1	1.038
	9.2	1.982	7.2	1.653	7.8	1.552
	14.7	2.282	11.6	2.013	12.0	1.825
	20.2	2.435	18.2	2.252	15.8	2.025
	25.4	2.566	25.7	2.446	20.8	2.188
	31.0	2.651	33.5	2.578	27.4	2.336
	40.2	2.754	43.5	2.664	35.0	2.455
	49.3	2.809	53.5	2.706	43.5	2.526
	56.9	2.811	71.3	2.743	55.1	2.593
					69.2	2.666
					82.7	2.680

TABLE II

Variation of Isosteric Heats of Adsorption with the Amount Adsorbed

Adsorbate	Amount Adsorbed mmol/g solid	$-\Delta H_s$ kcal/gmol	ΔH_c kcal/gmol
CH_3Cl	2.0	6.36	4.85-5.05
	2.5	6.38	
	3.0	6.43	
	3.5	6.41	
	4.0	6.46	
	4.5	6.48	
CH_2Cl_2	2.0	10.31	6.89-7.05
	2.5	9.48	
	3.0	9.44	
	3.5	9.14	
	4.0	8.70	
	4.5	9.26	
$CHCl_3$	1.4	11.20	7.53-7.77
	1.8	9.40	
	2.2	8.75	
	2.6	8.15	
	3.0	8.05	
	3.3	8.27	
CCl_4	0.9	10.34	7.39-7.70
	1.2	8.79	
	1.5	7.83	
	1.8	7.98	
	2.1	8.08	
	2.4	8.43	

TABLE III

Monolayer Coverages and Area per Molecule Calculated by Using BET Model

Adsorbate	T(°K)	Area Per Molecule $Ax10^{19}(m^2/Molecule)$	Surface Coverage m^2/g solid	Monolayer Coverage N_m(mmol/g)
CH_3Cl	288	2.55	739.9	4.82
	293	2.64	739.0	4.65
	298	2.68	738.9	4.58
CH_2Cl_2	288	4.73	740.3	2.60
	293	4.79	741.1	2.57
	298	4.88	740.3	2.52
$CHCl_3$	288	5.61	739.6	2.19
	293	5.67	740.7	2.17
	298	5.75	740.8	2.14
CCl_4	288	7.74	740.9	1.59
	293	7.84	741.0	1.57
	298	7.96	738.0	1.54

TABLE IV

Henry's Law Constants for the Systems Investigated

Adsorption System	T(°K)	K_ℓ (mmol/g.atm)	b_o (atm^{-1})
CH_3Cl - Silica Gel	288	211	$1x10^{-5}$
	293	178	
	298	128	
CH_2Cl_2 - Silica Gel	288	315	$8x10^{-6}$
	293	257	
	298	244	
$CHCl_3$ - Silica Gel	288	620	$4x10^{-6}$
	293	570	
	298	467	
CCl_4 - Silica Gel	288	860	$1x10^{-6}$
	293	758	
	298	673	

TABLE V

Best Fit Model Parameters

System	T(°K)	m (mmol/g)	K_1 (mmHg)	$-K_2$ $(mmHg)^{-1}$	Absolute Average % Deviation
CH_3Cl-Silica gel	288	6.95	215	0.000171	0.851
	293	6.75	230	0.000137	0.784
	298	6.50	250	0.000090	1.041
CH_2Cl_2-Silica gel	288	5.80	34	0.001332	1.201
	293	5.70	40	0.000912	1.674
	298	5.50	50	0.000815	1.921
$CHCl_3$-Silica gel	288	3.95	10.8	0.013296	1.236
	293	3.90	12.5	0.011124	1.557
	298	3.80	15.0	0.007558	1.714
CCl_4-Silica gel	288	3.10	7.8	0.04782	1.362
	293	3.00	8.5	0.03786	1.274
	298	2.90	9.5	0.03032	1.453

TABLE VI

Comparison of Model Correlations

Adsorbate	T(°K)	Average Absolute Percent Deviations		
		Langmuir	BET	Kuo and Hines Model
CH_3Cl	288	5.534	3.974	0.851
	293	6.791	5.406	0.784
	298	5.672	3.572	1.041
CH_2Cl_2	288	3.525	15.482	1.201
	293	3.817	11.881	1.674
	298	3.978	12.829	1.921
$CHCl_3$	288	2.836	14.263	1.236
	293	3.068	13.108	1.557
	298	3.271	13.258	1.714
CCl_4	288	2.217	16.083	1.362
	293	2.473	13.852	1.274
	298	2.746	14.986	1.453

LIST OF FIGURES

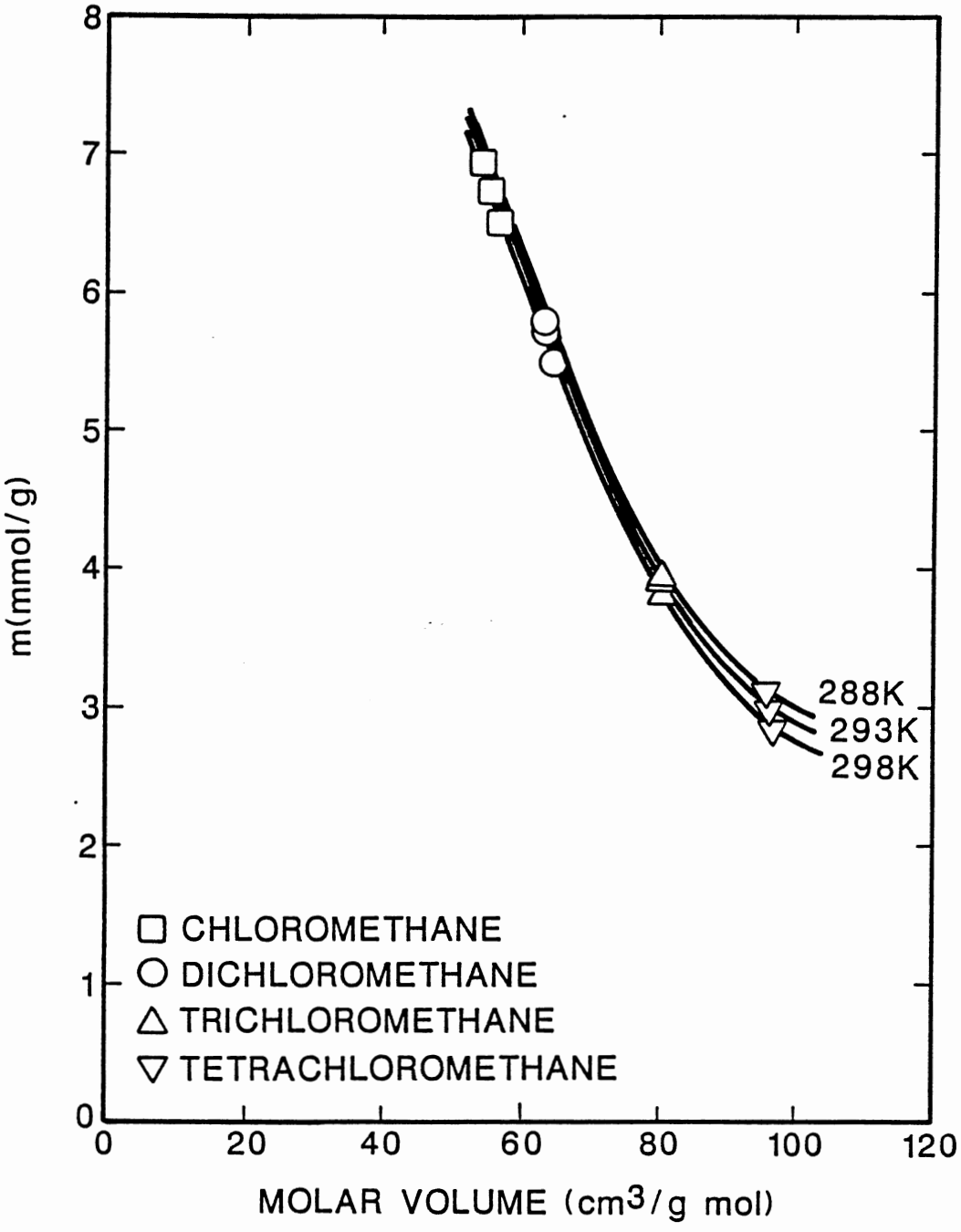

Figure 1. Plots of Maximum Adsorption Capacities as a Function of Molar Volume.

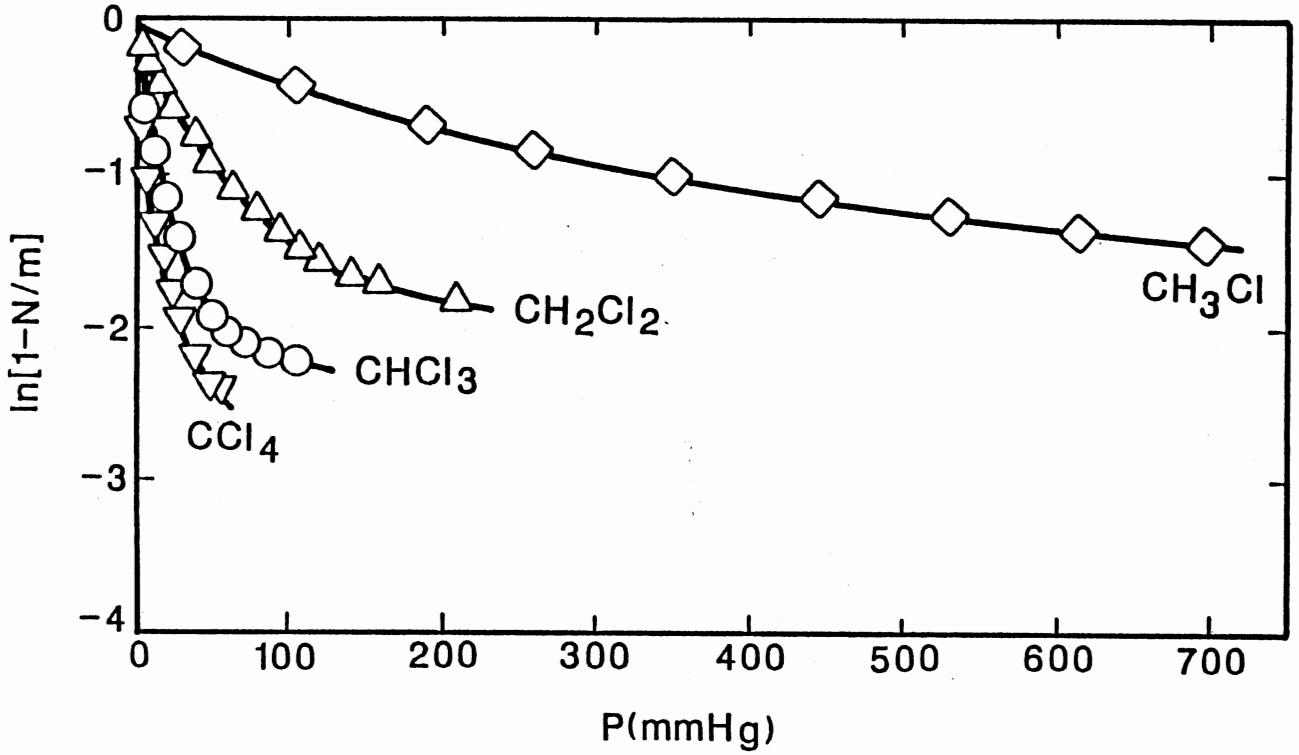

Figure 2. Linearized Jovanovic Plots for Chlorinated Hydrocarbons Adsorbed on Silica Gel at 288k.

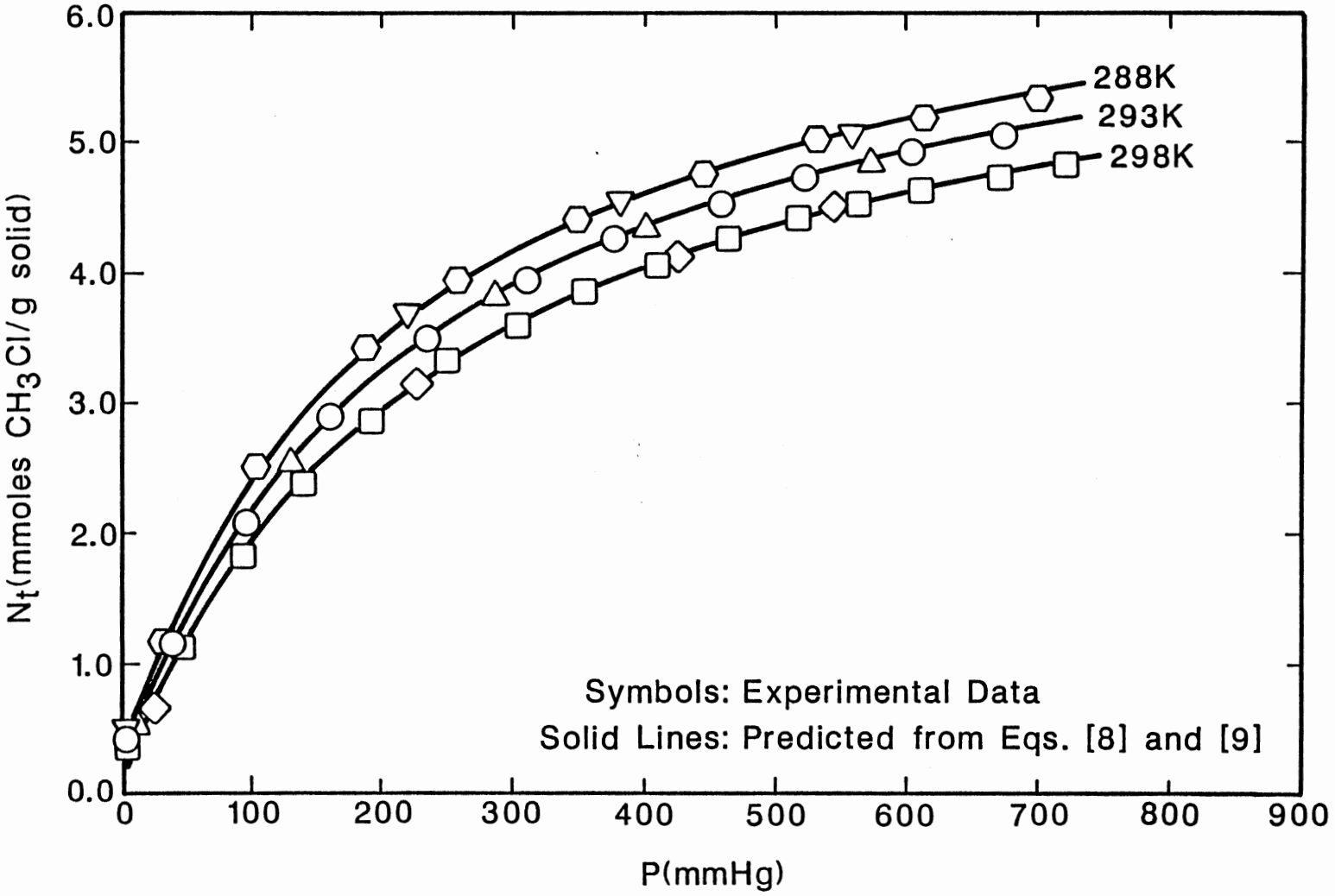

Figure 3. Adsorption of Chloromethane on Silica Gel.

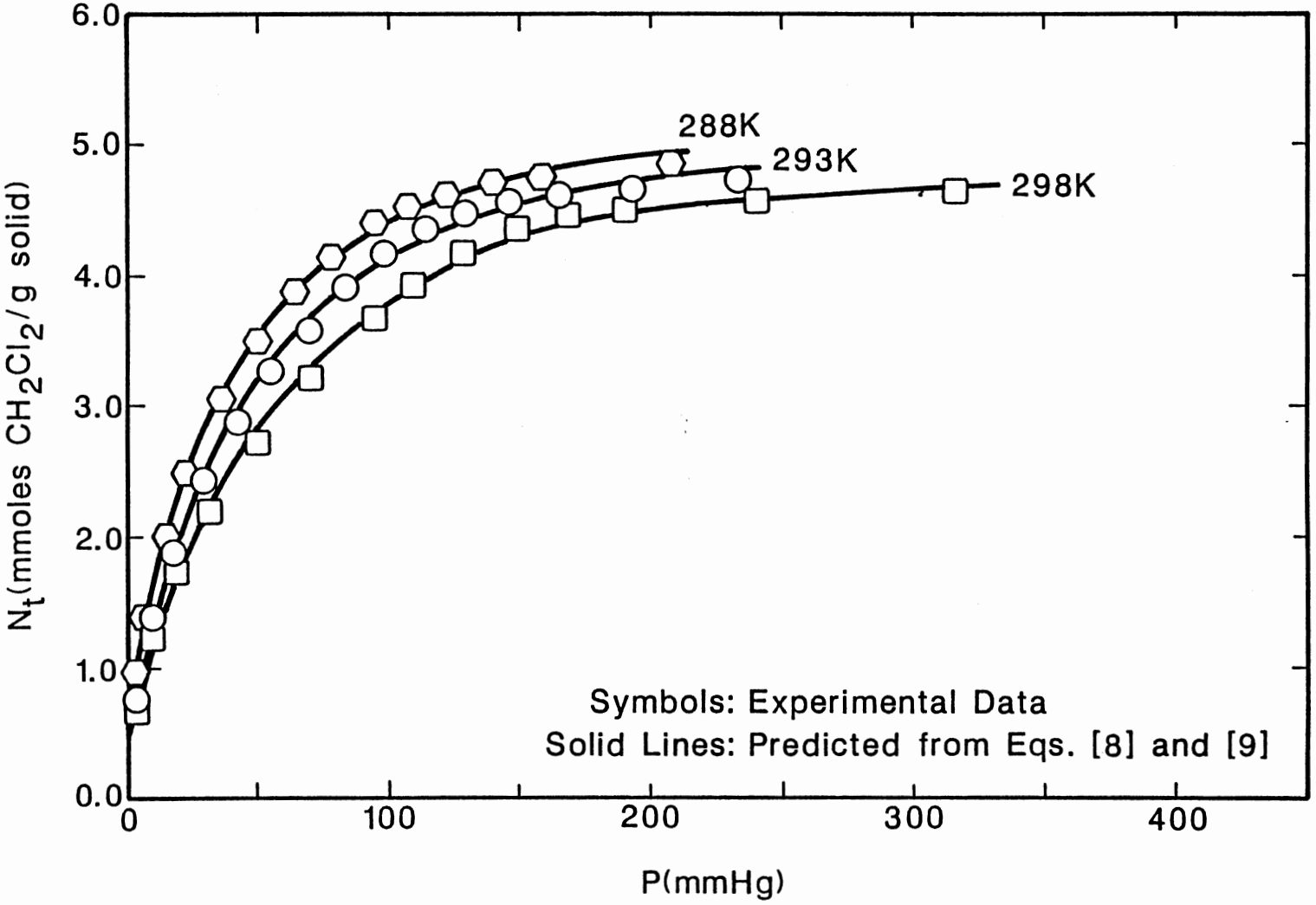

Figure 4. Adsorption of Dichloromethane on Silica Gel.

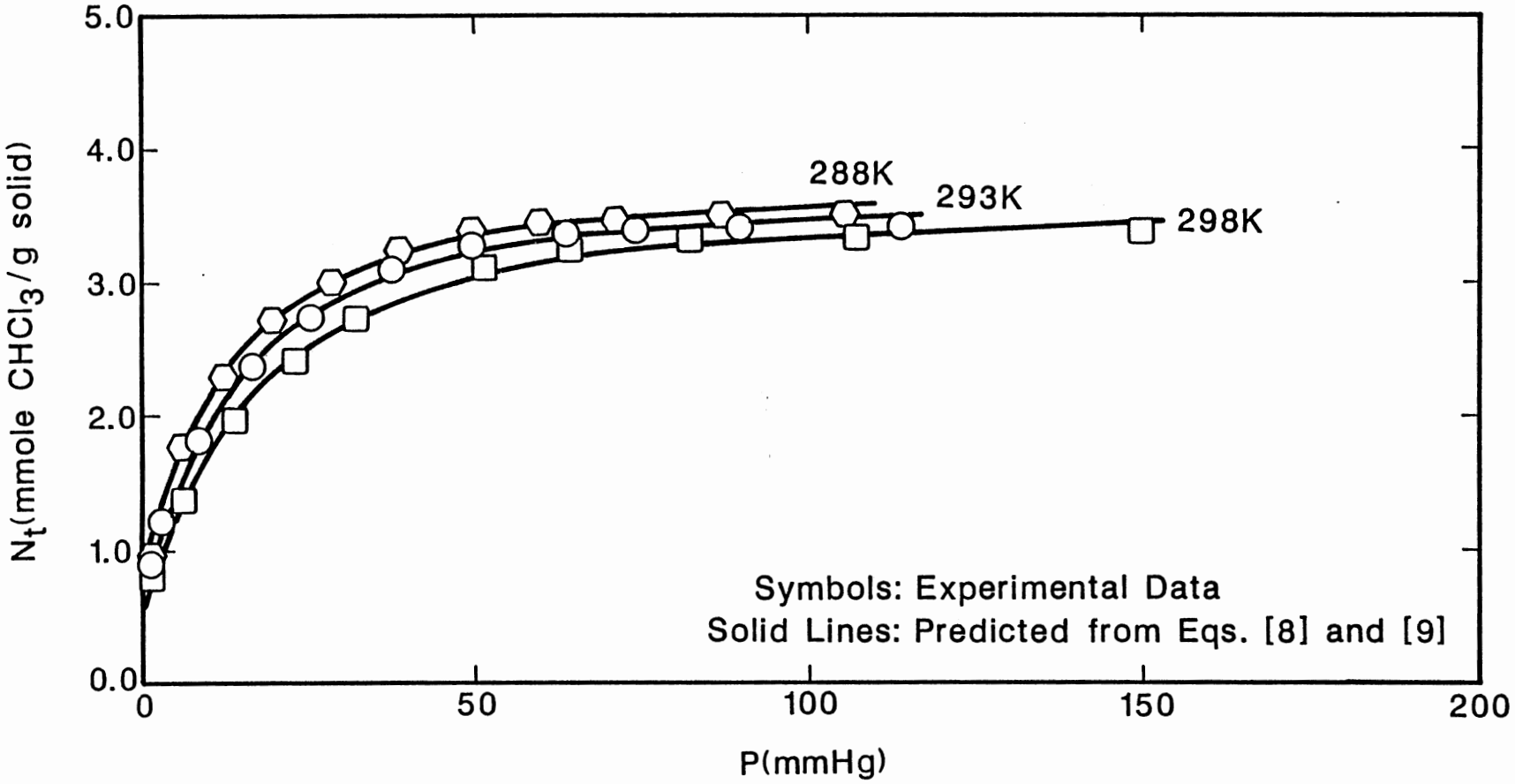

Figure 5. Adsorption of Trichloromethane on Silica Gel.

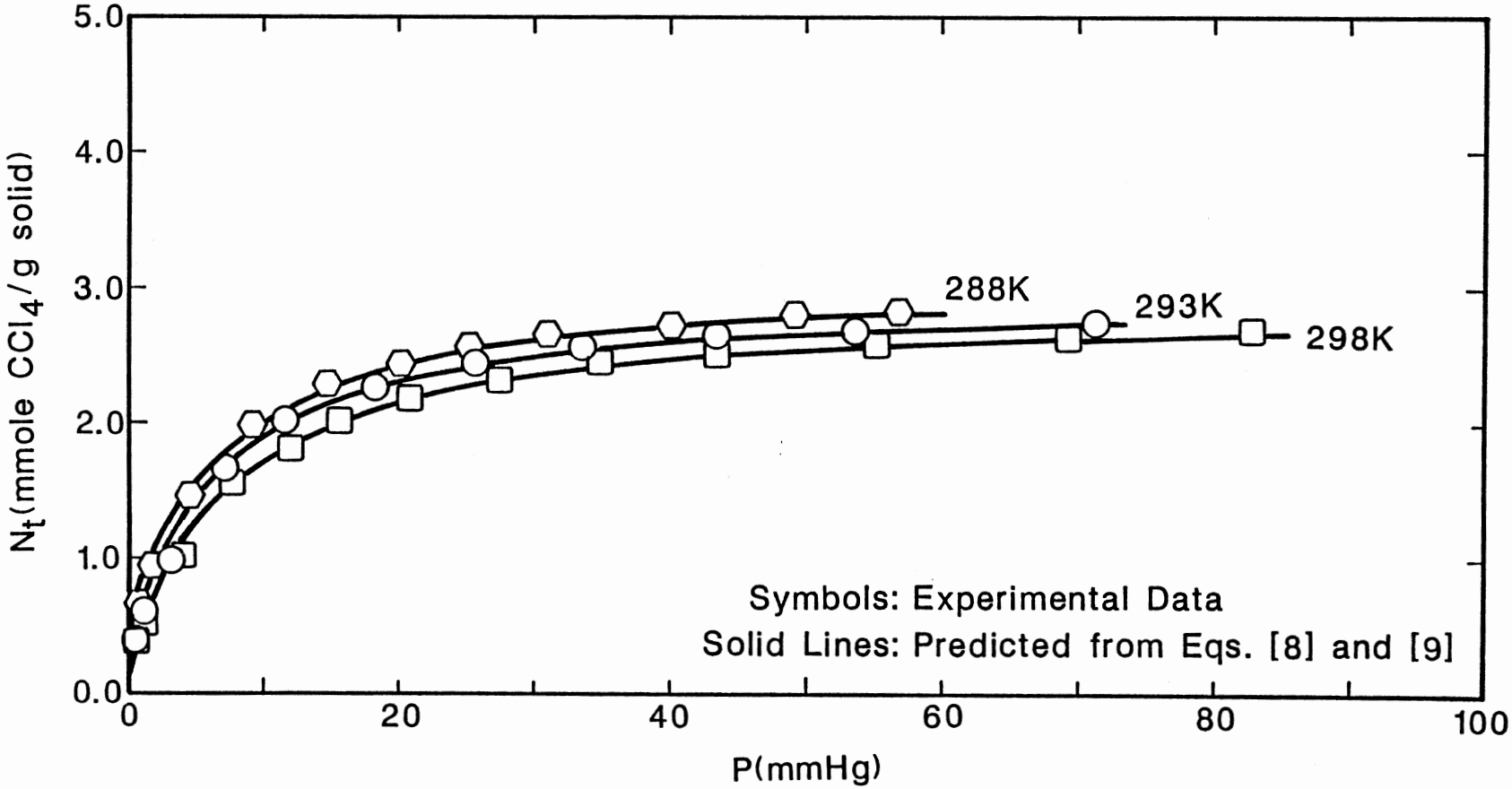

Figure 6. Adsorption of Tetrachloromethane on Silica Gel.

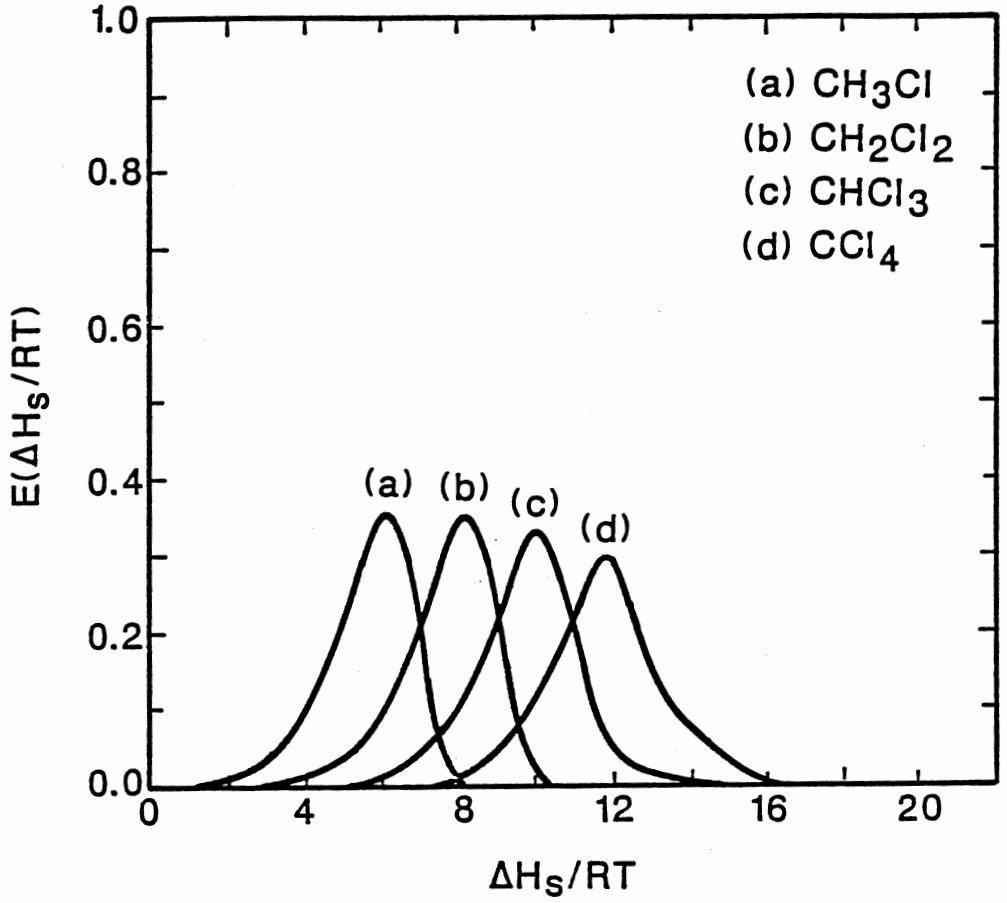

Figure 7. Energy Probability Density Function for Chlorinated Hydrocarbons on Silica Gel.

CHAPTER V

ADSORPTION OF 1,1,1-TRICHLOROETHANE AND TETROCHLOROETHYLENE ON SILICAL GEL

ADSORPTION OF 1,1,1-TRICHLOROETHANE AND TETRACHLOROETHYLENE ON SILICA GEL

Shing-Lin Kuo and Anthony L. Hines*

School of Chemical Engineering
Oklahoma State University
Stillwater, Oklahoma 74078

*To whom correspondence should be directed

ABSTRACT

Adsorption of 1,1,1-trichloroethane and tetrachloroethylene on silica gel were carried out at 288, 293, and 298K.

Experimental data were Type I isotherms and were correlated with the Kuo and Hines isotherm model as well as the Langmuir and the BET isotherm models. It was found that the Kuo and Hines isotherm model provided the best correlation of the experimental data. The Langmuir model also provided reasonably good correlations to the isotherm data. The BET model provided good correlations for the isotherm data only up to 35 percent saturation pressure for each adsorbate.

ADSORPTION OF 1,1,1-TRICHLOROETHANE AND TETRACHLOROETHYLENE ON SILICA GEL

INTRODUCTION

Two of the common indoor air pollutants that appear in most people's homes are 1,1,1-trichloroethane and tetrachloroethylene. The chlorinated hydrocarbon, 1,1,1-trichloroethane, comes into the home with aerosol sprays and is considered to be responsible for dizziness and irregular breathing. On the other hand, tetrachloroethylene finds its way into the home in the form of dry-cleaning fluids or fumes on clothes and is also considered to pose damage to human nerves, livers and kidneys.

Although indoor air pollution has drawn considerable attention from researchers in recent years (1,2,3), relatively few studies have been made in which the pollutants were removed from the air. An adsorption study using silica gel as an adsorbent to adsorb indoor air pollutants was made by Kuo and Hines (3). The work of Kuo and Hines was then extended to include the adsorption of the homologous series of chlorinated hydrocarbons chloromethane, dichloromethane, trichloromethane, and tetrachloromethane at several different temperatures (4).

This study extends the work of the previous investigation and contains equilibrium isotherms for 1,1,1-trichloroethane and tetrachloroethylene on silica gel at 288, 293, and 298K from low pressure up to saturation. The Langmuir and the BET isotherm models, as well as the heterogeneous adsorption isotherm model developed by Kuo and Hines (5) was used to correlate the equilibrium adsorption data.

EXPERIMENTAL SECTION

Materials and Apparatus. The adsorbent used in this study was type PA 40, 80-100 mesh silica gel supplied by Davidson Chemical Co. The 1,1,1-trichloroethane was obtained from J. T. Baker Chemical Co. and had a purity of 99.8%, and the tetrachloroethylene was obtained from Eastman Kodak Company with purity of 99.5%.

The experimental adsorption studies were carried out gravimetrically using a Cahn R-2000 electrobalance housed in a vacuum bottle assembly. The adsorption apparatus was designed such that either gases or vapors could be studied. The assembly was equipped with two sample hangdown tubes surrounded by a cylindrical shell through which water could flow to keep the balance temperature relatively constant during sample regeneration and during the adsorption process. The system was designed such that a sample weight of 3.5 grams could be tested. The sample weight was monitored with a strip chart recorder connected to the electrobalance control unit. A refrigerated-heated bath and circulator with a temperature control of ± 0.1K was used to control the adsorption temperature. A special vapor supply flask was used to introduce the liquid adsorbates into the system. A vacuum system which consisted of two vacuum pumps, a sorption trap, and a diffusion pump were used to obtain a vacuum of 1×10^{-4} mmHg for the adsorption system during regeneration. The leak rate of the complete system was approximately 0.05 mmHg/h. Two thermistor gauges were used to monitor the pressure when the system was being evacuated and during the adsorption runs. Pressures up to 760 mmHg were measured with a Wallace and Tiernan absolute pressure gauge with an accuracy of ± 0.02 mmHg. The error of the weight measurement was estimated to be ±10 μg.

Procedure. The electrobalance was calibrated to agree with the output signal of the recorder. The weight changes of the silica gel sample due to adsorption were detected by the electrobalance. The adsorbent was regenerated by evacuating the system and applying heat at 423K to the sample hangdown tube. Heating was continued until a constant sample weight was obtained, which typically required from 4 to 10h. After regeneration, the adsorbent was cooled to the adsorption temperature and the adsorbate was introduced into the system. After equilibrium was reached, as indicated by a constant sample weight, the pressure and weight were recorded. Equilibrium adsorption data were collected from very low pressures up to saturation. Following adsorption, desorption measurements were made by reducing the system pressure.

Buoyancy tests were conducted to determine the effects of the gas on the weight readings other than from the effect of actual gas adsorption. This procedure was exactly like the one used in collecting data, except that glass beads were placed in the sample pan rather than the adsorbent. The maximum error introduced by the buoyancy effect upon the measured adsorbed weight were estimated to be less than 0.5% for each adsorbate.

RESULTS AND DISCUSSION

Equilibrium Data: Adsorption isotherms were obtained for 1,1,1-trichloroethane and tetrachloroethylene on silica gel at 288, 293, and 298k after overnight regeneration of the adsorbent at 423k in vacuo. The experimental data are presented in Table I. The weight of the sample was measured to within 10 μg. Since the regenerated sample weight

was 0.0856g, the error in weight measurement was 0.012%. Pressures were measured with an accuracy of ±0.1 mmHg. Except for the lowest pressures, the maximum error in pressure measurement was less than 0.5%. The average error over the entire adsorption range was estimated to be less than 1%. Several of the data points were reproduced with an error no greater than 1%.

The adsorption data for both 1,1,1-trichloroethane and tetrachloroethylene on silica gel were Type I according to the Brunauer classification (6) and showed no apparent hysteresis when desorbing. The absence of capillary condensation, as shown by the adsorption isotherm data, indicates that silica gel contains mostly micropores. The amount of adsorbate removed by the silica gel increased as the molecular weight of adsorbate increased as shown in Table 1. The fact that the maximum uptake of both adsorbates by the silica gel was in the range of 0.444-0.472g adsorbate/g silica gel suggests that silica gel is an effective adsorbent for removing either one of the chlorinated hydrocarbons. The maximum uptake of each adsorbate was also plotted with respect to the molar volume of each adsorbate as shown in Figure 1. The maximum uptake data for the homologous series of chlorinated hydrocarbons studied by Kuo and Hines (4) were also presented in the figure for comparison purposes. It can be seen from the figure that the maximum uptake for all the six chlorinated hydrocarbons fall on a single curve for each temperature. This suggests that the maximum adsorption capacity curve may be used to predict the maximum uptake of other chlorinated hydrocarbons.

The isosteric heats of adsorption were calculated at constant adsorbent loading from the relationship

$$q = R\left[\frac{\partial(\ell nP)}{\partial(1/T)}\right]_N \qquad [1]$$

The heterogeneity of the adsorbent surface is usually caused by the differences among the adsorptive strength of the sites. The heterogeneity of the adsorption system can be detected from the shape of the adsorption isotherms and is usually evaluated by comparing the isosteric heats of adsorption at different loadings. As can be seen from Table II, the isosteric heats of adsorption in the beginning of the adsorption process exhibit the commonly observed trend of a decreasing amount of heat being given off as the loading on the surface is increased. This is due to pore filling in that the more active sites will adsorb gas molecule first. As the adsorption proceeds, most of the more active sites will be filled with the adsorbed molecules and the remaining less active sites will give off less amount of heat due to less amount of adsorption. However, the heats of adsorption remains practically constant after certain surface loading, which is considered to be near monolayer coverage, is reached. The fact that the heats of adsorption remains constant at different loadings indicates that the surface of the adsorbent is homogeneous. Previous works by Kuo and Hines (4) and Rojas (7) on the adsorption of homologous series chlorinated hydrocarbons and water, respectively, also confirmed that PA 40 on silica gels consists of homogeneous surface. Since the heats of adsorption shown in Table II are of the same order of magnitude as the heat of condensation, it may be concluded that the adsorption of 1,1,1-trichloroethane and tetrachloroethylene on silica gel are primarily the result of physical forces.

Data Correlation. The Langmuir model (8-10) was used to correlate the equilibrium data. The Langmuir equation, which can be derived by using statistical thermodynamics or kinetic considerations, has the form

$$N_\ell = \frac{maP}{1 + aP} \qquad [2]$$

where N_ℓ is the equilibrium uptake, P is the pressure, m is a characteristic constant defined as the amount of adsorption which would saturate the unit surface with a monolayer, and the term a is a characteristic constant often defined as the "capillarity" of the substances. When Eq. [2] was used to correlate the adsorption data by applying a regressional analysis technique, it was found that the Langmuir model provided a reasonably good correlation for the adsorption isotherm data of both chlorinated hydrocarbons on silica gels studied in this work. The average absolute percent deviation for the correlation is shown in Table VI.

The BET isotherm (11) was also used to correlate the adsorption isotherm data obtained in this study. The BET model, which was obtained by extending the Langmuir isotherm to apply to multilayer adsorption, has the form

$$\frac{P}{N_\ell(P_s - P)} = \frac{1}{CN_m} + \frac{(C - 1)}{CN_m}\frac{P}{P_s} \qquad [3]$$

where P_s is the saturation or vapor pressure, C is a constant for the particular adsorption system, N_ℓ is the uptake, and N_m is the monolayer adsorption capacity. If $P/[(P_s - P)N_\ell]$ is plotted versus P/P_s, a straight line should be obtained over the region in which the BET

equation holds. This line will have a slope of $(C-1)/(CN_m)$ and an intercept of $1/(CN_m)$. When such plots were made, it was found that the BET model correlate the experimental data successfully only for the region $P/P_s \leq 0.35$ for each of the adsorbates investigated in this work. This is not surprising considering that the BET model satisfies the Henry's law requirement in the low pressure region and it holds primarily for Type II and III isotherms. Since the BET model holds for the low pressure region, it was used to obtain the monolayer coverage and the surface area occupied by the molecules. The results are shown in Table III. As can be seen from the table and the equilibrium data, multilayer coverage occured for all of the adsorbates on the silica gels. The calculated surface area occupied by one molecule of the adsorbates was found to be in the range of $4.28\text{-}5.68 \times 10^{-19}$ m^2/molecule.

For a large class of solid-vapor systems, the heterogeneous structure of the adsorbent phase plays an important role in the process of physical adsorption. The traditional one-parameter models frequently fail in describing the adsorption behavior on microporous adsorbents. Most of the traditional isotherm models do not even conform to the basic constraints imposed by the physics of adsorption thermodynamics (12). The popular approach for the adsorption on a heterogeneous surface is to assume that the heterogeneous adsorbent consists of a distribution of energetically distinct sites and the overall adsorption isotherm can be obtained by the integration of the contribution of each site (13). This can be expressed as

$$N(P,T) = \int_0^\infty N_\ell(P,T,g) \quad E(g)\, dg \qquad [4]$$

where N(P,T) is the overall adsorption isotherm on the heterogeneous adsorbent, $N_\ell(P,T,g)$ describes a specific adsorption isotherm for homogeneous sites of adsorptive energy g, and E(g) is the site energy distribution for g.

In the previous studies by Kuo and Hines, (4,5) it was assumed that the local isotherm for homogeneous sites can be described by Jovanovic model (14) as

$$N_\ell(P,T,g) = m[1 - e^{-bP}] \qquad [5]$$

with the energy distribution function being represented by a Morse-type probability function (15) given by

$$E(g) = \frac{K_1}{1 - K_1K_2}\left[e^{-K_1 g} - K_2 e^{-g}\right] \qquad [6]$$

In Eqs. [5] and [6], m is the saturation adsorption capacity, K_1 and K_2 are parameters in the energy distribution function, and b is the Jovanovic parameter which can be related to the heat of adsorption by

$$b = b_o \exp[-q/RT] \qquad [7]$$

The resulting overall adsorption isotherm for adsorption on a heterogeneous adsorbent is

$$N(P,T) = m\left[1 - \left(\frac{1}{1 - K_1K_2}\right)\left(\frac{K_1}{P + K_1} - \frac{K_1K_2}{P + 1}\right)\right] \qquad [8]$$

where m, K_1, and K_2 are related to the Henry's law constant, K_ℓ, by

$$m\left[\frac{1 - K_1^2K_2}{K_1 - K_1^2K_2}\right] = K_\ell \quad \text{as} \quad P \to 0 \qquad [9]$$

In deriving Eqs. [8] and [9] Kuo and Hines (5) neglected the b_o contribution to the overall isotherm equation, since b_o is usually very small ($b_o < 10^{-4}$) for most systems.

Equations [8] and [9] were used to correlate the adsorption data for 1,1,1-trichloroethane and tetrachloroethylene on silica gel. The adsorbates showed varying degrees of affinity of adsorption on silica gel as indicated by the differences in the Henry's law constants and b_o values given in Table IV. According to the Jovanovic model, a plot of $\ell n(1 - \frac{N}{m})$ versus pressure should yield a straight line with a slope equals to -b. Two examples of such plots for the systems studied using the isotherm data at 298k are shown in Figure 2. The nonlinearity of the plots indicated that the silica gel was heterogeneous for both adsorbates, and a more sophisticated isotherm model would be necessary to correlate the adsorption isotherm data. Equations [8] and [9] were then used by employing a trial and error procedure to obtain the best fit parameters. The Henry's law constants were estimated from the initial slopes of the isotherms. A value of m was chosen and K_2 was calculated using Eq. [9] for different value of K_1. The entire isotherm was then generated using Eq. [8]. If the calculated isotherm was not within ± 2% of the experimental data over the entire pressure range, a

new value of m was chosen and the procedure repeated. The best fit model parameters are given in Table V.

Figures 3 and 4 show the experimental data and the best fit curves obtained from Eqs. [8] and [9] for 1,1,1-trichloroethane and tetrachloroethylene on silica gel. As shown in the figures, the heterogeneous isotherms obtained by using the Kuo and Hines model describes the isotherm data extremely well over the entire range of pressure and temperature. The absolute errors between the values calculated by the Kuo and Hines model and the experimental data ranged from 0.841% to 1.244%.

The energy probability density function E(q/RT) may be obtained by defining the energy parameter $g = b_o[\exp(q/RT) - 1]$ and combining it with Eqs. [6] and [7] as

$$E(q/RT) = \frac{K_1}{1 - K_1K_2}\left[e^{-K_1 g} - K_2 e^{-g}\right][g + b_o] \qquad [10]$$

Figure 5 shows graphs of E(q/RT) versus q/RT for both of the systems at 288K. As noted in the figure, Eq. [10] gives skewed Gaussian-like energy distribution functions, which are characteristic of the Morse-type probability density function. Figure 5 also shows that silica gel is more heterogeneous when adsorbing tetrachloroethylene than when 1,1,1-trichloroethane is adsorbed. However, 1,1,1-trichloroethane showed larger maximum for the energy distribution function. In addition, the chlorinated hydrocarbons studied earlier by Kuo and Hines

(4) demonstrated the same degree of heterogeneity with respect to the silica gel as does 1,1,1-trichloroethane.

Comparison of the experimental equilibrium data correlations using different isotherm models can be made by calculating the average absolute percent deviation over the entire pressure range for each adsorption system. The adsorption isotherm data for 1,1,1-trichloroethane and tetrachloroethylene on silica gel at three temperatures were correlated by using the Langmuir, BET, and Kuo and Hines models, and the results of the average absolute percent deviation predicted by each model are shown in Table VI. As can be seen from the table, the Kuo and Hines model provided the best correlation for the experimental isotherm data. The Langmuir model also provided a reasonably good correlation for the isotherm data, while the BET model gave very poor correlations for both of the adsorbates. This is not surprising when considering that the BET model only holds for pressures up to 35% saturation of the adsorbates studied in this work.

CONCLUSIONS

The adsorption of 1,1,1-trichloroethane and tetrachloroethylene was investigated using silica gel as the adsorbent. The adsorption isotherms of both chlorinated hydrocarbons were determined gravimetrically at 288, 293, and 298K and pressures up to saturation. The maximum adsorption capacities for the two chlorinated hydrocarbons fell on a single curve for each temperature, which suggests that the maximum capacity curve can be used to predict the maximum uptakes of other chlorinated hydrocarbons. On the basis of this study, it was

concluded that silica gel can be effectively used to adsorb many chlorinated hydrocarbons.

The isotherm data for the adsorption of 1,1,1-trichloroethane and tetrachloroethylene on silica gel were correlated by using the Kuo and Hines adsorption isotherm model as well as the Langmuir and the BET models. It was found that the Kuo and Hines model provided the best correlation for the experimental isotherm data. The Langmuir model also provided pretty good correlations for the isotherm data, while the BET model provided good correlations for the isotherm data only up to 35 percent saturation pressure for each of the adsorbates studied in this work.

NOTATIONS

A	=	Surface area of a molecule
a	=	Langmuir parameter defined by Eq. [2]
b	=	Jovanovic parameter defined by Eq. [5]
b_o	=	Limiting value of b at infinite temperature
C	=	BET constant defined in Eq. [3]
E	=	Energy distribution function
g	=	Adsorption energy parameter
K_1	=	Parameter in Morse-type energy distribution function
K_2	=	Parameter in Morse-type energy distribution function
K_ℓ	=	Henry's law constant
m	=	Saturation adsorption capacity
N	=	Overall adsorption isotherm
N_ℓ	=	Local adsorption isotherm
N_m	=	Monolayer adsorption capacity
P	=	System pressure
P_s	=	Saturation pressure
q	=	Isosteric heat of adsorption
q_c	=	Heat of condensation
R	=	Universal gas constant
T	=	System temperature

LITERATURE CITED

1. Consumer Reports, October, 60 (1985).

2. U. S. News and World Report, September, 71 (1985).

3. S. L. Kuo and A. L. Hines, "Adsorption of Chlorinated Hydrocarbon Pollutants on Silica Gel," Submitted for review, 1987.

4. S. L. Kuo and A. L. Hines, "Application of a New Heterogeneous Isotherm Model to Predict the Adsorption of Chlorinated Hydrocarbons on Silica Gel." Submitted for review, 1987.

5. S. L. Kuo and A. L. Hines, "New Theoretical Isotherm for Adsorption on Heterogeneous Adsorbents," Submitted for review, 1987.

6. S. Brunauer, The Adsorption of Gases and Vapors, Vol. 1, Princeton University Press, Princeton, New Jersey (1945).

7. F. J. Rojas V., M.S. Thesis, Colorado School of Mines, Colorado (1981).

8. I. Langmuir, J. Am. Chem. Soc., 38, 2221 (1916).

9. I. Langmuir, J. Am. Chem. Soc., 39, 1848 (1917).

10. I. Langmuir, J. Am. Chem. Soc., 40, 1361 (1918).

11. S. Brunauer, P. H. Emmett, and E. Teller, J. Am. Chem. Soc., 60, 309 (1938).

12. S. Sircar and R. Gupta, AIChE J., 27, 806 (1981).

13. S. Ross and J. P. Oliver, On Physical Adsorption, Wiley, New York (1964).

14. D. S. Jovanovic, Kolloid-Z. Z., Polym. 235, 1203 (1969).

15. P. M. Morse, Phys. Rev., 34, 57 (1929).

LIST OF TABLES

TABLE I

Adsorption Isotherm Data for 1,1,1-Trichloroethane and Tetrachloroethylene on Silica Gel

Adsorbate	288°K		293°K		298°K	
	P,mmHg	N,mmol/g	P,mmHg	N,mmol/g	P,mmHg	N,mmol/g
1,1,1-Trichloroethane	1.2	1.608	0.9	1.200	0.8	0.876
	3.4	2.373	2.3	1.576	2.9	1.388
	7.0	2.903	6.8	2.531	6.6	2.062
	12.2	3.131	11.5	2.846	10.3	2.430
	21.1	3.205	16.7	2.969	17.2	2.745
	29.8	3.258	23.2	3.061	25.8	2.916
	40.6	3.310	31.3	3.135	34.7	3.017
	49.7	3.354	41.3	3.209	46.0	3.118
	59.5	3.389	50.0	3.253	58.3	3.205
	64.0	3.402	61.0	3.301	68.5	3.244
	69.8	3.411	69.8	3.336	79.1	3.275
	34.0	3.266	78.8	3.363	88.8	3.297
	25.8	3.240	85.0	3.376	99.0	3.315
	8.5	2.999	55.0	3.280	104.5	3.323
			34.3	3.170	85.3	3.284
			7.8	2.601	40.2	3.074
					15.6	2.684
Tetrachloroethylene	0.2	1.602	0.20	1.469	0.15	1.160
	0.7	2.098	0.75	1.978	0.65	1.550
	1.4	2.365	1.60	2.315	1.30	2.053
	2.2	2.522	2.30	2.448	2.00	2.265
	3.0	2.625	2.8	2.509	2.75	2.388
	3.8	2.685	3.8	2.608	3.80	2.500
	4.7	2.725	5.1	2.675	4.50	2.541
	5.9	2.768	6.3	2.705	5.60	2.591
	7.0	2.800	8.1	2.738	7.10	2.643
	8.5	2.822	9.8	2.765	8.40	2.650
	9.8	2.833	11.3	2.777	9.80	2.675
	6.2	2.775	5.0	2.665	11.50	2.680
	1.0	2.210	2.2	2.422	13.70	2.685
	0.3	1.805	0.8	2.002	12.50	2.682
					5.80	2.600
					2.25	2.309
					0.85	1.798

TABLE II

Variation of Isosteric Heats of Adsorption with the Amount Adsorbed

Adsorbate	Amount Adsorbed mmol/g solid	-q kcal/gmol	q_c kcal/gmol
$C_2H_3Cl_3$	1.2	31.79	7.14-7.34
	1.6	19.17	
	2.0	17.69	
	2.4	17.07	
	2.8	18.06	
	3.2	18.35	
C_2Cl_4	1.6	23.16	8.08-8.32
	1.8	18.35	
	2.0	14.65	
	2.2	11.14	
	2.4	11.25	
	2.6	11.80	

TABLE III

Monolayer Coverages and Area per Molecule Calculated by Using BET Model

Adsorbate	T(°K)	Area Per Molecule $Ax10^{19}$ (m^2/Molecule)	Surface Coverage m^2/g solid	Monolayer Coverage N_m(mmol/g)
$C_2H_3Cl_3$	288	4.28	739.5	2.87
	293	4.32	738.6	2.85
	298	4.38	740.9	2.81
C_2Cl_4	288	5.52	741.0	2.23
	293	5.60	738.3	2.19
	298	5.68	742.0	2.17

TABLE IV

Henry's Law Constants for the Systems Investigated

Adsorption System	T(°K)	K_ℓ (mmol/g.atm)	b_o (atn^{-1})
$C_2H_3Cl_3$ - Silica Gel	288	1475	5×10^{-7}
	293	1283	
	298	1008	
C_2Cl_4 - Silica Gel	288	8660	1×10^{-7}
	293	6830	
	298	5770	

TABLE V

Best Fit Model Parameters

System	T(°K)	m (mmol/g)	K_1 (mmHg)	$-K_2$ $(mmHg)^{-1}$	Absolute Average % Deviation
$C_2H_3Cl_3$-Silica Gel	288	3.56	2.70	0.1423	1.244
	293	3.53	5.00	0.1067	0.962
	298	3.50	7.50	0.0527	0.841
C_2Cl_4-Silica Gel	288	2.97	0.20	2.0507	1.124
	293	2.90	0.25	1.7173	0.974
	298	2.80	0.30	1.2112	0.918

TABLE VI

Comparison of Model Correlations

Adsorbate	T(°K)	Average Absolute Percent Deviation		
		Langmuir	BET	Kuo and Hines
$C_2H_3Cl_3$	288	1.748	29.486	1.244
	293	1.326	32.129	0.962
	298	1.284	36.472	0.841
C_2Cl_4	288	1.654	20.764	1.124
	293	1.398	23.951	0.974
	298	1.267	23.413	0.918

LIST OF FIGURES

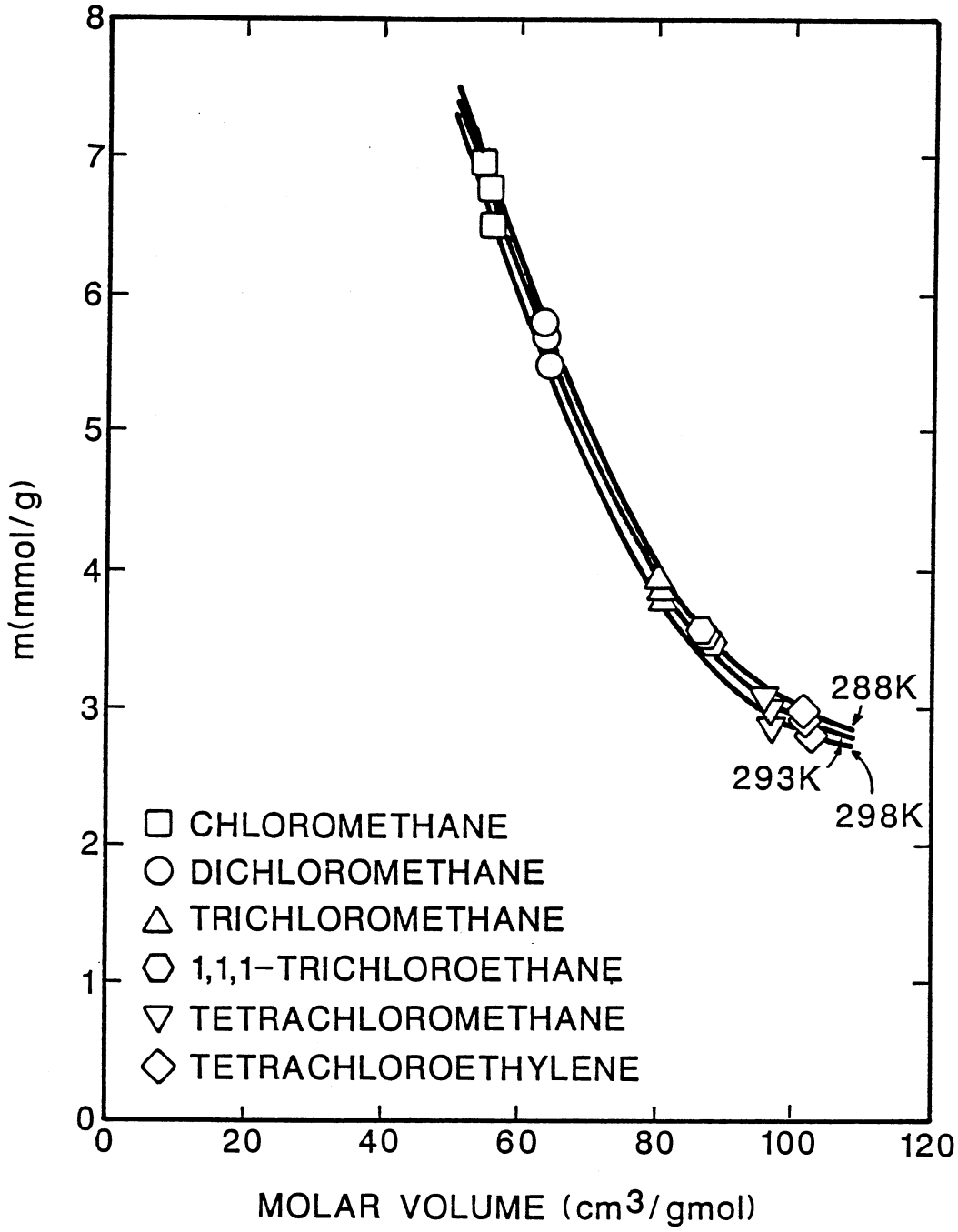

Figure 1. Plots of Maximum Adsorption Capacities as a Function of Molar Volume.

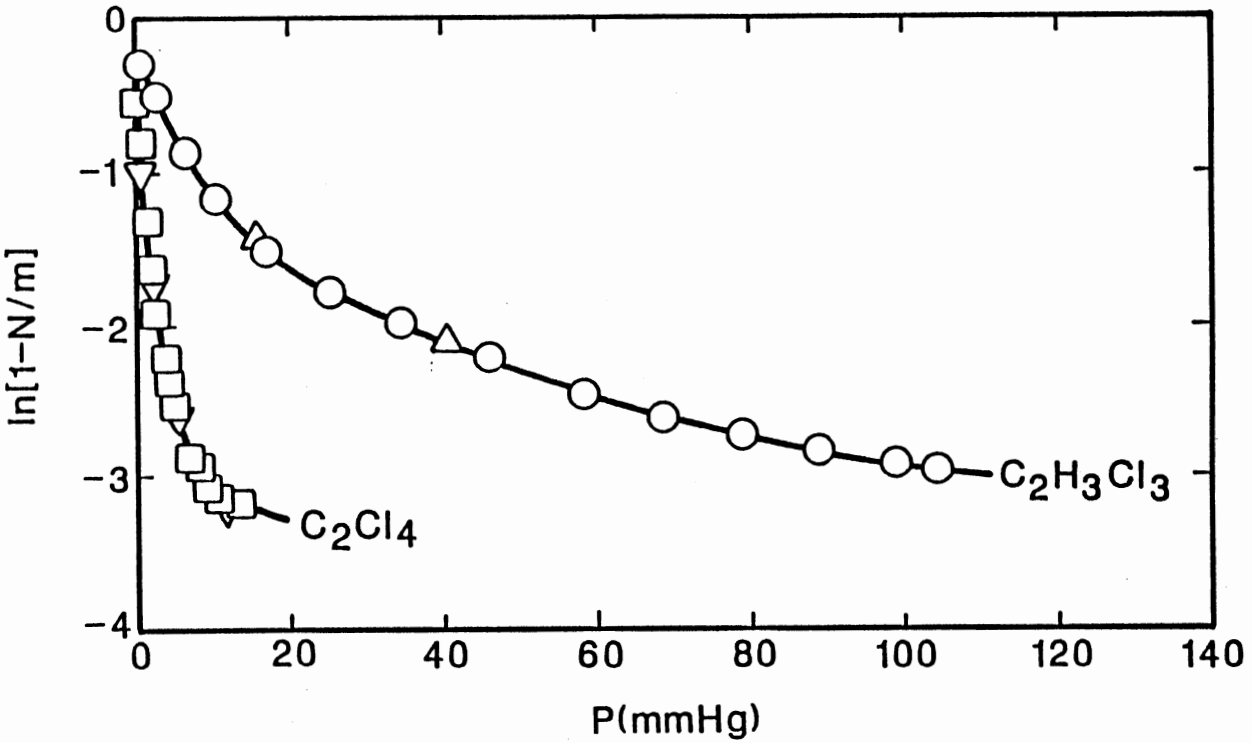

Figure 2. Linearized Jovanovic Plots for 1,1,1-Trichloroethane and Tetrachloroethylene on Silica Gel at 298K.

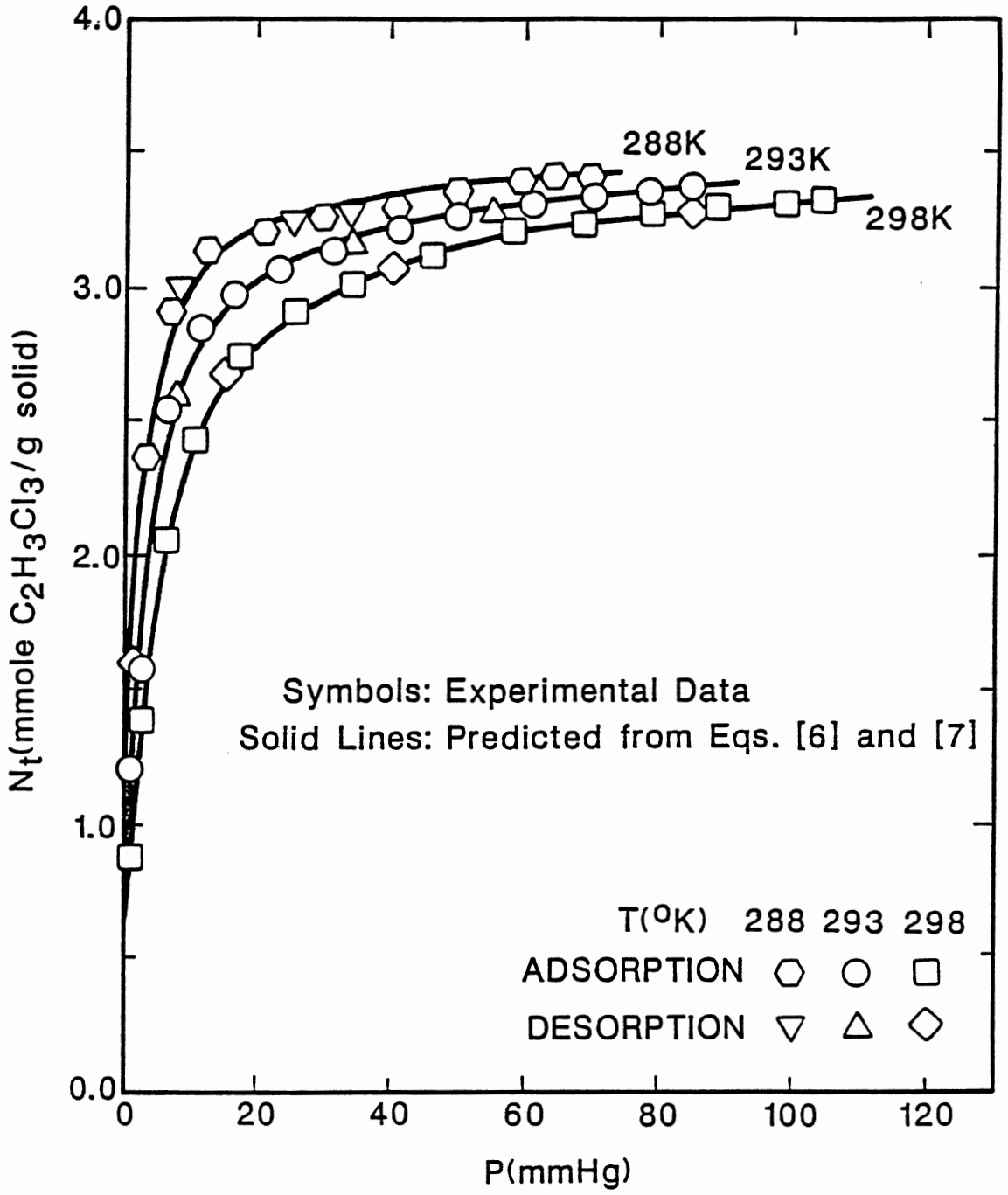

Figure 3. Adsorption of 1,1,1-Trichloroethane on Silica Gel.

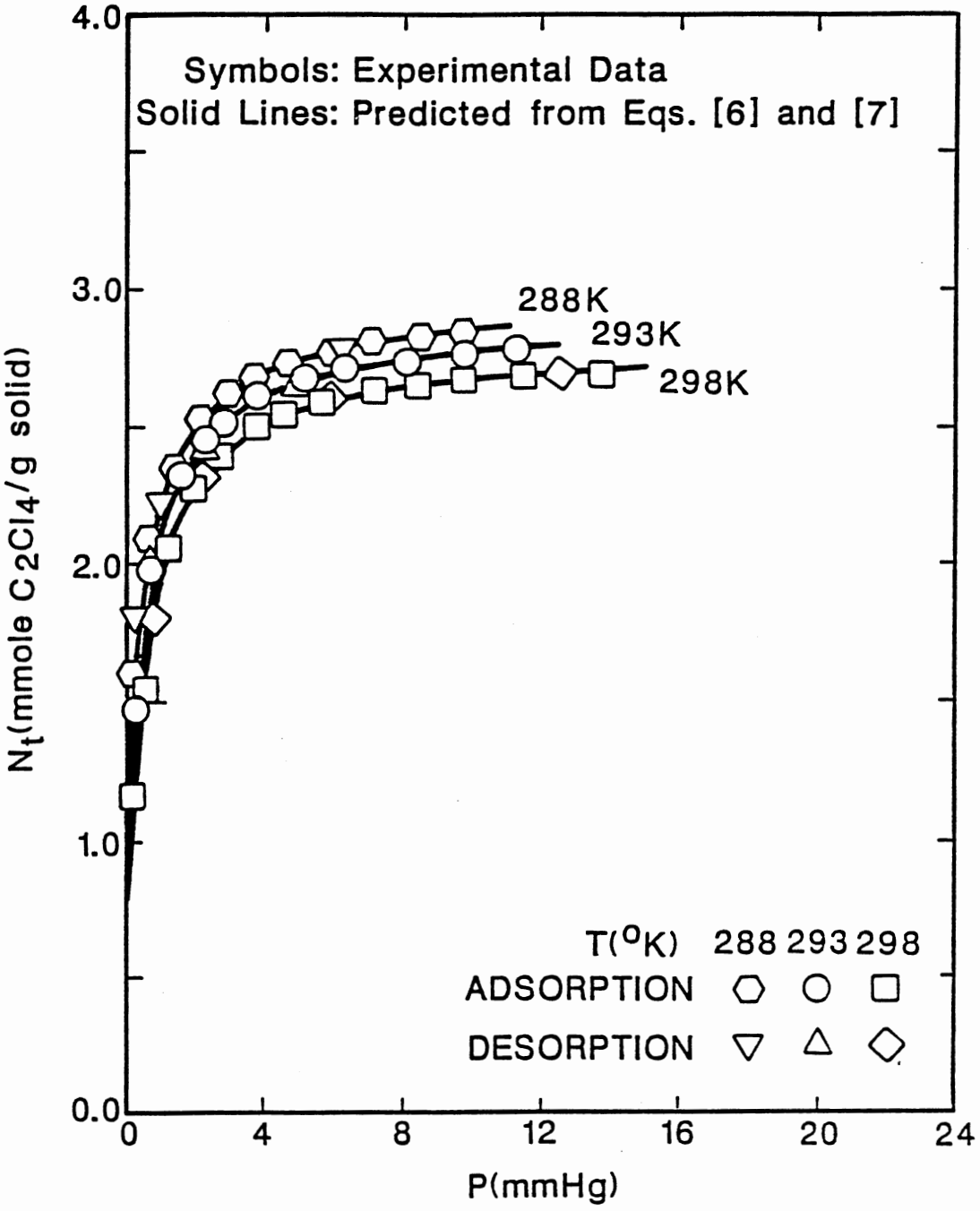

Figure 4. Adsorption of Tetrachloroethylene on Silica Gel.

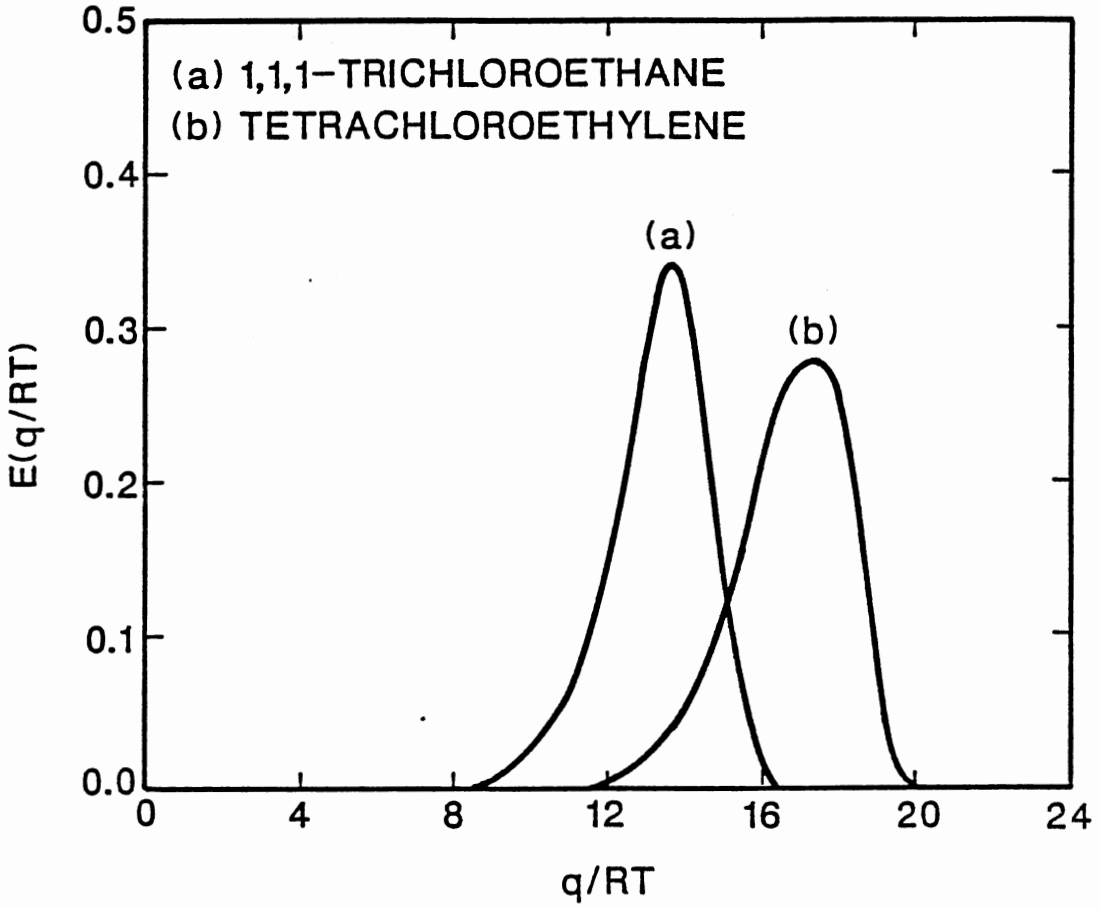

Figure 5. Energy Probability Density Function for 1,1,1-Trichloroethane and Tetrachloroethylene on Silica Gel.

CHAPTER VI

DIFFUSION OF CHLORINATED HYDROCARBONS IN SPHERICAL SILICA GEL BEADS

DIFFUSION OF CHLORINATED HYDROCARBONS IN SPHERICAL SILICA GEL BEADS

Shing-Lin Kuo and Anthony L. Hines*

School of Chemical Engineering
Oklahoma State University
Stillwater, OK 74078

*To whom correspondence should be directed.

ABSTRACT

The diffusion coefficients of six chlorinated hydrocarbons chloromethane, dichloromethane, trichloromethane, tetrachloromethane, 1,1,1-trichloroethane, and tetrachloroethylene were investigated using a gravitational apparatus. It was found that the diffusion processes of the above hydrocarbons on spherical silica gel beads were controlled by surface diffusion which exhibits liquid phase diffusion characteristics in the multilayer region. Concentration effects on the diffusion coefficients were found to be insignificant. The fact that the silica gel bead exhibited homogeneous-like surface behavior implied that diffusion coefficients for the above systems were very weak functions of concentration and could be treated, for all practical purposes, as constant at specific temperatures.

DIFFUSION OF CHLORINATED HYDROCARBONS IN SPHERICAL SILICA GEL BEADS

INTRODUCTION

Transport of a substance within an adsorbed phase is known as surface diffusion and is important in cases, such as adsorption, catalysis, and membrane-separation processes. The diffusion and flow of gases through porous materials can occur by several different mechanisms. Testin and Stuart (1) and Leyva-Ramos and Geankoplis (2) gave vivid descriptions of several diffusion mechanisms. The transport processes occurring in diffusion and adsorption include (a) external gas molecule diffusion, (b) pore volume diffusion, (c) adsorption of the gas molecule, (d) molecular motion along the surface, (e) desorption of the molecule, and (f) surface diffusion. Steps (c) and (e) are apparently very rapid so that the kinetics of adsorption and desorption may be too rapid to measure (3,4). If it is assumed that steps (c) and (e) are nearly instantaneous, a measurable adsorption rate would consist primarily of migration of the molecule to the surface and motion of the molecule along the surface. For solids with a relatively narrow pore size distribution, several distinct regimes of behavior are observed, depending on the ratio of the mean free path of gas molecules to the mean pore diameter. Knudsen diffusion of nonadsorbed gases occurs at large values of this ratio and is often encountered with high surface area materials at moderate pressures. For gases which adsorb appreciably, flows of an unusually large magnitude, in comparison with the Knudsen flow of nonadsorbed gases, have been observed. These anomalously large transport rates can be attributed to the migration of adsorbed molecules along the internal surfaces of the

porous solids. Since most adsorbents are microporous that display strong adsorptive properties, an understanding of surface transport is important in characterizing the total transport of gases within these materials.

Surface diffusion for gas-solid adsorption systems is commonly measured by using either gravimetric or volumetric adsorption methods (5). The experiment consists of contacting the gaseous adsorbate with the solid adsorbent and monitoring the subsequent changes in the gas phase pressure of the system (volumetric method) or the changes in the weight of adsorbent (gravimetric method) with time. The adsorbent typically consists of a few granules of the solid with a known geometry. The amount adsorbed is then determined as a function of time by carrying out a material balance between the gas and the adsorbed phases. The diffusivity is then estimated by using different models to match the measured uptake.

Of all the diffusion models, the Wicke model is one of the most commonly used for mass transport studies inside porous media. The Fickian model was derived based on the following assumptions:

(1) The porous particles exhibit isothermal behavior during the entire diffusion measurement.

(2) The pore system inside the particles is homogeneous and isotropic.

(3) The diffusivity is independent of the adsorbate concentration inside the adsorbent particle.

Although the Wicke model is most frequently used because of its mathematical simplicity, many variations of the model have been proposed in the literature to account for nonuniform particle geometry (6), non-

uniform particle size distribution (6), polydisperse pore structures of the adsorbent (7-11) and concentration dependence of the diffusion coefficient (12,14,15). However, all of these models assume isothermal behavior.

The purpose of this work is to study the diffusion of six chlorinated hydrocarbons through silica gel at 288, 293, and 298K. The effects of temperature and pressure on the diffusion coefficients were also investigated.

EXPERIMENTAL

Materials and Apparatus. The silica gel used in this study was 8 mesh Spherical Bead Gel B06-08-4X1925, supplied by Davison Chemical Co. It had a surface area of approximately $800 m^2/g$. A pore volume of $0.45 cm^3/g$, an average bulk density of 48 lb/ft^3, and an average pore diameter of 22 Å. The chlorinated hydrocarbons consisted of the homologous series chloromethane, dichloromethane, trichloromethane, and tetrachloromethane and two additional chlorinated hydrocarbons, 1,1,1-trichloroethane and tetrachloroethylene. The methyl chloride was obtained from Union Carbide and had a purity of 99.5%. The methylene chloride, chloroform, and carbon tretrachloride were obtained from Fisher Scientific Company with purities of 99.9%, 99.9%, and 99.5%, respectively. The 1,1,1-trichloroethane was obtained from J. T. Baker Chemical Company with a purity of 99.8%, and the tetrachloroethylene was obtained from Eastman Kodak Company with a purity of 99.5%.

The experimental diffusion studies were measured gravimetrically using a Cahn R-2000 electrobalance housed in a vacuum bottle assembly. The apparatus was designed such that either gases or vapors could be

studied. The assembly was equipped with two sample hangdown tubes surrounded by a cylindrical shell through which water could flow to keep the balance temperature constant during the diffusion process. A sample weight up to 3.5 grams could be tested. Two sample hangdown rings were placed inside the sample hangdown tubes; the sample hangdown rings were designed to be very thin so that they could support a spherical silica gel bead while blocking only a very small portion of the bead's surface. The sample weight was monitored with a strip chart recorder connected to the electrobalance control unit. A refrigerated-heated bath and circulator with a temperature control of ±0.1C was used to control the diffusion temperature. A special vapor supply flask was used to introduce the liquid adsorbates into the system. A vacuum system which consisted of two vacuum pumps, a sorption trap, and a diffusion pump were used to obtain a vacuum of $1x10^{-4}$mmHg for the diffusion apparatus. The leak rate of the complete system was approximately 0.05mmHg/h. Two thermistor gauges were used to monitor the pressure when the system was evacuated and during the diffusion measurements. Pressures up to 760 mmHg were measured with a Wallace and Tiernan absolute pressure gauge with an accuracy of ± 0.02 mmHg. The error of the weight measurement was estimated to be 10 μg. A schematic diagram of the apparatus is shown in Figure 1.

Procedure. The spherical silica gel bead was regenerated by evacuating the system and applying heat at 423K to the sample hangdown tube. Heating was continued until a constant sample weight was obtained, which typically required from 4 to 10h. After regeneration, the silica gel bead was cooled to the adsorption temperature and the adsorbate was introduced into the system. The weight change of the

silica gel due to diffusion of the adsorbate was detected by the electrobalance, which was calibrated to agree with the output signal of the recorder. During the diffusion process, the weight change of the bead was recorded as a function of time. After reaching equilibrium at a specific pressure, the system pressure was increased and the process repeated until the silica gel bead was saturated. In order to hold the temperature inside the particles constant, pressure increases were made as small as possible. Measurements were made at three different temperatures in order to investigate the temperature effect on the diffusion coefficients.

Buoyancy tests were conducted to determine the effects of the gas on the weight readings from effects other than the effects of actual gas uptake. The procedure was exactly the same as the one used in collecting data, except that glass beads were placed on the sample ring rather than the silica gel bead. The maximum error introduced by the buoyancy effect upon the measured weight was estimated to be less than 0.5% for each adsorbate.

ESTIMATION OF DIFFUSION COEFFICIENTS

It can be shown that for cases in which the adsorbent is microporous and the rate determining step for the diffusion processes is surface diffusion, the analysis is simplified by the fact that the uptake only takes place at the surface of the adsorbent particles. Following the approach used by Wicke (16), in which he assumed that mass transfer was controlled by diffusion in the porous sphere and described the overall adsorption process in terms of unsteady diffusion into a

sphere, the differential equation that describes the diffusion process can be expressed as

$$\frac{1}{r^2}\frac{\partial}{\partial r}\left(Dr^2\frac{\partial C}{\partial r}\right) = \frac{\partial C}{\partial t} \qquad [1]$$

with the boundary conditions

$$\text{BC1:}\quad C = C_o \quad \text{at } t = 0, \text{ for } r < R \qquad [2]$$

$$\text{BC2:}\quad C = C_1 \quad \text{at } r = R, \text{ for all } t \qquad [3]$$

$$\text{BC3:}\quad \frac{\partial C}{\partial r} = 0 \quad \text{at } r = 0, \text{ for all } t \qquad [4]$$

Eq. [1] can be solved by using the separation-of-variable method to give

$$\frac{C - C_o}{C_1 - C_o} = 1 + \frac{2R}{\pi r}\sum_{n=1}^{\infty}\frac{(-1)^n}{n}\sin\frac{n\pi r}{R}\exp\left(-\frac{n^2\pi^2 Dt}{R^2}\right) \qquad [5]$$

The amount of uptake, M_t, relative to the amount of uptake after infinite time, M_∞, is expressed by the relationship

$$\frac{M_t}{M_\infty} = 1 - \frac{6}{\pi^2}\sum_{n=1}^{\infty}\frac{1}{n^2}\exp\left(-\frac{n^2\pi^2 Dt}{R^2}\right) \qquad [6]$$

Diffusion coefficients can then be determined by using Eq. [6] to match the measured uptake data as a function of time. This was done by injecting a gas into the system at a specific pressure and obtaining the amount of uptake at specified times. A diffusion coefficient was calculated for each value of uptake and time. As many as thirty values of the diffusivity were obtained for each pressure and temperature.

RESULTS AND DISCUSSION

Diffusion coefficients were measured for chloromethane, dichloromethane, trichloromethane, tetrachloromethane, 1,1,1-trichloroethane, and tetrachloroethylene on spherical silica gel beads at 288, 293, and 298K, after overnight regeneration of the adsorbent at 423K in vacuo. The weight of the sample was measured to within 10 μg. Since the regenerated sample weight was 0.1098g, the error in the weight measurement was 0.0091%. The average error during the entire diffusion process was estimated to be less than 1%. Several of the data were reproduced with an error no greater than 1%. The maximum uptakes for all of the chlorinated hydrocarbon-silica gel bead systems agreed very well with those obtained for the adsorption isotherms in the previous studies (18,19). Therefore, the spherical silica gel beads used in this study may be considered to be representative of the diffusion through other similar silica gels. The experimental uptake versus time data for chloromethane, dichloromethane, trichloromethane, tetrachloromethane on a 0.440 cm diameter spherical silica gel bead at 288, 293, and 298K are shown in Figures 2 through 4 while the experimental uptake versus time data for 1,1,1-trichloroethane and tetrachloroethylene on a 0.398 cm diameter spherical silica gel bead at 288, 293, and 298K are shown in Figures 5 through 7. As can be seen from the figures, the spherical silica gel beads were saturated faster with the lighter chlorinated hydrocarbons than with the heavier ones. This is reasonable considering that heavier materials usually diffuse slower than the lighter materials. The effect of temperature on the rate of saturation for a specific chlorinated hydrocarbon could be seen by comparing Figures 2-4 and Figures 5-7. It was found that for all the chlorinated

hydrocarbons, the spherical silical gel beads were saturated faster at higher temperatures as a result of the higher diffusion rates.

The experimental uptake versus time data for all the chlorinated hydrocarbons were correlated using Eq. [6]; average values for the calculated effective diffusion coefficients are shown in Table I. As can be seen from the data, the maximum deviation for any of the calculated effective diffusion coefficients differs by only 3.42% from the average value. Average effective diffusion coefficients for all of the chlorinated hydrocarbons fall in the range of 10^{-9} to 10^{-10} m^2/s, which is the characteristic of physical adsorption processes (17). The magnitude of the effective diffusion coefficients decreased as the molecular weight of chlorinated hydrocarbons increased. The effective diffusion coefficient for each chlorinated hydrocarbon was plotted with respect to the molecular diffusion volume (13); the result is shown in Figure 8. It can be seen from the figure that the effective diffusion coefficients for all the chlorinated hydrocarbons fall on a single curve for each temperature. This suggests that these curves may be used to predict the effective diffusion coefficients of similar chlorinated hydrocarbons through silica gel beads.

The effects of pressure on the effective diffusion coefficient was investigated by measuring the effective diffusion coefficients of chloromethane through silica gel bead at 25°C for three pressures. The effective diffusion coefficients were found to be 1.336×10^{-9} m^2/s, 1.319×10^{-9} m^2/s and 1.320×10^{-9} m^2/s when the gas pressure in the system was 626 mmHg, 378 mmHg, and 257 mmHg, respectively. This indicates that the effective diffusion coefficients are a very weak function of concentration. Since all of the chlorinated hydrocarbon-silica gel

systems exhibited similar characteristics (18,19), it is assumed that the effect of pressure on the chloromethane-silica gel bead system was the representative of all of the chlorinated hydrocarbons.

The effects of temperature on the effective diffusion coefficients were also investigated. Table I shows that the effective diffusion coefficients for all of the chlorinated hydrocarbons are strong functions of system temperature, with the diffusion coefficients increasing as the system temperature increases. A plot of lnD versus reciprocal temperature is shown in Figure 9. It can be seen from the figure that these plots for all of the chlorinated hydrocarbons resulted in straight lines. This suggests that the effective diffusion coefficients for all the chlorinated hydrocarbons may be correlated by an Arrhenius-type expression

$$D = D_o \exp(-\frac{E_a}{RT}) \qquad [7]$$

where D is the measured effective diffusion coefficient, D_o is the preexponential or frequency factor, and E_a is the activation energy which may be visualized simply as the energy required to raise an atom over an energy barrier. According to Eq. [7], a plot of lnD versus 1/T should yield a straight line with a slope of $-E_a/R$ and an intercept of $\ln D_o$. Table II shows the correlated D_o and E_a values for all six hydrocarbons. The isosteric heats of adsorption for these chlorinated hydrocarbons were calculated by Kuo and Hines (18,19) in previous studies and are also included in Table II. As can be seen from the table, the activation Energy (E_a) is markedly lower than the isosteric

heats of adsorption (ΔH_s), which suggests the existence of surface transport in the diffusion process (11).

In order to analyze the diffusion mechanisms, the Kundsen diffusion coefficient, the gas diffusivity and surface diffusion coefficients for each diffusion system were calculated. Knudsen diffusion coefficients and gas diffusivities were calculated from kinetic theory (20) and the Equation of Fuller et al. (21), respectively, while the surface diffusion coefficient was determined by using the expression

$$\frac{1}{D} = \frac{1}{D_k} + \frac{1}{D_g} + \frac{1}{D_s} \qquad [8]$$

where D represents the observed effective diffusion coefficients; D_k is the Knudsen diffusion coefficients; D_g is the gas diffusivity; and D_s is the surface diffusion coefficient. Values for these diffusion coefficients are listed in Table III. As can be seen from the data, gas diffusivities for all the chlorinated hydrocarbons fall in the range of 10^{-5} to 10^{-7} m^2/s, and the Knudsen diffusion coefficients are in the range of 10^{-7} m^2/s. When comparing the combined effects of gas diffusion and Knudsen diffusion on the diffusion process with the observed effective diffusion coefficients, which falls in the range of 10^{-10} m^2/s, it was found that the resistances due to Knudsen and gas diffusion were much smaller than the overall diffusion resistance. The difference between the overall and the combined gas and Knudsen diffusion resistance is attributed to surface diffusion. Since the combined gas and Knudsen diffusion resistances contribute less than 1% to the overall diffusion resistance, it may be concluded that the

transport of all the chlorinated hydrocarbons through the silica gel beads was dominated by surface diffusion.

Surface diffusion is characterized by migration of the molecule from one surface site to another. However, in the multilayer adsorption region, the adsorbed film assumes a liquid-like character, and diffusion further into the pore probably occurs by movement of the molecules over each other. Testin and Stuart (1) and Sladek et al. (17) have shown that this diffusion is similar to liquid phase diffusion. In order to justify this liquid-like character for the systems investigated in this study, the liquid phase diffusion coefficients for all the chlorinated hydrocarbons was calculated by using Wilke and Chang Equation (22) and the result are included in Table III. The liquid phase diffusion coefficients are about 5 to 10 times larger than the surface diffusion coefficients. This difference is the result in the differences in the bonding energies associated with these two diffusion mechanisms. For liquid phase diffusion the only bonding energy that has to be overcome is the liquid intramolecule bonding energy, while for surface diffusion to occur, the energy barrier includes not only the liquid-liquid bonding energy but also the much stronger liquid-solid bonding energy, which is caused by the Van der Waals forces.

Table IV summarizes some of the results of surface diffusion data of various gas-silica gel systems given in the literature. The surface diffusivity data obtained in this study are also included for comparison. It is noted that the surface diffusion coefficients for all of the gases diffusing through silica gels are usually of the order 10^{-9} to 10^{-10}, except for nitrogen diffusion. Nemeth and Stuart (24) performed N_2 diffusion through silica gels and claimed that it was

reasonable to obtain higher diffusion coefficients when the adsorption layer becomes fluid enough in the multilayer region. The surface diffusion coefficients of CF_2Cl_2 studied by Carman and Raal (23) were found to be of the order of 10^{-9}, which are of the same order of magnitude as the surface diffusion coefficients of the chlorinated hydrocarbons investigated in this study. Comparisons of the surface diffusion coefficients of the chlorinated hydrocarbons obtained in this study with these for other gases showed that the surface diffusion coefficients for all of the adsorbates listed in Table IV are of the same order of magnitude. This suggests that when silica gel is used as the adsorbent, the diffusion mechanisms for most of the gases listed in Table IV are very similar and surface diffusion may be the rate-determining step for the diffusion processes.

CONCLUSIONS

The uptake versus time data and the diffusion coefficients of six chlorinated hydrocarbons through spherical silica gel beads were studied using a gravimetric apparatus at temperatures of 288, 293, and 298K. The effective diffusion coefficients for all the chlorinated hydrocarbons fell on a single curve for a fixed temperature, which suggests that the effective diffusion coefficient curve may be used to predict the diffusion coefficients for other similar chlorinated hydrocarbons through silica gel. Temperature effects on the diffusion coefficients were significant while pressure effects on the diffusion coefficients was found to be very small which indicated that the diffusion coefficients for all the chlorinated hydrocarbons in silica gel beads are very weak functions of concentration. Thus, the diffusion

coefficients for all of the systems investigated may be treated as though they are independent of concentration at specific temperatures. The diffusion rate controlling step was found to be surface diffusion while the effects of gas and Knudsen diffusions were found to be less significant. Surface diffusion coefficients were found to be within an order of magnitude of the liquid phase diffusion coefficients, which suggests that surface diffusion exhibits liquid-like characteristics for multimolecular layer coverage of the solids.

NOTATIONS

C	=	Concentration profile of chlorinated hydrocarbons inside a spherical bead
C_o	=	Initial gas concentration
C_1	=	Surface concentration of gas
D	=	Effective diffusion coefficient
D_g	=	Gas diffusivity
D_k	=	Knudsen diffusion coefficient
D_ℓ	=	Liquid diffusivity
D_o	=	Preexponential or frequency factor
D_s	=	Surface diffusion coefficient.
E_a	=	Activation energy of surface diffusion
ΔH_s	=	Isosteric energy of adsorption
M_t	=	Amount of uptake
M_∞	=	Amount of uptake at $T \rightarrow \infty$
R	=	Radius of a spherical bead
T	=	Temperature

REFERENCES

1. R. F. Testin and E. B. Stuart, Chem. Eng. Progr. Symposium, Ser. No. 74, 63, 10 (1966).

2. R. Leyva-Ramos and C. J. Geankoplis, Chem. Eng. Sci., 40, 799 (1985).

3. J. W. McBain, Trans. Faraday Soc., 14, 202 (1919).

4. S. Brunauer, The Adsorption of Gases and Vapors, Princeton Univ. Press., N.J. (1945).

5. V. Ponec, Z . Knor, and S. Cerny, Adsorption on Solids, Butterworth, London (1974).

6. D. M. Ruthven and K. F. Loughlin, Chem. Eng. Sci., 26, 577 (1971).

7. Y. H. Ma and T. Y. Lee, AIChE J., 22, 147 (1976).

8. M. Kodrik and A. Zikanova, Ind. Eng. Chem. Fundam., 13, 347 (1974).

9. E. Ruckenstein, A. S. Vaidyanathan, and G. R. Youngquist, Chem. Eng. Sci., 26, 1305 (1971).

10. M. M. Dubinin, I. T. Erashko, O. Kadlec, V. I. Ulrn, A. M. Voloshchuk, and P. P. Zolotarev, Carbon, 13, 193 (1975).

11. L. K. Lee, H. Yucel, and D. M. Ruthven, Molecular Sieves II, ACS Symposium Series No. 40, 417 (1977).

12. Krückels, W. W., Chem. Eng. Sci., 28, 1565 (1973).

13. E. N. Fuller, P. D. Schettler, and J. C. Giddings, Ind. Eng. Chem., 58, 19 (1966).

14. D. R. Garg and D. M. Ruthven, Chem. Eng. Sci., 27, 417 (1972).

15. E. R. Gilliland, R. F. Baddour, G. P. Perkinson, and K. J. Sladek, Ind. Eng. Chem. Fundam., 13, 95 (1974).

16. V. E. Wicke, Kolloid Z., 86, 167 (1939).

17. K. J. Sladek, E. R. Gilliland, and R. F. Baddour, J. Ind. Eng. Chem. Fundam., 13, 100 (1974).

18. S. L. Kuo and A. L. Hines, "Application of a New Heterogeneous Isotherm Model to Predict the Adsorption of Chlorinated Hydrocarbons on Silica Gel." Submitted for review, 1987.

19. S. L. Kuo and A. L. Hines, "Adsorption of 1,1,1-trichloroethane and Tetrachloroethylene on Silica Gel." Submitted for review, 1987.

20. J. M. Smith, Chemical Engineering Kinetics, McGraw-Hill Inc., New York (1970).

21. E. N. Fuller, P. D. Schettler, and J. C. Giddings, Ind. Eng. Chem., 58, 19 (1966).

22. C. R. Wilke and P. Chang, AIChE J., 1, 264 (1955).

23. P. C. Carman and F. A. Raal, Proc. Roy. Soc. 201A, 38 (1951).

24. E. J. Nameth and E. B. Stuart, AIChE J., 16, 999 (1970).

25. P. Schneider and J. M. Smith, AIChE J., 14, 886 (1968).

26. R. A. W. Haul, Z Physik. Chem., 1, 153 (1954).

27. A. A. Pesaran, Ph.D. Thesis, University of California, Los Angeles, CA (1983).

LIST OF TABLES

TABLE I

Effective Diffusion Coefficients of Chlorinated Hydrocarbons through Spherical Silica Gel Beads

Adsorbate	T(°K)	Average Effective Diffusivity $Dx10^9(m^2/s)$	Maximum Deviation in the Calculated Effective Diffusion Coefficients
CH_3Cl	288	1.1162	2.62
	293	1.2179	2.89
	298	1.3227	3.01
CH_2Cl_2	288	0.5396	3.42
	293	0.5896	2.96
	298	0.6341	3.01
$CHCl_3$	288	0.2851	3.06
	293	0.3112	2.53
	298	0.3435	2.87
CCl_4	288	0.1486	2.57
	293	0.1615	2.85
	298	0.1824	3.10
$C_2H_3Cl_3$	288	0.1264	3.14
	293	0.1413	2.79
	298	0.1579	3.08
C_2Cl_4	288	0.1050	2.98
	293	0.1179	2.94
	298	0.1331	3.17

TABLE II

Activation Energy of Chlorinated Hydrocarbons

Adsorbate	$D_o x 10^7 (m^2/s)$	E_a(kcal/gmol)	ΔH_s(kcal/gmol)
CH_3Cl	1.7553	2.8944	6.2254
CH_2Cl_2	1.2205	3.1047	8.1868
$CHCl_3$	1.1072	3.3678	8.0674
CCl_4	0.7263	3.5482	7.1171
$C_2H_3Cl_3$	0.5951	3.7954	17.307
C_2Cl_4	0.2323	4.0446	13.685

TABLE III

Diffusion Coefficients of Chlorinated Hydrocarbons

Adsorbate	T(^{o}K)	$D_g x10^7$ (m^2/s)	$D_k x10^7$ (m^2/s)	$D_s x10^9$ (m^2/s)	$D_\ell x10^9$ (m^2/s)
CH_3Cl	288	5.185	2.549	1.124	7.559
	293	4.542	2.570	1.227	7.967
	298	5.207	2.592	1.333	8.405
CH_2Cl_2	288	14.163	1.965	0.541	3.370
	293	13.897	1.982	0.592	3.572
	298	15.039	1.999	0.636	3.791
$CHCl_3$	288	38.539	1.658	0.285	2.580
	293	31.338	1.672	0.312	2.698
	298	37.251	1.686	0.344	2.935
CCl_4	288	42.050	1.460	0.149	1.488
	293	46.100	1.473	0.163	1.621
	298	43.760	1.485	0.183	1.769
$C_2H_3Cl_3$	288	18.135	1.568	0.127	1.087
	293	19.825	1.582	0.141	1.211
	298	22.803	1.595	0.158	1.334
C_2Cl_4	288	134.762	1.406	0.105	0.808
	293	133.910	1.419	0.118	0.889
	298	160.906	1.431	0.133	0.984

TABLE IV

Surface Diffusivities of Various Gas-Silica Gel Systems

Adsorbate	Temperature (^{o}K)	$D_s(m^2/s)$	Reference
CF_2Cl_2	251.7	$1.9\text{-}7.0\times10^{-9}$	(23)
SO_2	273.2	$2.6\text{-}9.2\times10^{-9}$	(23)
N_2	90.6	$1.7\text{-}9.6\times10^{-8}$	(24)
	109.5	$1.3\text{-}4.2\times10^{-7}$	(24)
CH_4	323.2	5.5×10^{-9}	(25)
C_3H_8	323.2	1.5×10^{-9}	(25)
nC_4H_{10}	323.2	7.3×10^{-9}	(25)
	2.63-323.2	$16\text{-}5.4\times10^{-9}$	(26)
H_2O	303.2	$0.03\text{-}0.30\times10^{-9}$	(27)
	333.2	$0.50\text{-}0.59\times10^{-9}$	(27)
$CHCl_3$	288-293	$1.12\text{-}1.33\times10^{-9}$	(this work)
CH_2Cl_2	288-293	$0.54\text{-}0.64\times10^{-9}$	"
$CHCl_3$	288-293	$0.29\text{-}0.34\times10^{-9}$	"
CCl_4	288-293	$0.15\text{-}0.18\times10^{-9}$	"
$C_2H_3Cl_3$	288-293	$0.13\text{-}0.16\times10^{-9}$	"
C_2Cl_4	288-293	$0.11\text{-}0.13\times10^{-9}$	"

LIST OF FIGURES

SYMBOLS INDEX FOR FIGURE 1

A	Adjustable relief valve - 1/4"
B	Needle valve - 1/4"
C	Bellows vacuum valve - 1/4"
D	Bellows vacuum valve - 1/2"
E	Bellows vacuum valve - 1/2"
F	Bellows vacuum valve - 1/2"
G	Needle valve - 1/4"
H	Needle valve - 1/4"
BF	Constant temperature bath or furnace
CU	Balance control unit
DIT	Dry ice trap
DP	Difussion pump
FB	Feed bottle
HT	Hangdown tube
MP	Mechanical vacuum pump, holding pump
RC	Recorder
RP	Mechanical vacuum pump, roughing pump
TVG	Thermistor vacuum gauage
WTG	Wallace and Tiernan gauge

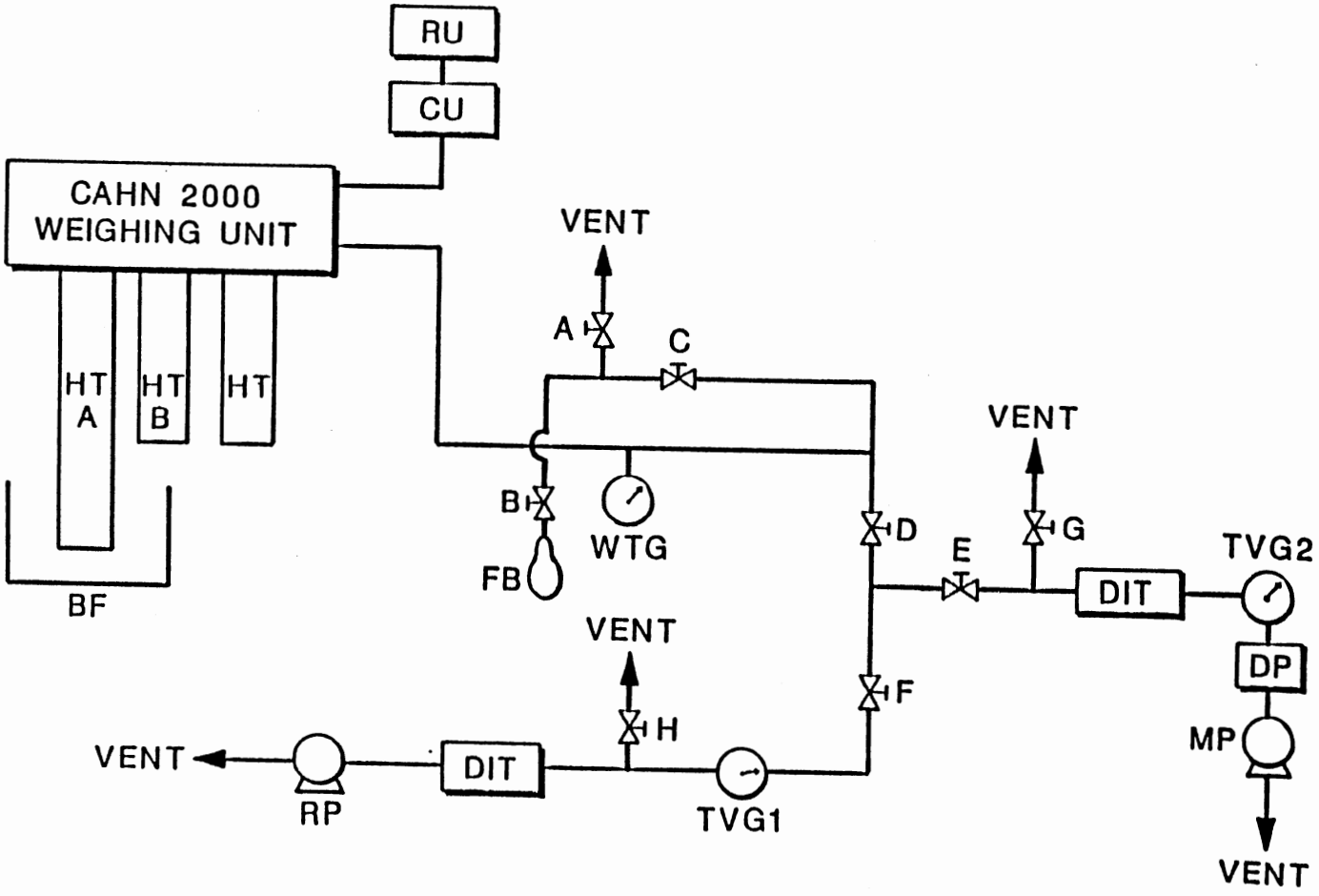

Figure 1. Schematic Diagram of Experimental Apparatus.

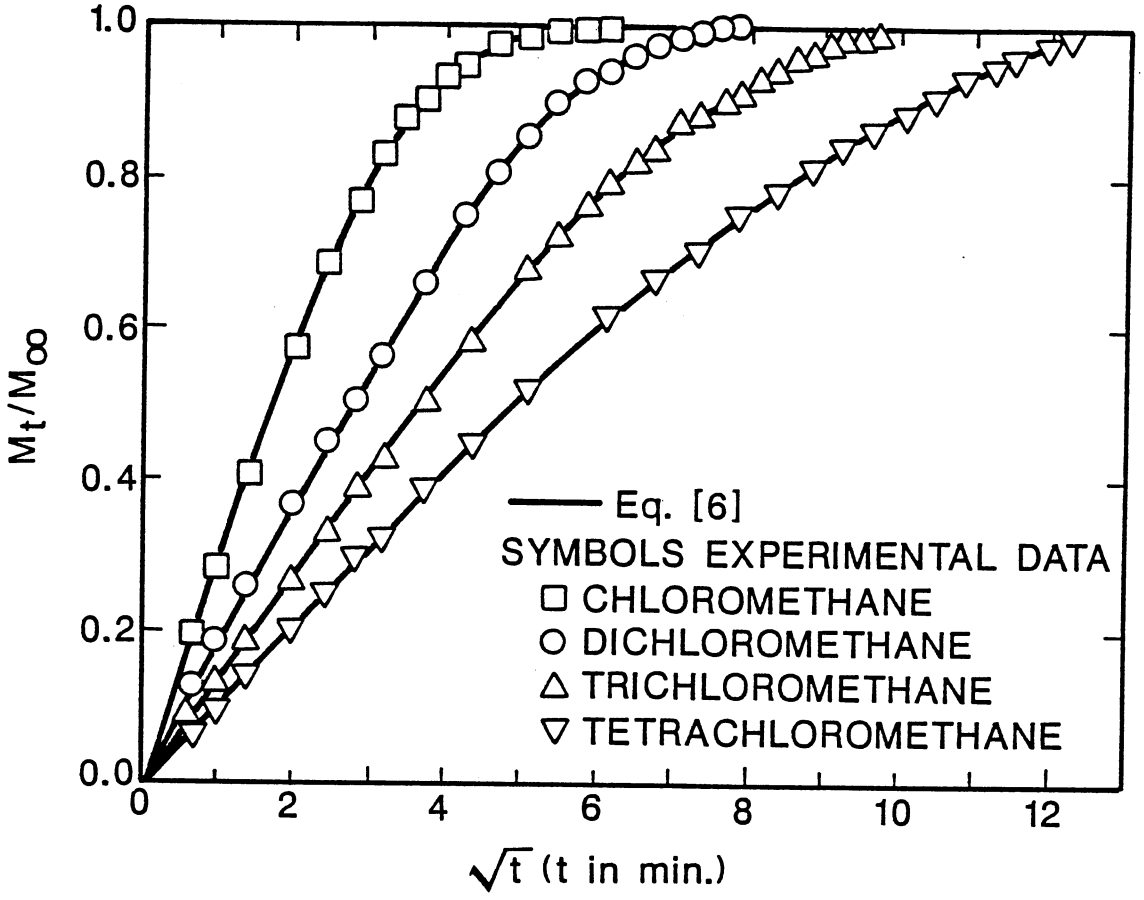

Figure 2. Adsorption Curve for Chloromethane, Dichloromethane, Trichloromethane, and Tetrachloromethane on 0.440 cm Diameter Spherical Silica Gel Bead at 288K.

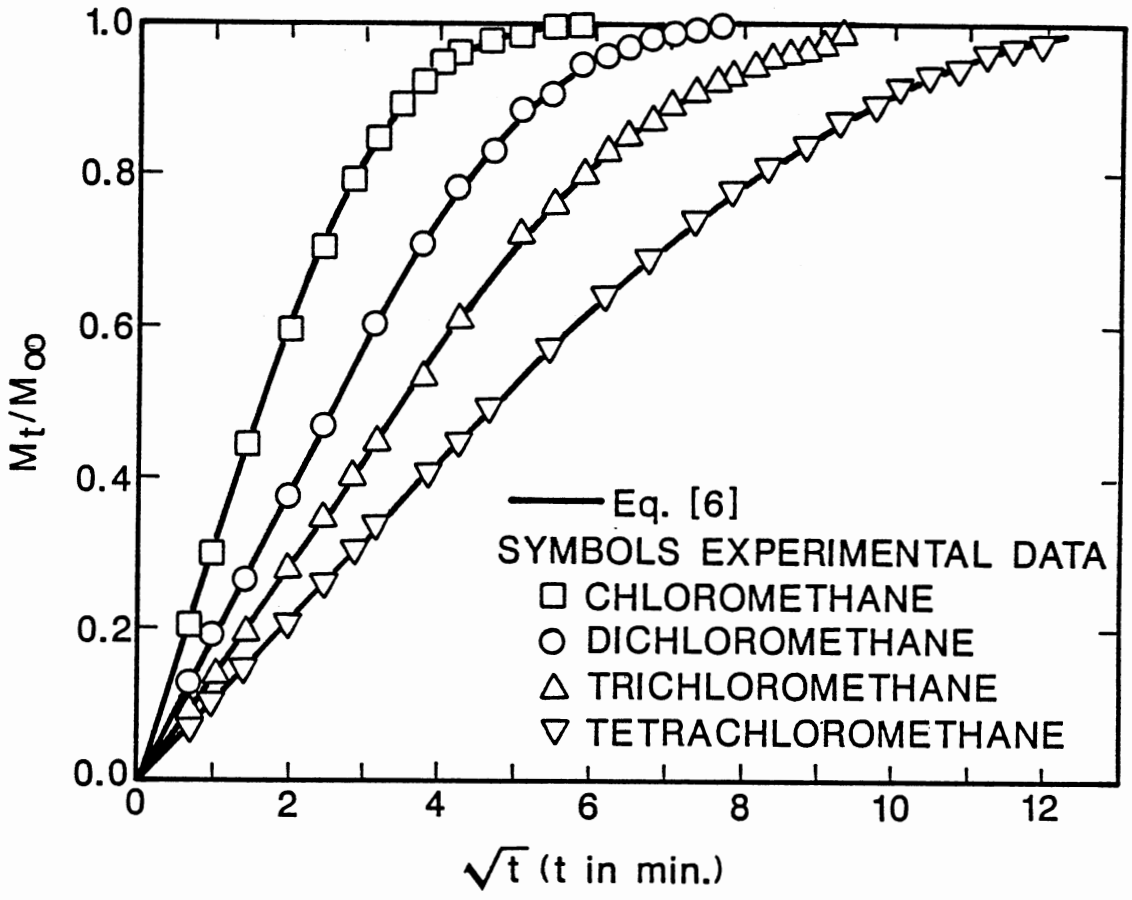

Figure 3. Adsorption Curve for Chloromethane, Dichloromethane, Trichloromethane, and Tetrachloromethane on 0.44 cm Diameter Spherical Silica Gel Bead at 293K.

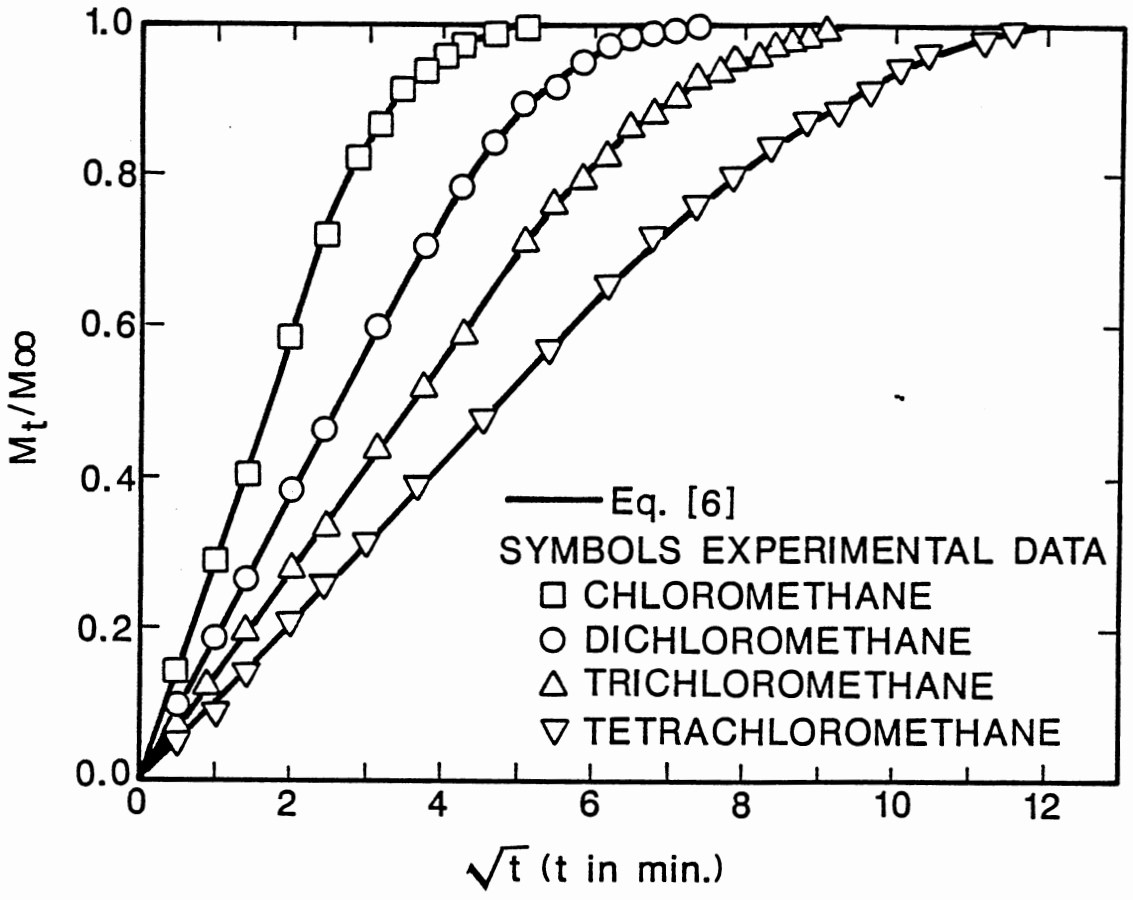

Figure 4. Adsorption Curve for Chloromethane, Dichloromethane, Trichloromethane, and Tetrachloromethane on 0.44 cm Diameter Spherical Silica Gel Bead at 298K.

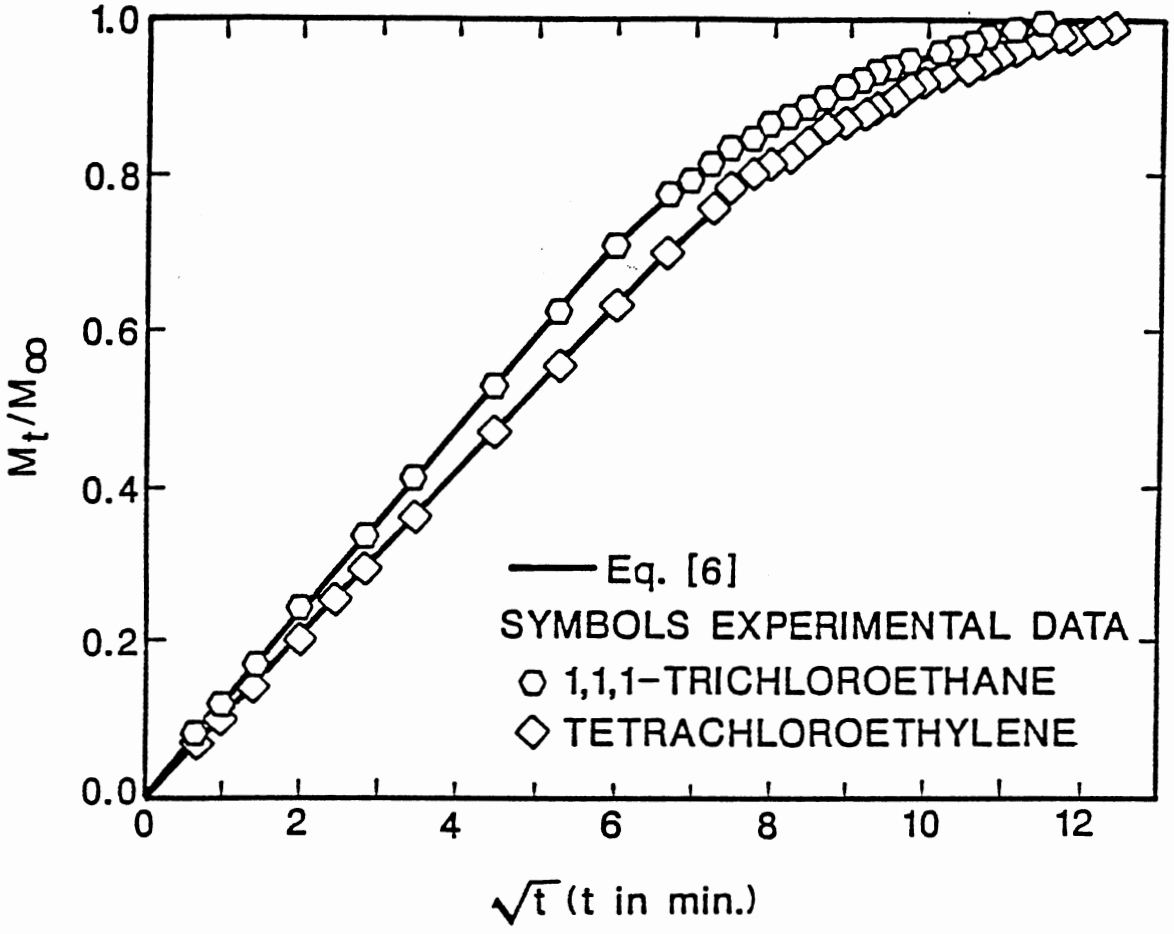

Figure 5. Adsorption Curve for 1,1,1-Trichloroethane and Tetrachloroethylene on 0.398 cm Diameter Spherical Silica Gel Bead at 288K.

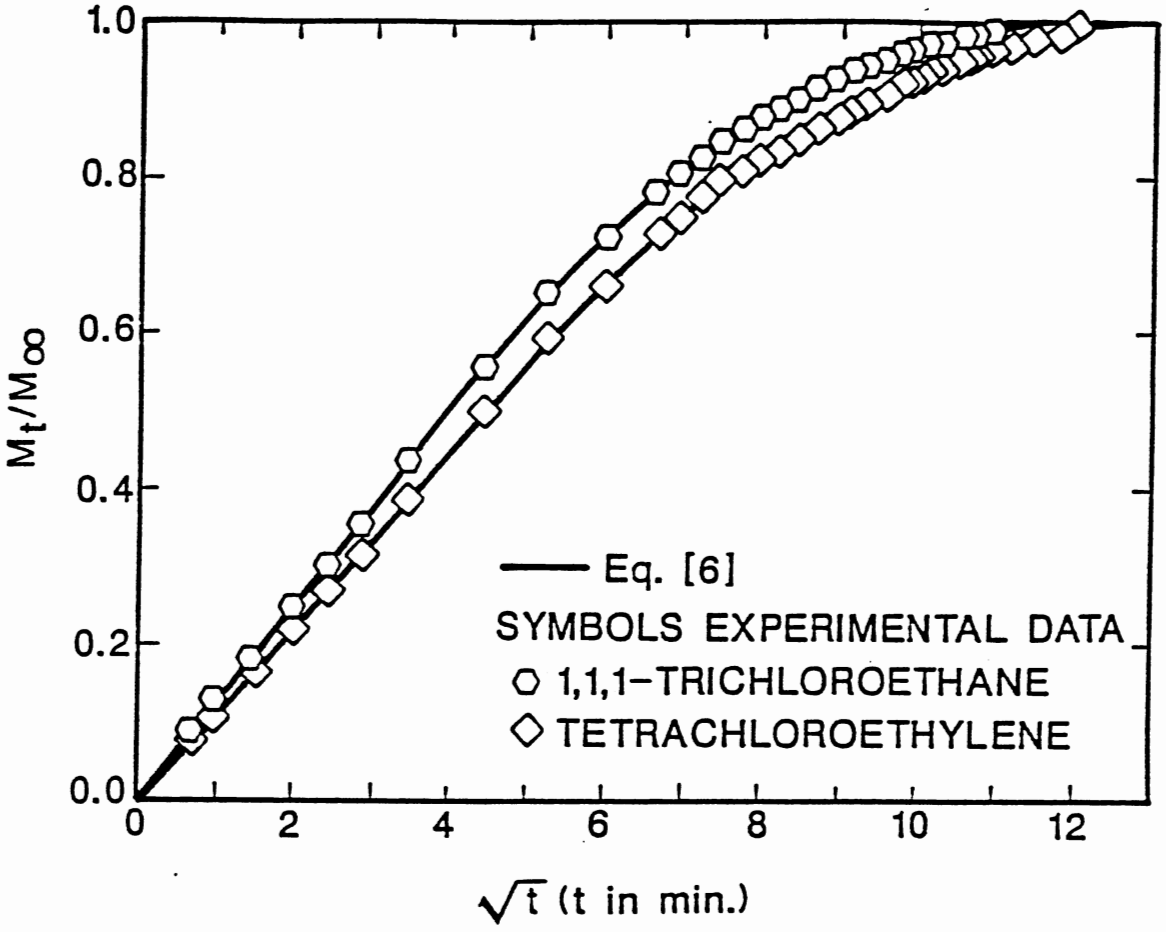

Figure 6. Adsorption Curve for 1,1,1-Trichloroethane and Tetrachloroethylene on 0.398 cm Diameter Spherical Silica Gel Bead at 293K.

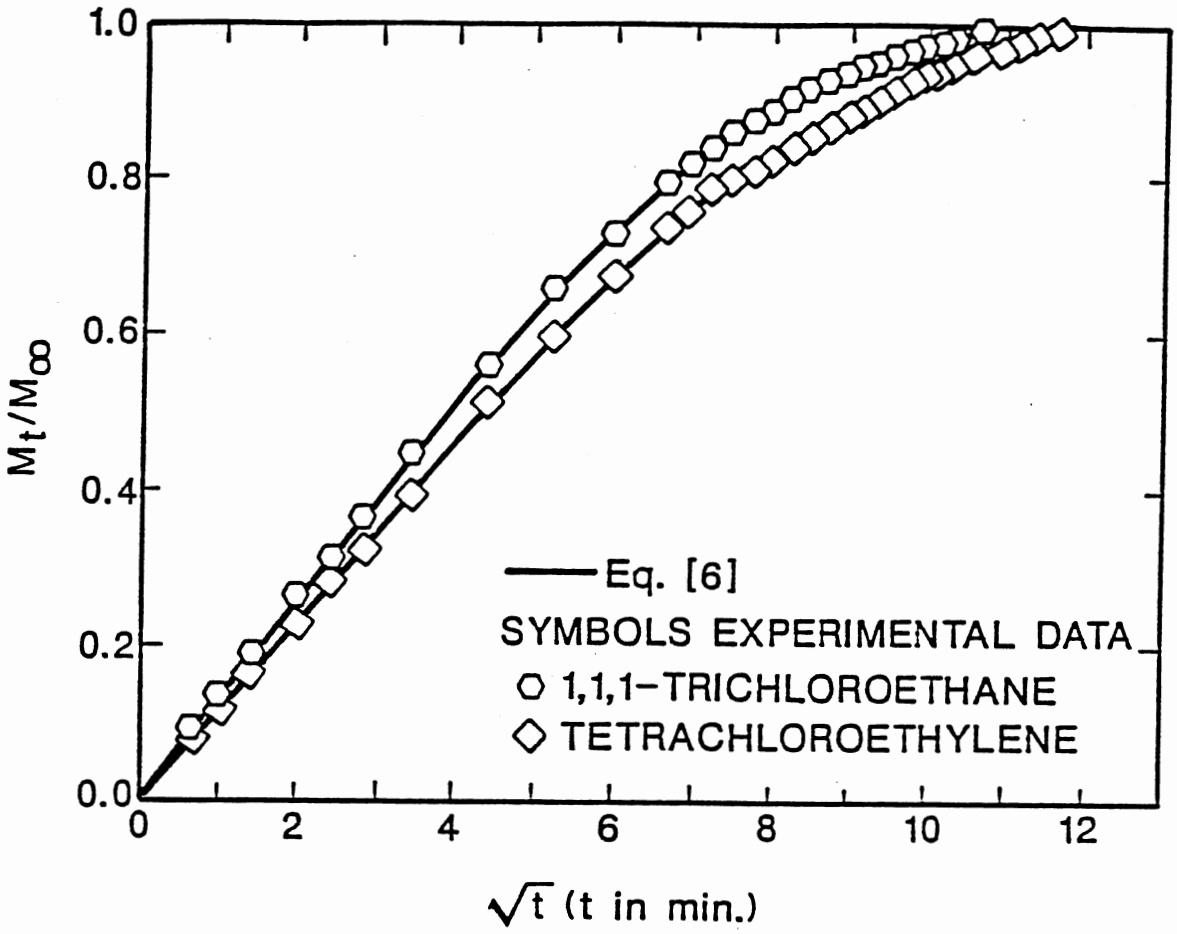

Figure 7. Adsorption Curve for 1,1,1-Trichloroethane and Tetrachloroethylene on 0.398 cm Diameter Spherical Silica Gel Bead at 298K.

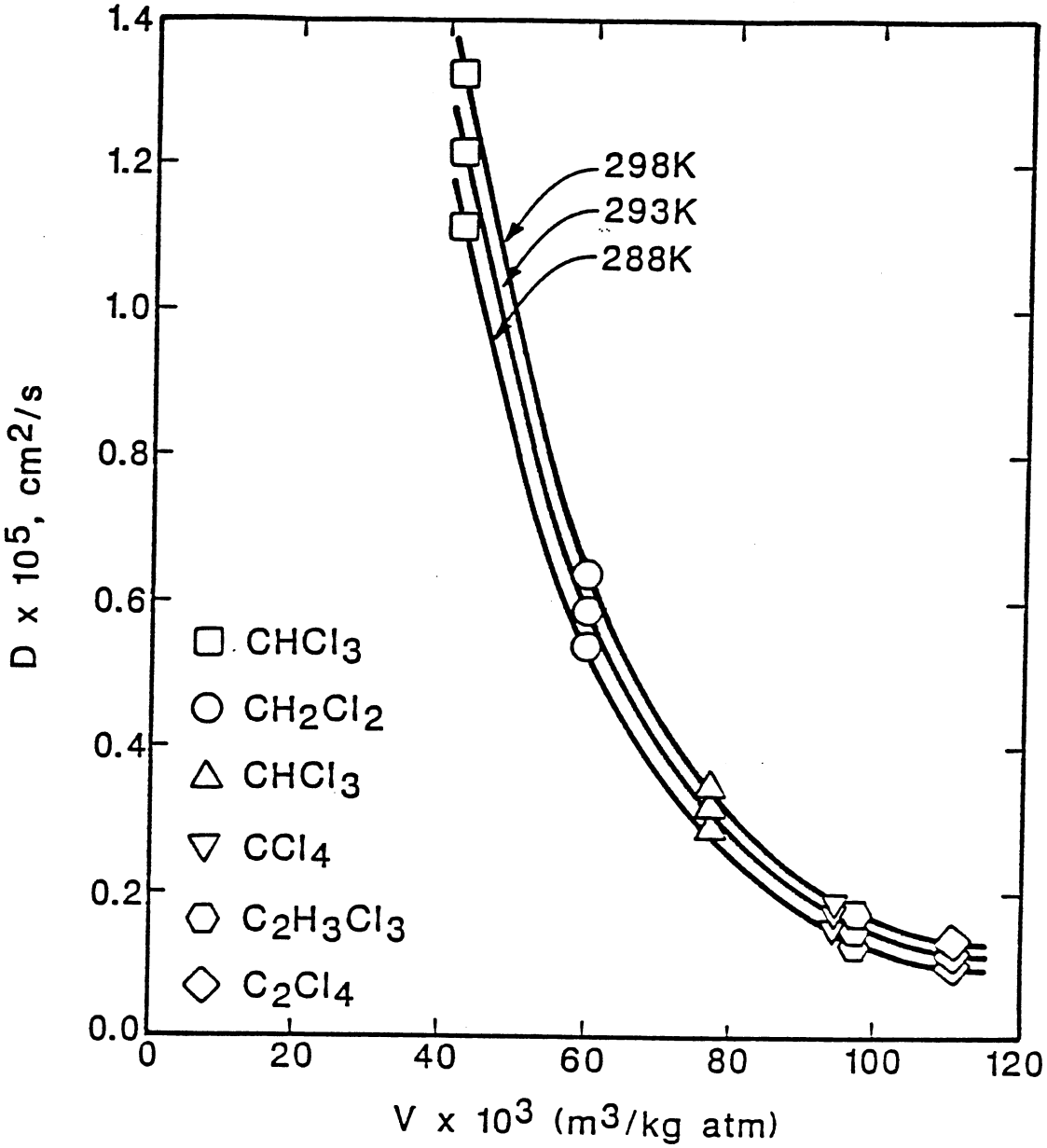

Figure 8. Plots of Diffusion Coefficients as a Function of Molecular Diffusion Volumes.

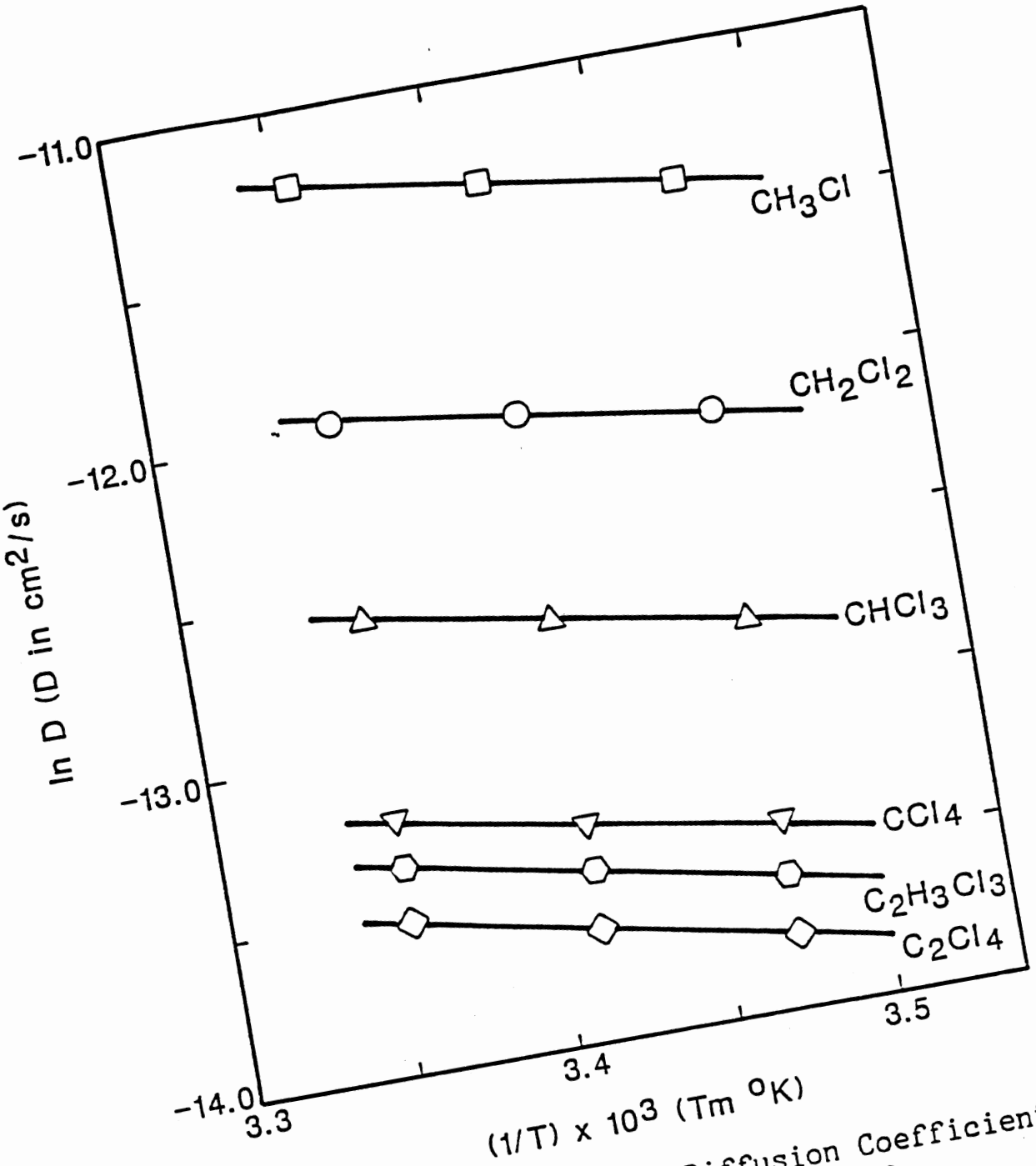

Figure 9. Variation of Diffusion Coefficients with System Temperature

CHAPTER VII

CONCLUSIONS AND RECOMMENDATIONS

CONCLUSIONS

The following conclusions can be drawn from the results of this work:

1. The removal of six chlorinated hydrocarbon pollutants on silica gel was performed and the results suggested that silica gel can be effectively used to remove pollutant from dry air.

2. A new theoretical heterogeneous isotherm, using the local Jovanovic isotherm and a Morse-type probability density function, was developed and tested. The new analytical isotherm developed in this study provides an excellent correlation of the experimental adsorption data for various gas-solid systems. A comparison of the new model with other heterogeneous isotherm equations showed that the new model gives a more accurate and yet simpler description of adsorption behavior on heterogeneous adsorbents.

3. The isotherm data for the adsorption of six chlorinated hydrocarbons on silica gels were correlated by using the new adsorption isotherm model as well as Langmuir and BET models. It was found that new isotherm model provided the best correlation of the experimental isotherm data. The Langmuir model provided better correlations for the isotherm data for the heavier adsorbates than for lighter ones, while the BET model provided good correlations to the isotherm data only up to 35% saturation pressure for each adsorbate.

4. Diffusion studies of the chlorinated hydrocarbons in spherical silica gel beads showed that the diffusion rate controlling step was surface diffusion while the effects of gas and Knudsen diffusions were found to be less significant. Surface diffusion coefficients were found

to be within an order of magnitude of the liquid phase diffusion coefficients.

RECOMMENDATIONS

For further investigation the following recommendations are made:

1. Extend the adsorption studies to other indoor air pollutants such as formaldehyde and radon gas.

2. A study should be undertaken to measure the effect of water vapor on the adsorption of chlorinated hydrocarbons.

3. Competitive adsorption that include two or more chlorinated hydrocarbons should be performed in future studies.

4. Adsorption studies of chlorinated hydrocarbons on adsorbents other than the silica gels used in this work should be made.

BIBLIOGRAPHY

CHAPTER II

(1) U.S. News and World Report, Sept. 23, 71 (1985).

(2) Consumer Reports, October 600 (1985).

(3) Meyer, E., Chemistry of Hazardous Materials, Prentice-Hall, Englewood Cliffs, New Jersey (1977).

(4) Brunauer, S., P. H. Emmett, and E. J. Teller, Am. Chem. Soc., 60, 309 (1938).

(5) Brunauer, S., L. S. Deming, W. E. Deming, and E. J. Teller, Am. Chem. Soc., 62, 1723 (1940).

(6) Polamyi, M. Z. Physik, 2, 111 (1920).

(7) Polamyi, M., Verh. Deut. Physik, Ges., 18, 55 (1916).

(8) Dubinin, M. M., Chem. Rev., 60, 235 (1960).

(9) Bering, B. P., M. M. Dubinin, and V. V. Superinsky, J. Colloid Interface Sci., 21, 378 (1966).

(10) Bering, B. P., M. M. Dubinin, and V. V. Superinsky, J. Colloid Interface Sci., 38, 186 (1972).

(11) Dubinin, M. M., J. Colloid Interface Sci., 23, 487 (1967).

CHAPTER III

(1) Cerofolini, G. F., M. Jaroniec, and S. Sokolowski, J. Colloid and Polymer Sci., 256, 471 (1978).

(2) Hill, T. L., An Introduction to Statistical Thermodynamics, Addison-Wesley, Reading, Mass. (1955).

(3) House, W. A., and M. J. Jaycock, J. Colloid and Polymer Sci., 256, 52 (1978).

(4) Jaroniec, M., Surface Sci., 50, 553 (1975).

(5) Jaroniec, M., A. Patrykiejiew, and M. Borowko, Progress in Surface and Membrane Science, Vol. 14, Academic Press, New York (1981).

(6) Jovanovic, D. S., Kolloid-Z. Z. Polym., 235, 1203 (1969).

(7) Misra, D. N., J. Colloid Interface Sci., 43, 85 (1973).

(8) Misra, D. N., J. Chem. Phys., 52, 5499 (1970).

(9) Misra, D. N., Surface Sci., 18, 367 (1969).

(10) Morse, P. M., Phys. Rev., 34, 57 (1929).

(11) Ponec, V., Z. Knor, and S. Cerry, Adsorption on Solids, CRC Press, Ohio (1974).

(12) Reich, R., Ph.D. Dissertation, Georgia Institute of Technology, Georgia (1974).

(13) Ross, S., and I. D. Morrison, Surface Sci., 52, 103 (1975).

(14) Ross, S., and J. P. Oliver, On Physical Adsorption, Wiley, New York (1964).

(15) Rudzinski, W., and M. Jaroniec, Surface Science, 42, 552 (1974).

(16) Sing, K. S. W., Adsorption at the Gas/Solid Surface: Colloid Science I, Bertholomew Press, Dorking (1973).

(17) Sips, R., J. Chem. Phys., 18, 1024 (1950).

(18) Sircar, S., J. Colloid and Interface Sci., 101, 452 (1984).

(19) Sircar, S., J. Colloid and Interface Sci., 98, 306 (1984).

(20) Sircar, S., Carbon 19, 153 (1981).

(21) Sircar, S., and Gupta R., AIChE J., 27, 806 (1981).

CHAPTER IV

(1) Consumer Reports, October, 60 (1985).

(2) U. S. News and World Report, September, 71 (1985).

(3) Kuo, S. L. and A. L. Hines, "Adsorption of Chlorinated Hydrocarbon Pollutants on Silica Gel," Submitted for review (1987).

(4) Kuo, S. L. and A. L. Hines, "New Theoretical Isotherm for Adsorption on Heterogeneous Adsorbents," submitted for review (1987).

(5) Brunauer, S. The Adsorption of Gases and Vapors, Vol. 1, Princeton University Press, Princeton, New Jersey (1945).

(6) Rojas V., F. J., M.S. Thesis, Colorado School of Mines, Colorado (1981).

(7) Langmuir, I., J. Am. Chem. Soc., 38, 2221 (1916).

(8) Langmuir, I., J. Am. Chem. Soc., 39, 1848 (1917).

(9) Langmuir, I., J. Am. Chem. Soc., 40, 1361 (1918).

(10) Brunauer, S., P. H. Emmett, and E. Teller, J. Am. Chem. Soc., 60, 309 (1938).

(11) Sircar, S. and R. Gupta, AIChE J., 27, 806 (1981).

(12) Ross, S., and J. P. Oliver, On Physical Adsorption, Wiley, New York (1964).

(13) Sircar, S., J. Colloid and Interface Sci., 98, 306 (1984).

(14) Sircar, S., J. Colloid and Interface Sci., 101, 452 (1984).

(15) Jovanovic, D. S., Kolloid-Z. Z., Polym. 235, 1203 (1968).

(16) Morse, P. M., Phys. Rev., 34, 57 (1929).

CHAPTER V

(1) Consumer Reports, October, 60 (1985).

(2) U. S. News and World Report, September, 71 (1985).

(3) Kuo, S. L. and A. L. Hines, "Adsorption of Chlorinated Hydrocarbon Pollutants on Silica Gel," Submitted for review (1987).

(4) Kuo, S. L. and A. L. Hines, "Application of a New Heterogeneous Isotherm Model to Predict the Adsorption of Chlorinated Hydrodcarbons on Silica Gel." Submitted for review (1987).

(5) Kuo, S. L. and A. L. Hines, "New Theoretical Isotherm for Adsorption on Heterogeneous Adsorbents." Submitted for review (1987).

(6) Brunauer, S., The Adsorption of Gases and Vapors, Vol. 1, Princeton University Press, Princeton, New Jersey (1945).

(7) Rojas V., F. J., M.S. Thesis, Colorado School of Mines, Colorado (1981).

(8) Langmuir, I., J. Am. Chem. Soc., 38, 2221 (1916).

(9) Langmuir, I., J. Am. Chem. Soc., 39, 1848 (1917).

(10) Langmuir, I., J. Am. Chem. Soc., 40, 1361 (1918).

(11) Brunauer, S., P. H. Emmett, and E. Teller, J. Am. Chem. Soc., 60, 309 (1938).

(12) Sircar, S. and R. Gupta, AIChE J., 27, 806 (1981).

(13) Ross, S. and J. P. Oliver, On Physical Adsorption, Wiley, New York (1964).

(14) Jovanovic, D. S., Kolloid-Z. Z., Polym. 235, 1203 (1969).

(15) Morse, P. M., Phys. Rev., 34, 57 (1929).

CHAPTER VI

(1) Testin, R. F. and E. B. Stuart, Chem. Eng. Progr. Symposium, Ser. No. 74, 63, 10 (1966).

(2) Leyva-Ramos, R. and C. J. Geankoplis, Chem. Eng. Sci., 40, 799 (1985).

(3) McBain, J. W., Trans. Faraday Soc., 14, 202 (1919).

(4) Brunauer, S., The Adsorption of Gases and Vapors, Princeton Univ. Press., N.J. (1945).

(5) Ponec, V., Z . Knor, and S. Cerny, Adsorption on Solids, Butterworth, London (1974).

(6) Ruthven, D. M. and K. F. Loughlin, Chem. Eng. Sci., 26, 577 (1971).

(7) Ma, Y. H. and T. Y. Lee, AIChE J., 22, 147 (1976).

(8) Kodrik, M. and A. Zikanova, Ind. Eng. Chem. Fundam., 13, 347 (1974).

(9) Ruckenstein, E., A. S. Vaidyanathan, and G. R. Youngquist, Chem. Eng. Sci., 26, 1305 (1971).

(10) Dubinin, M. M., I. T. Erashko, O. Kadlec, V. I. Ulrn, A. M. Voloshchuk, and P. P. Zolotarev, Carbon, 13, 193 (1975).

(11) Lee, L. K., H. Yucel, and D. M. Ruthven, Molecular Sieves II, ACS Symposium Series No. 40, 417 (1977).

(12) Kruckels, W. W., Chem. Eng. Sci., 28, 1565 (1973).

(13) Fuller, E. N., P. D. Schettler, and J. C. Giddings, Ind. Eng. Chem., 58, 19 (1966).

(14) Garg D. R. and D. M. Ruthven, Chem. Eng. Sci., 27, 417 (1972).

(15) Gilliland, E. R., R. F. Baddour, G. P. Perkinson, and K. J. Sladek, Ind. Eng. Chem. Fundam., 13, 95 (1974).

(16) Wicke, V. E., Kolloid Z., 86, 167 (1939).

(17) Sladek, K. J., E. R. Gilliland, and R. F. Baddour, J. Ind. Eng. Chem. Fundam., 13, 100 (1974).

(18) Kuo, S. L. and A. L. Hines, "Application of a New Heterogeneous Isotherm Model to Predict the Adsorption of Chlorinated Hydrocarbons on Silica Gel." Submitted for review, 1987.

(19) Kuo, S. L. and A. L. Hines, "Adsorption of 1,1,1-trichloroethane and Tetrachloroethylene on Silica Gel." Submitted for review, 1987.

(20) Smith, J. M., Chemical Engineering Kinetics, McGraw-Hill Inc., New York (1970).

(21) Fuller, E. N., P. D. Schettler, and J. C. Giddings, Ind. Eng. Chem., 58, 19 (1966).

(22) Wilke, C. R. and P. Chang, AIChE J., 1, 264 (1955).

(23) Carman, P. C. and F. A. Raal, Proc. Roy. Soc. 201A, 38 (1951).

(24) Nameth, E. J. and E. B. Stuart, AIChE J., 16, 999 (1970).

(25) Schneider, P. and J. M. Smith, AIChE J., 14, 886 (1968).

(26) Haul, R. A. W., Z Physik. Chem., 1, 153 (1954).

(27) Pesaran, A. A., Ph.D. Thesis, University of California, Los Angeles, CA (1983).

APPENDIX A

SAMPLE CALCULATION FOR ENERGY PROBABILITY DENSITY FUNCTIONS

SAMPLE CALCULATION FOR ENERGY PROBABILITY DENSITY FUNCTIONS

Energy distribution on the adsorbent can be described by a modified Morse-type probability density function of the energy parameter g

$$\int_o^\infty \frac{K_1}{1-K_1K_2}\,[e^{-K_1g} - K_2e^{-g}]dg = 1$$

where the energy parameter g can be related to the Jovanovic parameter b_o and isosteric heat of adsorption q by the following expression:

$$g = b_o[\exp(q/RT) - 1]$$

Thus, for fixed values of b_o and K_2, the energy distribution function, E, can be expressed for different K_1 in either g or q/RT domains. For example, if we set $b_o = 1.0\times10^{-4}$ and $K_2 = -0.01$, the energy distribution function becomes

$$\int_o^\infty \frac{K_1}{1 + 0.01K_1}\,[e^{-K_1g} + 0.01e^{-g}]dg = 1.0$$

or

$$\int_o^\infty \frac{K_1}{1 + 0.01K_1}\,[e^{-K_1g} + 0.01e^{-g}]\,[g + b_o]d(\frac{q}{RT}) = 1.0$$

For the case in which $K_1 = 10$, the energy distribution function can be calculated by using either one of the two equations shown above. The results are

g	E(g)	q/RT	E(q/RT)
0	9.091	0	0
0.01	8.316	4.615	0.084
0.02	7.532	5.303	0.151
0.05	5.600	6.217	0.281
0.10	3.427	6.909	0.343
0.25	0.817	7.824	0.204
0.50	0.116	8.517	0.058
1.00	0.034	9.210	0.034

APPENDIX B

SAMPLE CALCULATION FOR PREDICTION OF ADSORPTION ISOTHERMS USING THE NEW HETEROGENEOUS ISOTHERM MODEL

SAMPLE CALCULATION FOR PREDICTION OF ADSORPTION ISOTHERMS USING THE NEW HETEROGENEOUS ISOTHERM MODEL

The equations proposed by the new heterogeneous model for correlating the adsorption isotherms are

$$N(p,T) = m[1 - e^{-b_o P}(\frac{1}{1 - K_1K_2})(\frac{K_1}{P + K_1} - \frac{K_1K_2}{P + 1})]$$

$$m[b_o + \frac{1 - K_1^2K_2}{K_1 - K_1^2K_2}] = K_\ell \qquad \text{as } p \to o$$

Before the new model can be used to predict the adsorption isotherms, the Henry's law constant, K_ℓ, for each adsorption system has to be calculated a priori. This can be done by plotting the uptake/pressure data versus the system pressure and exropolating the curve to zero pressure to obtain the Henry's law constant. This procedure usually requires only a few good low pressure data points. For the CH_3Cl - silica gel system at 298K, the Henry's law constant was calculated according to procdure discussed above and was found to have the value of 128 mmol/g atm. After the Henry's law constants were calculated, the equations shown above can be combined into the following equation:

$$N(P,T) = K_\ell[\frac{K_1 - K_1^2K_\ell}{b_o(K_1 - K_1^2K_2) + (1 - K_1^2K_2)}][1 - e^{-b_o P}(\frac{1}{1 - K_1K_2})(\frac{K_1}{P + K_1}) - \frac{K_1K_2}{P + 1})]$$

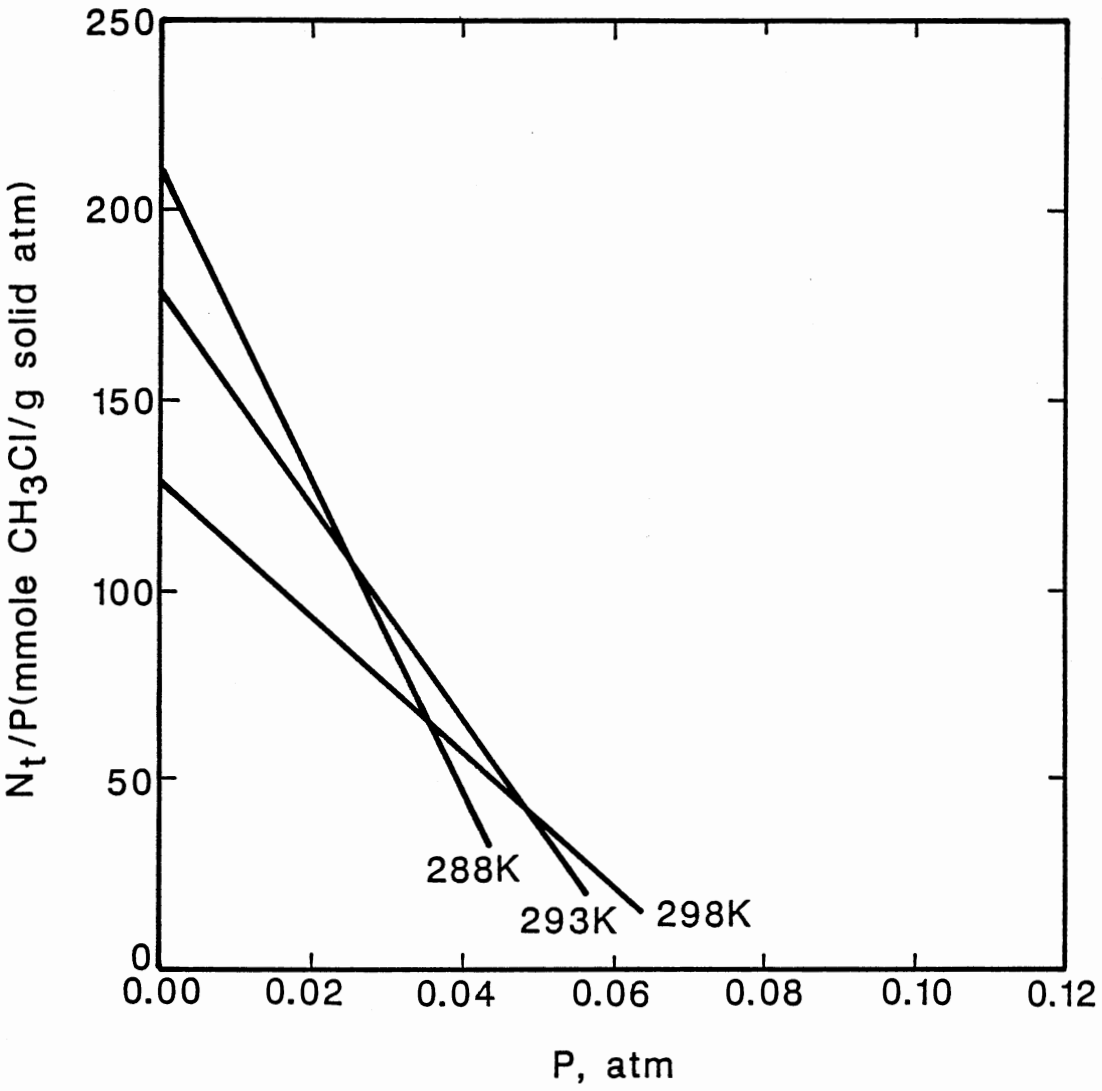
250
200
150
100
50
0
N_t/P(mmole CH_3Cl/g solid atm)
288K
293K
298K
0.00
0.02
0.04
0.06
0.08
0.10
0.12
P, atm

At this point, the new heterogeneous model is ready to be used to correlate the adsorption isotherm data. A trial and error procedure was used to obtain the best fit model parameters K_1 and K_2. A value of m and b_o were chosen and K_2 was calculated for different values of K_1. The entire isotherm was then generated. If the calculated isotherm was not within ±2% of the experimental data in the entire pressure range, a new value of m was chosen and the procedure repeated. For the CH_3Cl - silica gel system at 298K, the best fit model parameters were found to be:

$$K_1 = 250 \text{ mmHg}$$

$$K_2 = -0.00009 \text{ (mmHg)}^{-1}$$

$$b_o = 1.3158 \times 10^{-8} \text{ (mmHg)}^{-1}$$

$$m = 6.50 \text{ mmol/g}$$

Thus, the new isotherm model becomes

$$N(P,T) = 6.50\left[1 - 0.9780 \left(\frac{250}{P + 250} + \frac{0.0225}{P + 1}\right)\right]$$

The correlated isotherm data can be obtained by using the above equation and the results are:

P(mmHg)	N ($\frac{\text{mmol}}{\text{g}}$)
10	0.3745
50	1.1997
100	1.9593
150	2.5269
200	2.9683
250	3.3215
300	3.6104
400	4.0550
500	4.3810
600	4.6303
700	4.8269

APPENDIX C

SAMPLE CALCULATION FOR ISOSTERIC HEATS OF ADSORPTION

SAMPLE CALCULATION FOR ISOSTERIC HEATS OF ADSORPTION

The isosteric heats of adsorption were calculated at constant adsorbent loading from the relationship

$$\Delta H_s = R\left[\frac{\partial(\ell nP)}{\partial(1/T)}\right]_N$$

According to the above equation, a plot of ℓnP versus 1/T at constant adsorbent loading should yield a straight line with a slope of $\Delta H_s/R$. For the CH_3Cl - silica gel system at a loading of 2.0 gmmol/g solid, the corresponding temperatures and pressures were obtained from the experimental isotherms and are shown below.

P,mmHg	ℓnP	T(°K)	$1/T \times 10^3$
73	4.290	288	3.4722
87	4.466	293	3.4129
106	4.663	298	3.3557

After plotting these three data points, a straight line with a slope of $\Delta H_s/R = -3.202 \times 10^3$ was obtained. Therefore, the isosteric heat of adsorption can be calculated as shown:

$$\Delta H_s = -(3.202 \times 10^3)(1.987) = -6.36 \text{ cal/gmol}$$

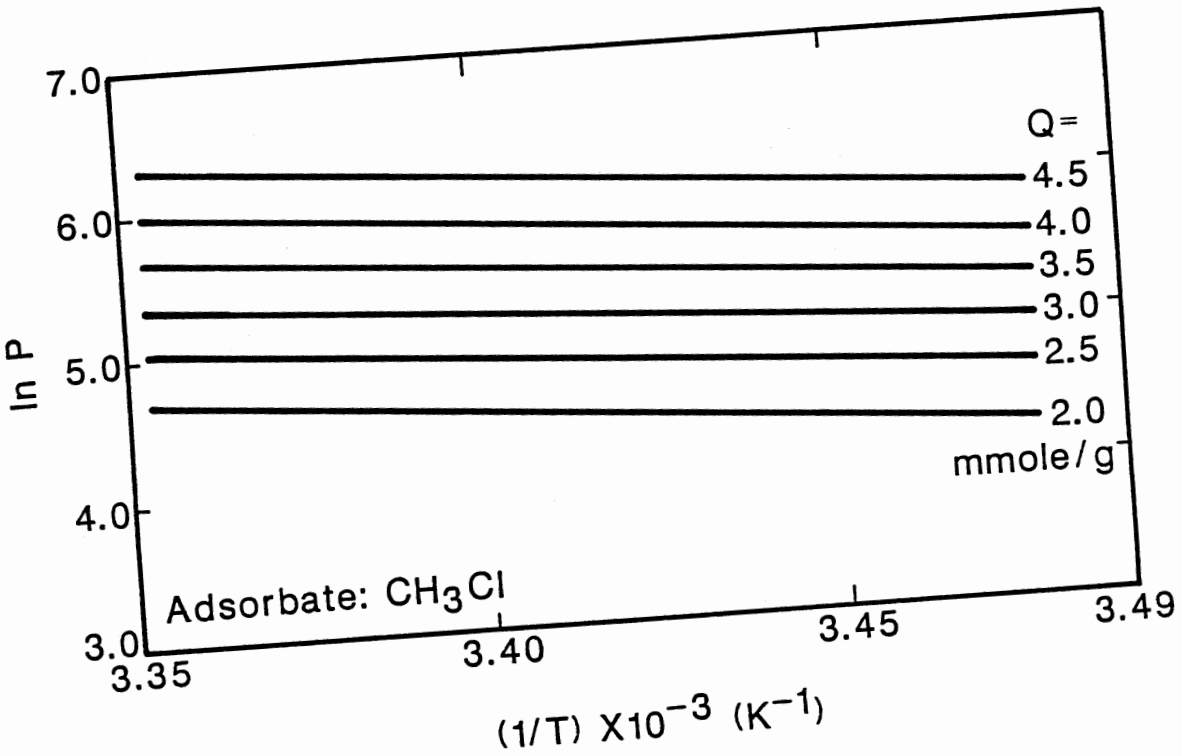
7.0
6.0
5.0
4.0
3.0
ln P
Q=
4.5
4.0
3.5
3.0
2.5
2.0
mmole/g
Adsorbate: CH_3Cl
3.35
3.40
3.45
3.49
(1/T) X10^{-3} (K^{-1})

APPENDIX D

SAMPLE CALCULATION FOR DIFFUSION COEFFICIENTS

SAMPLE CALCULATION FOR DIFFUSION COEFFICIENTS

Effective diffusion coefficients can be determined by using the equation

$$\frac{M_t}{M_\infty} = 1 - \frac{6}{\pi^2} \sum_{n=1}^{\infty} \frac{1}{n^2} \exp\left(-\frac{n^2 \pi^2 Dt}{R^2}\right)$$

To match the measured uptake data as a function of time. This was done by injecting a gas into the system at specific pressure and obtaining the amount of uptake at specific times. A diffusion coefficient was calculated for each value of uptake and time. As many as thirty values of the effective diffusivity were obtained for each pressure and temperature. Sample calculations are shown for the system CH_3Cl - silica gel bead at 298K and 112.6 mmHg.

For t = 1320 sec., $M_t/M_\infty = 0.9835$, and R = 0.220 cm, we have

$$0.9835 = 1 - \frac{6}{\pi^2} \sum_{n=1}^{\infty} \frac{1}{n^2} \exp\left[-\frac{n^2 \pi^2 D(1320)}{0.22 \times 10^{-2}}\right]$$

The effective diffusion coefficient can then be obtained from the equation shown above and the result is

$$D = 1.3401 \times 10^{-9} m^2/s$$

The complete uptake and time data were used to calculate the diffusion coefficients and the result is shown below

t(sec)	$\frac{M_t}{M_\infty}$	D x 10^{-9}(m^2/s)	Deviation from D_{avg} (%)
360	0.7479	1.2898	2.49
480	0.8132	1.2893	2.53
600	0.8791	1.3414	1.41
720	0.9176	1.3625	3.01
840	0.9341	1.3167	0.45
960	0.9560	1.3414	1.41
1080	0.9725	1.3459	1.75
1320	0.9835	1.3401	1.32
1560	0.9890	1.2871	2.69
1800	0.9945	1.3023	1.54
∞	1.0000	-	

$$D_{avg} = 1.3227 \times 10^{-9}$$

Knudsen diffusion occurs when a gas diffuses through a porous medium and the pores are very small or the gas density is very low, and the molecules collide more often with the walls than with each other. Knudsen diffusion coefficients are independent of the absolute pressure, and are directly proportional to the pore radius and the square root of temperature. A dimensional equation for Knudsen diffusion coefficient is

$$D_k = 97r\left(\frac{T}{M_A}\right)^{1/2} \quad m^2/s$$

For the CH_3Cl - silica gel bead system at 298K, the Knudsen diffusion coefficient is

$$D_k = (97)(11 \times 10^{-10})\left(\frac{298}{50.49}\right)^{1/2}$$
$$= 2.592 \times 10^{-7} m^2/s$$

Ordinary diffusion occurs when the molecules of the gas collide with each other more frequently than with the pore walls. The equation proposed by Fuller et al. (Reference 21, Chapter VI) can be used to

calculate the gas diffusion coefficients. Their equation, which results from a curve fit to available experimental data, is

$$D_{AB} = \frac{1.0 \times 10^{-9} T^{1.75}}{P[(\Sigma V)_A^{1/3} + (\Sigma V)_B^{1/3}]^2} \left(\frac{1}{M_A} + \frac{1}{M_B}\right)^{1/2} \quad m^2/s$$

For the CH_3Cl - silica gel bead system at 298K and 112.6 mmHg

$$T = 298K,\ P = 0.148\ atm,\ M_A = M_B = 50.49\ kg/kgmol$$

$$(\Sigma V)_A = (\Sigma V_B) = 16.5 + 3(1.98) + 19.5 = 41.94\ m^3/kgmol$$

Thus, the gas phase diffusion coefficient is

$$D_g = \frac{1.0 \times 10^{-9}(298)^{1.75}}{0.148\ [(41.94)^{1/3} + (41.94^{1/3})]^2} \left(\frac{1}{50.49} + \frac{1}{50.49}\right)^{1/2}$$

$$= 5.207 \times 10^{-7} m^2/s$$

Surface diffusion is the transport of adsorbed molecules along the adsorbent surface. Surface diffusion coefficients can be calculated from the following equation

$$\frac{1}{D} = \frac{1}{D_g} + \frac{1}{D_k} + \frac{1}{D_s}$$

where D_s is the surface diffusivity and D is the overal effective diffusion coefficient. For the CH_3Cl - silica gel bead system at 298K, the surface diffusion coefficient is

$$\frac{1}{D_s} = \frac{1}{D} - \frac{1}{D_g} - \frac{1}{D_k}$$

$$= \frac{1}{1.3227 \times 10^{-9}} - \frac{1}{5.207 \times 10^{-7}} - \frac{1}{2.592 \times 10^{-7}}$$

$$D_s = 6.305 \times 10^{-9}\ m^2/s$$

Finally, liquid phase diffusion coefficients can be calculated by using the Wilke and Change (Reference 22, Chapte VI) equation

$$D_{AB} = \frac{1.17 \times 10^{-13} (\xi_B M_B)^{1/2} T}{V_A^{0.6} \mu}$$

For $CH_3C\ell$ at 298K

$T = 298K$, $M_B = 50.49$ kg/kgmol, $\mu = 0.1768$ cP

ξ_B = association factor for the liquid = 1.0

$V_A = [14.8 + 3(3.7) + 24.6] \times 10^{-3} = 50.5 \times 10^{-3} m^3/kgmol$

Thus, the liquid phase diffusion coefficient is

$$D_{\ell} = \frac{1.17 \times 10^{-13} (1 \times 50.49)^{1/2} (298)}{(50.5 \times 10^{-3})^{0.6} (0.1768)} = 8.405 \times 10^{-9} \ m^2/s$$

APPENDIX E

SAMPLE CALCULATION OF ACTIVATION ENERGIES

SAMPLE CALCULATION OF ACTIVATION ENERGIES

Activation energy is visualized simply as the energy required to raise an atom over an energy barrier and it may be related to the effective diffusion coefficient and temperature by an Arrhenius expression

$$D = D_o \exp(-\frac{E_a}{RT})$$

where D is the effective diffusion coefficient, D_o is the preexponential or frequency factor, and E_a is the activation energy. According to the above equation, a plot of ℓnD versus 1/T should yield a straight line with a slope of $-E_a/R$ and an intercept of ℓnD_o. For the CH_3Cl - silica gel bead system, diffusion coefficients at each temperature were correlated by the Arrhenius expression shown above and the results are given below.

T(°K)	$1/Tx10^3$	$Dx10^9(m^2/s)$	ℓnD
288	3.4722	1.1162	-11.4030
293	3.4130	1.2179	-11.3158
298	3.5557	1.3227	-11.2333

After plotting these three data points, a straight line with an intercept of $\ell nD_o = 15.556$ and a slope of $-E_a/R = -1.4567x10^3$ was obtained. Thus, the preexponential factor and the activation energy are

$$D_o = 1.7553x10^{-7}\ m^2/s$$

$$E_a = 2.8944\ kcal/gmol$$

APPENDIX F

SAMPLE CALCULATION FOR BUOYANCY EFFECTS

Sample Calculation for Buoyancy Effects

The buoyancy effect on the sample weight, when working with the electrobalance, can be evaluated by applying the following equation:

$$b = m_s(\rho_g/\rho_s) - (V_{cw}\rho_g + C)$$

where

b = buoyance, g

m_s = mass of the sample, g

ρ_g = density of vapor or gas phase, g/cm^3

ρ_s = density of the sample, g/cm^3

V_{cw} = effective volume of counterweight, cm^3

C = correction term, g

The above equation represents the contributions of sample buoyancy, counterweight buoyance and the nonlinear effects such as thermomolecular flow.

For the CH_3Cl-silica gel system at 298K and 1 atm

m_s = 0.2137g

ρ_s = 0.7688 g/cm^3

ρ_g = 0.00206 g/cm^3

V_{cw} = 0.2 cm^3

$C \simeq 0$

Therefore, the buoyance effect for this system is

$$b = (0.2137)\left(\frac{0.00206}{0.7688}\right) - [(0.2)(0.00206) + 0] = 0.0001606g$$

The maximum error introduced by the buoyancy effect is

$$\frac{0.0001606g}{0.2137g} \times 100\% = 0.075\%$$

APPENDIX G

SAMPLE CALCULATION FOR MONOLAYER COVERAGE AND AREA OF AN ADSORBED MOLECULE

Sample Calculation for Monolayer Coverage and Area of an Adsorbed Molecule

The monolayer coverage can be calculated from the linear correlation given by the BET equation in the low pressure range.

$$\frac{P}{N_\ell(P_s - P)} = \frac{1}{N_m C} + \frac{C - 1}{N_m C}\frac{}{P_s}$$

For CCl_4 at 298K, P_s = 108 mmHg

The low pressure points are

P(mmHg)	N_ℓ(mmol/g)	P/P_s	$P/N_\ell(P_s - P)$
0.6	0.405	0.0056	0.01379
1.2	0.559	0.0111	0.0201
4.1	1.038	0.0380	0.0380

A plot of $P/ N_\ell (P_s - P)$ versus P/P_s gives

$$S = \text{slope} = 0.6365$$

$$I = \text{Y-axis intercept} = 0.011$$

$$C = \frac{S}{I} + 1 = \frac{0.6365}{0.011} + 1 = 58.868$$

$$N_m = \frac{1}{CI} = \frac{1}{(0.011)(58.868)} = 1.5443 \text{ (mmol/g)}$$

The number of layers, n, can be estimated using the adsorption data obtained in the neighborhood of the saturation pressure, since $N_\ell/N_m \sim n/2$. For CCl_4 at 298K and P/P_s = 0.766, N_ℓ = 2.680 mmol/g

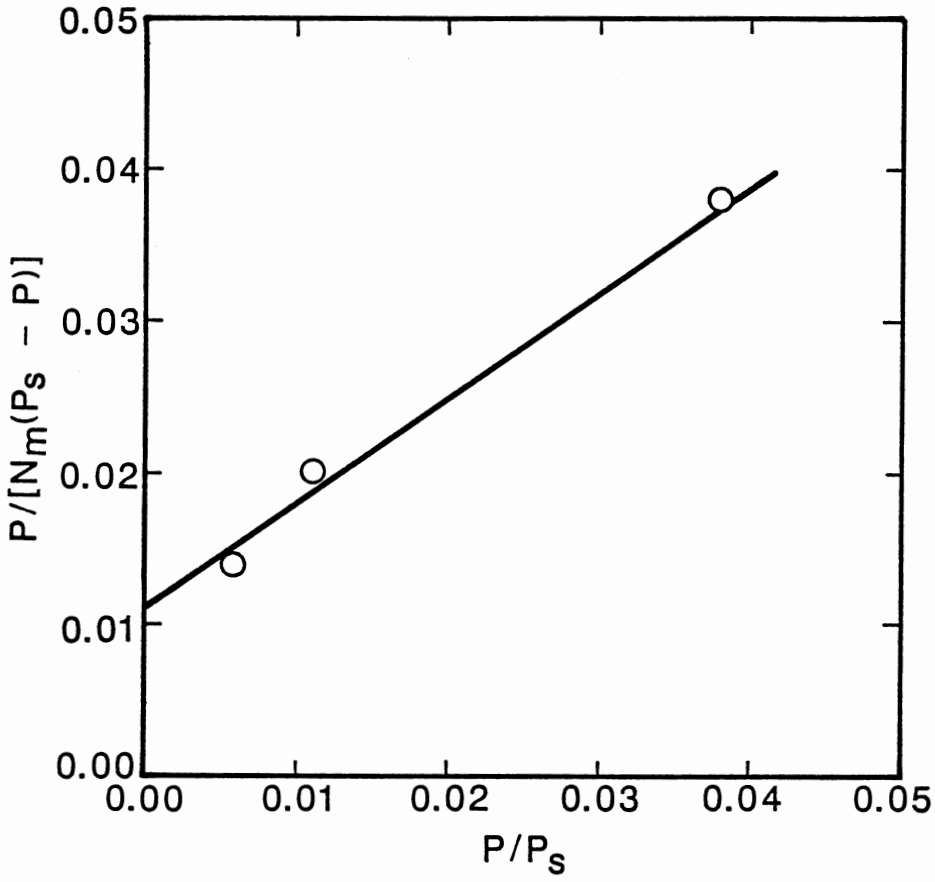
0.05
0.04
0.03
0.02
0.01
0.00
0.00
0.01
0.02
0.03
0.04
0.05
P/[Nm(Ps - P)]
P/Ps

$$\frac{n}{2} \sim \frac{2.680}{1.5443}$$

$$n \sim 4$$

The monolar coverage N_m can be readily coverted to the number of molecules adsorbed. For CCl_4 at 298K, the number of molecules adsorbed for a monolayer coverage is:

$$1.5443\ (\frac{gmol}{g})(\frac{gmol}{1000\ mmol})(\frac{6.02x10^{23}molecules}{gmol}) = 9.297x10^{20}molecules$$

For PA 40 silica gel, the surface area is ranging from 720 to 760 $m^{2/}g$. If we consider the surface area of silica gel can be respresented by the average values, i.e. 740 m^2/g in this case, the area occupied by one molecule of CCl_4 at 298K is:

$$A = 740\ \frac{m^2}{g} \times \frac{10^4 cm^2}{m^2} / 9.297x10^{20}molecules = 7.9598\ cm^2/g\ molecule$$

APPENDIX H

SAMPLE CALCULATIONS FOR PREDICTIONS OF ADSORPTION ISOTHERMS USING THE LANGMUIR MODEL

Sample Calculations for Predictions of Adsorption Isotherms Using the Langmuir Model

Langmuir model (Reference 7 - 9, Chapter IV) was used to correlate the equilibrium data. The Langmuir model, which can be derived by using statistical thermodynamics or kinetic considerations, has the form

$$N_{\ell} = \frac{maP}{1 + aP}$$

where N_{ℓ} is the equilibrium uptake, P is the pressure, the term m is a constant defined as the amount of adsorption which would saturate the unit surface with a monolayer, and the term a is a characteristic constant often defined as the "capillarity" of the substance. If P/N_{ℓ} is plotted versus P, a straight line should be obtained over the region in which Langmuir equation holds. This line will have a slope of 1/m and an intercept of 1/(am). The complete model parameters for all the six chlorinated hydrocarbons investigated are:

Adsorbate	T(°K)	m(mmol/g)	$a(mmHg)^{-1}$
CH_3Cl	288	6.2732	0.007199
	293	5.8792	0.007392
	298	5.9408	0.005461
CH_2Cl_2	288	5.4076	0.04361
	293	5.3687	0.03411
	298	5.1996	0.02922
$CHCl_3$	288	3.7571	0.1548
	293	3.6837	0.1376
	298	3.6169	0.1102
CCl_4	288	3.0344	0.2262
	293	2.9414	0.2015
	298	2.8753	0.1658

$C_2H_3Cl_3$	288	3.4714	0.6251
	293	3.4568	0.3725
	298	3.4475	0.2339
C_2Cl_4	288	2.9009	3.6992
	293	2.8540	2.9403
	298	2.7753	2.4164

The model parameters listed above were then used to correlate the experimenal data. Some of the results are shown in the next few pages for the sample calculations. As can be seen from the figures, Langmuir model did not successfully correlate the lighter chlorinated hydrocarbons. However, the Langmuir model provided better correlations for the equilibrium data as the molecular weight of the chlorinated hydrocarbon increased.

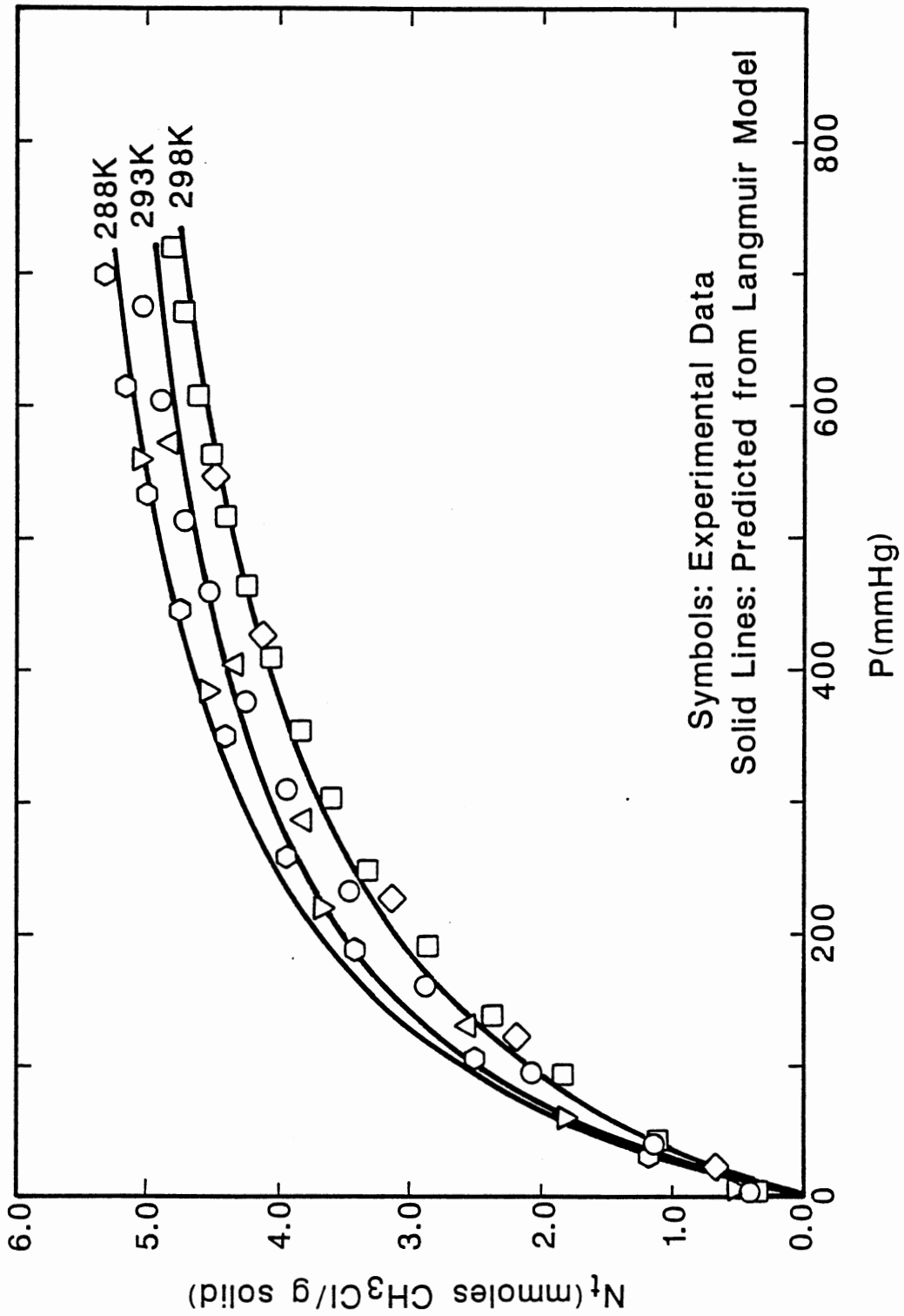
288K
293K
298K
Symbols: Experimental Data
Solid Lines: Predicted from Langmuir Model
N_t (mmoles CH_3Cl/g solid)
P(mmHg)
0.0
1.0
2.0
3.0
4.0
5.0
6.0
0
200
400
600
800

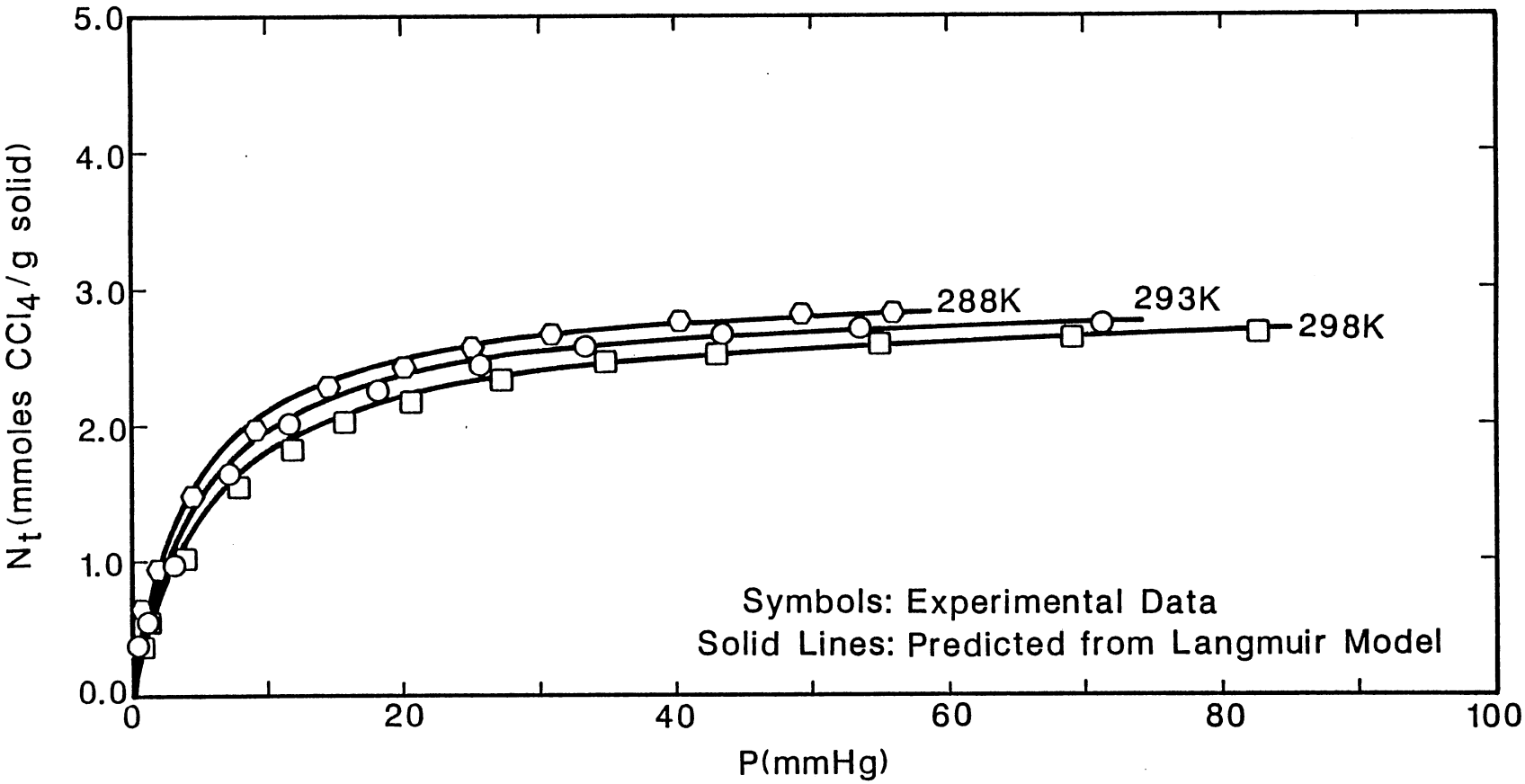
5.0
4.0
3.0
2.0
1.0
0.0
N_t(mmoles CCl_4/g solid)
0
20
40
60
80
100
P(mmHg)
288K
293K
298K
Symbols: Experimental Data
Solid Lines: Predicted from Langmuir Model

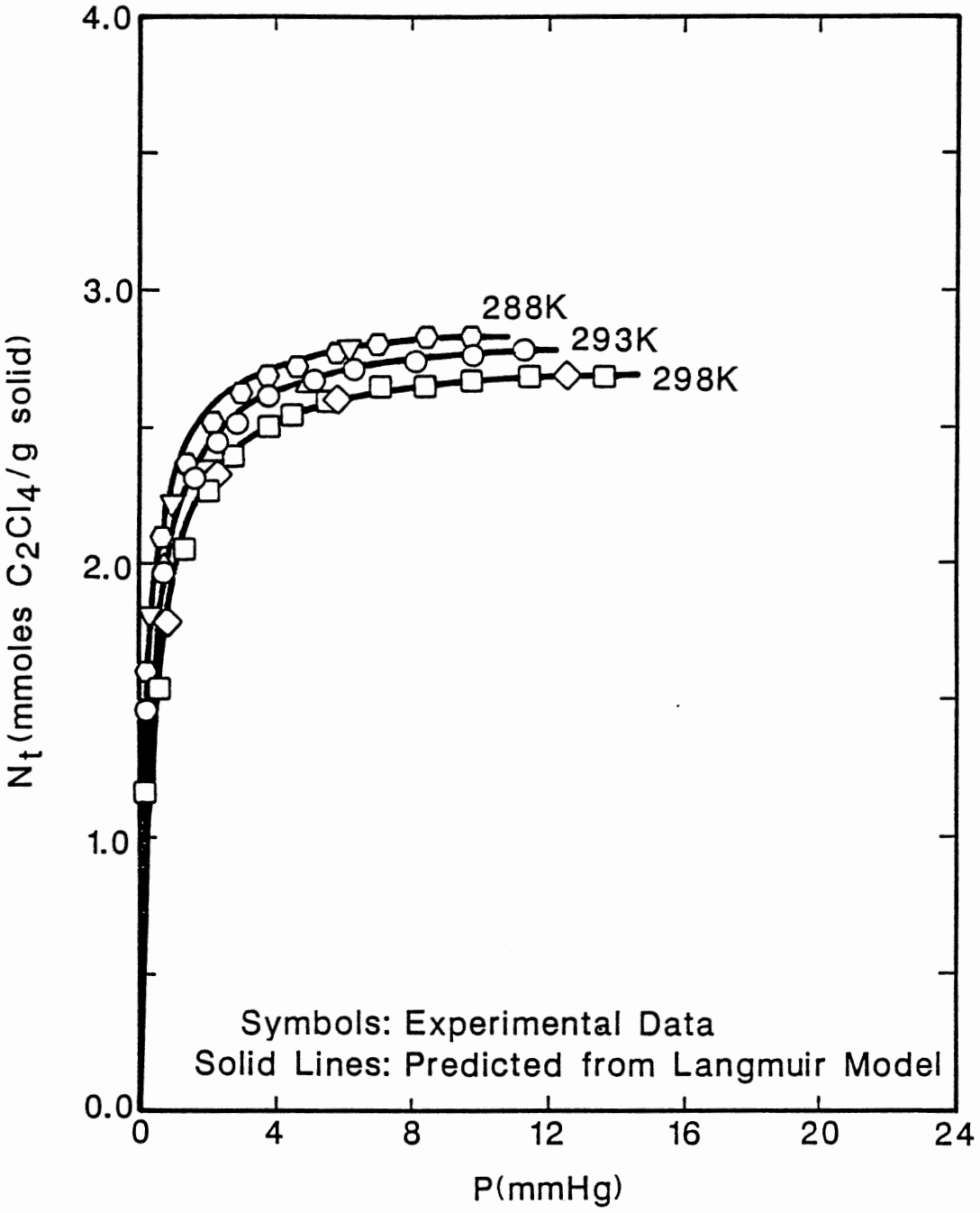
4.0
3.0
2.0
1.0
0.0
0
4
8
12
16
20
24
288K
293K
298K
Symbols: Experimental Data
Solid Lines: Predicted from Langmuir Model
N_t(mmoles C_2Cl_4/g solid)
P(mmHg)

APPENDIX I

SAMPLE CALCULATIONS FOR PREDICTION OF ADSORPTION ISOTHERMS USING THE BET MODEL

Sample Calculations for Prediction of Adsorption Isotherms Using the BET Model

BET isotherm (Reference 10, Chapter IV) was used to correlate the adsorption isotherm data. The BET model, which was obtained by extending the Langmuir isotherm to apply to multilayer adsorption, has the form

$$\frac{P}{N(P_s - P)} = \frac{1}{CN_m} + \frac{(C-1)}{N_m}\frac{P}{P_s}$$

where P_s is the saturation or vapor pressure, C is a constant for the particular adsorption system, N is the uptake and N_m is the monolayer adsorption capacity. If $P/(P_s - P)N$ is plotted versus P/P_s, a straight line should be obtained over the region in which BET equation holds. This line will have a slope of $(C-1)/(N_mC)$ and an intercept of $1/(CN_m)$. The plot of dichloromethane on silica gel is shown on next page as a sample calculation. As can be seen from the figure, the BET model correlates the data pretty well in the region $P/P_s \leq 0.35$. However, it did not hold for $P/P_s \geq 0.35$. This is not surprising considering that the BET model satisfies the Henry's law requirement in the low pressure region and it primarily holds for Types II and III isotherms. However, since the BET model holds for low pressure region, it can be used to obtain the monolayer coverage and area occupied by an adsorbed molecules from the slope and intercept of the straight lines.

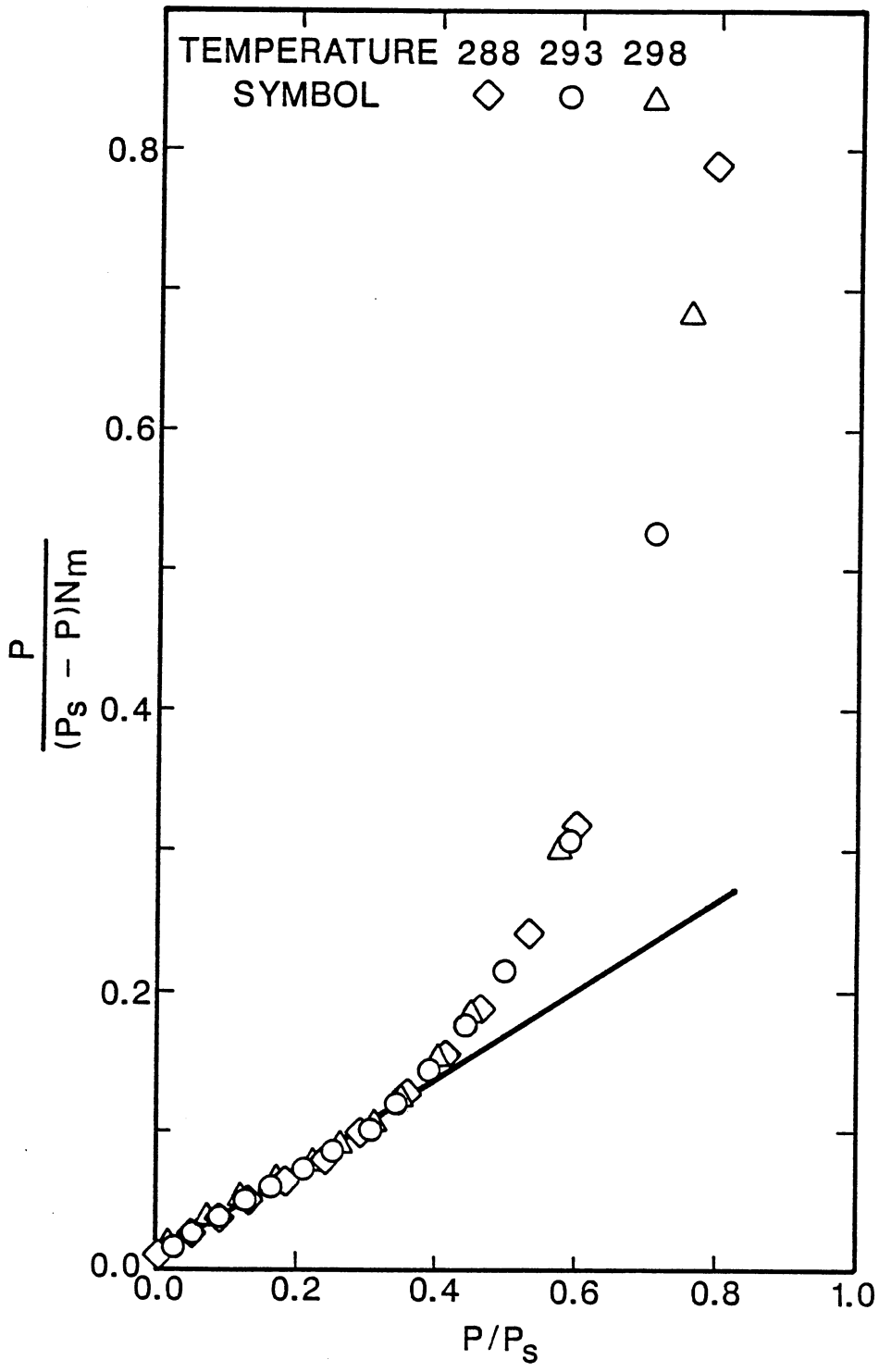
TEMPERATURE 288 293 298
SYMBOL
0.8
0.6
0.4
0.2
0.0
0.0
0.2
0.4
0.6
0.8
1.0
P/Ps
P / (Ps − P)Nm

VITA

Shing-Lin Kuo

Candidate for the Degree of

Doctor of Philosophy

Thesis: ADSORPTION OF CHLORINATED HYDROCARBON POLLUTANTS ON SILICA GELS

Major Field: Chemical Engineering

Biographical:

Personal Data: Born in Penghu, Taiwan, Rep. of China, February 4, 1954, the son of Shooa-Ren Kuo and Won-Chi Jen.

Education: Graduated from Penghu High School, Penghu, in May, 1973; received Bachelor of Engineering degree from Tamkang University, Taiwan, in May, 1977; received Master of Science degree from University of Wyoming in May, 1983; completed requirements for the Doctor of Philosophy degree of Oklahoma State University in December, 1987.

Professional Experience: Full-time Teaching Assistant, Chemical Engineering, Tamkang University, Taipei, Taiwan, from July, 1977, to July, 1980; Graduate Teaching and Research Assistant, Chemical Engineering, University of Wyoming, Laramie, Wyoming, from September , 1980, to July, 1983; Graduate Research Associate, School of Chemical Engineering, Oklahoma State University, Stillwater, Oklahoma, from September, 1983, to present.

Membership in Professional Societies: American Institute of Chemical Engineers; Chinese Institute of Chemical Engineers.